


Summer 8-23-2019

The dispersal pattern of *Thekopsora minima* in wild blueberry determined by a molecular detection method

Nghi Nguyen
nghi.nguyen@maine.edu

Follow this and additional works at: <https://digitalcommons.library.umaine.edu/etd>

 Part of the [Agricultural Science Commons](#), [Botany Commons](#), [Molecular Genetics Commons](#), [Plant Biology Commons](#), and the [Plant Pathology Commons](#)

Recommended Citation

Nguyen, Nghi, "The dispersal pattern of *Thekopsora minima* in wild blueberry determined by a molecular detection method" (2019). *Electronic Theses and Dissertations*. 3065.
<https://digitalcommons.library.umaine.edu/etd/3065>

This Open-Access Thesis is brought to you for free and open access by DigitalCommons@UMaine. It has been accepted for inclusion in Electronic Theses and Dissertations by an authorized administrator of DigitalCommons@UMaine. For more information, please contact um.library.technical.services@maine.edu.

**THE DISPERSAL PATTERN OF *THEKOPSORA MINIMA* IN WILD BLUEBERRY
DETERMINED BY A MOLECULAR DETECTION METHOD**

Nghi S. Nguyen

B.S University of North Texas, 2013

A THESIS

Submitted in Partial Fulfillment of the

Requirements for the Degree of

Master of Science

(in Botany and Plant Pathology)

The Graduate School

The University of Maine

August 2019

Advisory Committee:

Seanna Annis, Ph.D., Associate Professor of Mycology, Advisor, School of Biology and Ecology, Advisor

David Yarborough, Ph.D., Wild Blueberry Specialist, Professor of Horticulture, School of Food and Agriculture

Jianjun (Jay) Hao, Ph. D, Associate Professor of Plant Pathology, School of Food and Agriculture

Ek Han Tan, Ph. D, Assistant Professor of Plant Genetics, School of Biology and Ecology

© 2019 NGHI S. NGUYEN

All Rights Reserved

**THE DISPERSAL PATTERN OF *THEKOPSORA MINIMA* IN WILD BLUEBERRY
DETERMINED BY A MOLECULAR DETECTION METHOD**

By Nghi S. Nguyen

Thesis Advisor: Dr. Seanna Annis

An Abstract of the Thesis Presented
in Partial Fulfillment of the Requirements for the
Degree of Master of Science
(in Botany and Plant Pathology)
August 2019

Blueberry rust caused by *Thekopsora minima* is a common disease in wild blueberry (*Vaccinium angustifolium*) and other *Vaccinium* genera. Understanding the spore dispersal pattern and disease cycle of fungal pathogens in wild blueberry is crucial for the development of a more efficient disease management program. Molecular assays for rapid detection and quantification of *Thekopsora minima* were developed to be incorporated with a spore trap sampling method and weather data collection to examine spore dispersal pattern and production in three different fields: Blueberry Hill Farm in Jonesboro, East Machias, and Spring Pond in Deblois, Maine, in three years 2014, 2015 and 2017. A total of fifteen primer sets for PCR assays and one set of six Loop-mediated isothermal amplification assay (LAMP) primers developed from the internal transcribed spacer (ITS) regions of *T. minima* were tested for specificity and sensitivity towards *T. minima* DNA. There was one primer set (TMITS2F and TMITS2GR) that was specific to rust in both PCR and qPCR assay and could detect down to about 20 copies of DNA. Lower DNA level detection (about 2 copies) is possible but often nonreproducible. The LAMP assays results were found to be not reproducible. The qPCR with

the two primers TMITS2F and TMITS2GR was used to quantify rust spores in the spore trap tape DNA extracted by a Phenol-Chloroform method. Weather factors including temperature and leaf wetness duration (LWD) were collected using weather stations and button loggers placed in the fields. Calculated weekly sums of LWD and optimal temperature (17°C to 22°C) hour for uredinia production (TH) and weekly averages of other weather factors were analyzed with the weekly spore count numbers using a linear mixed model with the random effects from weeks, fields and years. There was a significant correlation between spore counts using a compound microscope and the qPCR method. There was no clear pattern of temperature, TH and LWD effects on spore numbers quantified by qPCR or microscopy. A linear mixed model (LMM) for disease severity in 2017 testing the effects of log of spore number quantified by qPCR assays, average temperature, LWD, and the random effects of weeks and fields, found that both temperature and LWD had significant negative effects on the disease severity ($p < 0.05$). The model could explain 94.38% of the variance in the disease severity and the fixed effects alone could explain 64.46% of the variance. This might indicate that higher weekly average temperature and LWD might decrease the disease severity for *T. minima*. This relationship could be due to the time required for spores to germinate and cause disease. The proposed preliminary models for disease severity and weather variables, as well as the relationship between the spore number and disease severity need to be tested with data from more years and fields to confirm the results. Nevertheless, the establishment of the molecular assay and predicting models for spore number in this study could be a useful tool for future research on disease management and development of a disease warning strategy for *T. minima* in wild blueberry.

ACKNOWLEDGEMENTS

I have received much support from several individuals and organizations for my project. Firstly, I would like to thank my advisor Dr. Seanna Annis and my committee members, Dr. Jay Hao, Dr. Dave Yarborough and Dr. Ek Han Tan for their incredible mentorship and expertise in this project. I am also grateful for my current and previous lab members Rachael Martin, Katie Ashley, Megan Correia, Kelly Xiao, Samari Stewart and Sarah Marcotte for their assistance and support during my project. I especially want to thank Dr. Jay Hao, and his graduate students Tongling Ge and Cody Li, who have allowed me access to their lab equipment and provided beneficial advice for my experiments. I want to thank Dr. Bill Halteman for his advice and help with statistical analysis in the project. I also appreciate the continuous collaboration of many Maine wild blueberry growers who granted us permission to collect samples on their farms and extension workers who assisted with our research. Funding for this project was provided by the Specialty Crop Block Grant from Maine Department of Agriculture, Conservation and Forestry, and Wild Blueberry Commission of Maine. I want to thank my undergraduate mentors, Dr. Jim Bidlack, Dr. Gloria Caddell at the University of Central Oklahoma and my internship mentors Dr. Matthew Paret and Dr. Fanny Iriarte who supported and inspired me to study Plant Pathology in graduate school. Lastly, I want to show my appreciation to my beloved family and friends who always provide tremendous emotional support and love to keep me on track of my academic career.

TABLE OF CONTENTS

ACKNOWLEDGEMENTS	vi
LIST OF TABLES	x
LIST OF FIGURES	xii
CHAPTER 1: LITERATURE REVIEW.....	1
1.1 Lowbush blueberry production overview.....	1
1.2 <i>Thekopsora minima</i> : history, life cycle and disease symptoms on blueberry.....	3
1.3 Molecular detection and quantification methodologies.....	7
1.4 Internal transcribed spacer regions in fungi.....	12
1.5 Airborne spore sampling methods and weather factor analysis for development of disease warning systems.....	13
1.6 Thesis objectives.....	17
CHAPTER 2: DEVELOPMENT OF MOLECULAR ASSAYS FOR DETECTION AND QUANTIFICATION OF <i>T. MINIMA</i>	19
2.1 Introduction.....	19
2.2 Material and Methods.....	22
2.2.1 <i>T. minima</i> urediniospores collection and DNA extraction.....	22
2.2.2 Identification of <i>T. minima</i> DNA in spore samples.....	24
2.2.3 DNA from non-target species.	25
2.2.4. Cloning and identification of possible <i>T. minima</i> PCR products.....	27
2.2.5 PCR and LAMP primer development.....	28
2.2.6 PCR and qPCR assay development.....	31
2.2.7 LAMP and qLAMP assays development.....	33

2.3 Results.....	35
2.3.1 Collection of DNA of <i>T. minima</i> and other species.....	35
2.3.2 PCR and gel electrophoresis for <i>T. minima</i> DNA.....	36
2.3.3 Plasmid cloning and estimation of DNA copies.....	37
2.3.4 PCR and qPCR assays development.....	39
2.3.5 LAMP and qLAMP assays development	57
2.4 Discussion and Conclusion.....	61
CHAPTER 3: ASSESSMENT OF WEATHER FACTORS EFFECTS ON DISPERSAL	
PATTERN AND DISEASE SEVERITY OF <i>T. MINIMA</i>.....	
3.1 Introduction.....	67
3.2 Materials and methods.....	71
3.2.1 Spore collection using spore trap samplers.....	71
3.2.2. Spore counting using microscopy.....	72
3.2.3 DNA extraction of spore trap tapes	73
3.2.4 Determining the detection threshold for qPCR assay.....	75
3.2.5 Spore tape quantification using qPCR.....	75
3.2.6 Weather data collection and data analyses	77
3.3 Results.....	81
3.3.1 Determining the detection threshold for the qPCR assay.....	81
3.3.2 Detection and quantification of rust DNA from spores on spore trap tapes.....	82
3.3.3 Comparison of spore quantification using microscopy, molecular method and disease severity rating.....	83
3.3.4 Analysis of weather data and spore numbers using molecular method.....	92
3.4 Discussion and Conclusion.....	104

CITED REFERENCES	111
APPENDICES.....	121
APPENDIX A LIST OF SEQUENCES USED TO DEVELOP PCR PRIMERS.....	121
APPENDIX B. LIST OF FIELDS AND WEEKS USED IN THE STUDY.....	124
BIOGRAPHY OF THE AUTHOR	126

LIST OF TABLES

Table 2.1 Summary of collected spore samples with confirmed <i>T. minima</i> presence.....	23
Table 2.2 List of non-target species used in assay specificity tests.....	26
Table 2.3 Primer set for LAMP that targets ITS regions of <i>T. minima</i>	31
Table 2.4 Plasmid extraction samples from two locations BBHF and Wesley.....	39
Table 2.5 PCR primer sequences list.	41
Table 2.6 List of 15 primer sets that were tested in PCR and qPCR assays development.....	42
Table 3.1 Spore trap location used and weather data collection.....	72
Table 3.2 Results of amplification of spore dilution series extracts.	82
Table 3.3 Average spore number quantified by microscopy and qPCR methods in three blueberry fields over three years.....	83
Table 3.4 Proportion of variance each of five principal components contributed to the variance of the weather data.....	93
Table 3.5 Factor loadings or the correlation coefficients between the variables and factors.....	94
Table 3.6 Summary of the linear mixed effects model of log spore quantified by qPCR and two weather factors of TH and LWD.	96
Table 3.7 Results of likelihood ratio test on the full model of log spore number with weather variables and three nested models.....	97
Table 3.8 The summary of the LMM model of disease severity rating, log of spore number and two weather factors TH and LWD.	98
Table 3.9 Results of likelihood ratio test on the full LMM model of disease severity with weather variables and two nested models.	99
Table 3.10 Summary of the LMM model of disease severity rating, log of spore number	

and two weather factors temperature and LWD.	102
Table 3.11 Summary of the likelihood ratio test on the full LMM model of disease severity with weather variables and two nested models.	103

LIST OF FIGURES

Figure 1.1 Wild blueberry leaves with rust urediniospores in a field in Maine (Photo: Annis Lab)	6
Figure 1.2 Internal transcribed spacer region of the fungal rDNA complex.....	12
Figure 1.3 A solar powered Burkard 7-day spore trap on a blueberry barren.....	15
Figure 2.1 Urediniospores collection from infected blueberry leaves.....	24
Figure 2.2 Illustration of LAMP primers' location (Source: Eiken Genome Site, Eiken Chemical Co. Ltd)	30
Figure 2.3 Gel electrophoresis of PCR products from three field samples.....	36
Figure 2.4 Gel electrophoresis of samples that were used for plasmid cloning.	38
Figure 2.5 Gel electrophoresis of initial tests of the 6 primer sets to amplify <i>T. minima</i>	43
Figure 2.6 Gel electrophoresis of initial tests to amplify using two <i>T. minima</i> DNA samples.	43
Figure 2.7 Specificity test results of primer set 2 (TMITS1B and TMITS2B).	45
Figure 2.8 Results of PCR specificity test for primer set 8 and 10.....	46
Figure 2.9 PCR detection limit tests for primer set 8 and 10.....	47
Figure 2.10 Specificity test of primer set 12.	48
Figure 2.11 Detection limit test of PCR assay using primer set 12.....	48
Figure 2.12 PCR detection limit and specificity results for primer set 13 and 14.	50
Figure 2.13 The gel electrophoresis of the qPCR detection limit and specificity tests for primer set 12.....	51
Figure 2.14 PCR detection limit test for primer set 15.....	52
Figure 2.15 Amplification curve in qPCR assay specificity test using primer set 15.....	53

Figure 2.16 Gel electrophoresis of qPCR for detection limit and specificity tests using primer set 15.....	53
Figure 2.17 Standard curve and melting peak diagram from a qPCR test using primer set 15 in the first run.....	55
Figure 2.18 Standard curve and melting peak diagram from a qPCR test using primer set 15 in the second run.	56
Figure 2.19 Standard curve and melting peak diagram from a qPCR test using primer set 15 in the third run.	56
Figure 2.20 Gel electrophoresis of temperature tests for LAMP primer set.	57
Figure 2.21 Gel electrophoresis of specificity for LAMP primer set.	58
Figure 2.22 Gel electrophoresis of detection limit for LAMP primer set.....	58
Figure 2.23 Gel electrophoresis of heating test and HNB dye using LAMP assay.	60
Figure 2.24 Gel electrophoresis of specificity test for LAMP primers.	61
Figure 3.1 Urediniospores (orange color) observed under 40X lens of the microscope.....	73
Figure 3.2 Graph of spore number quantified using microscopy and qPCR method.....	85
Figure 3.3 Graph of spore number in EM 2015.....	86
Figure 3.4 Graph of spore number in SP 2017.....	87
Figure 3.5 Graph of spore number and weather factors in BBHF and EM in 2014 and 2015.	90
Figure 3.6 Graph of spore number, disease severity and weather factors in BBHF in 2017.....	91

Figure 3.7 Graph of spore number, disease severity and weather variables in SP in 2017.....	92
Figure 3.8 A PCA biplot of the five weather variables (Temperature, TH, RH, LWD and dew point)	95
Figure 3.9 Residual plot of the linear model between log of spore number detected by qPCR and temperature, TH, LWD.....	97
Figure 3. 10 Residual plot between the residuals and fitted (or predicted) values.	100
Figure 3.11 Normal quantile-quantile plot of the LMM for disease severity.	100
Figure 3.12 Caterpillar plot of the intercepts of the random effects from each of the 11 weeks of 2017 (with first week converted to Julian date) in the disease severity model.....	101
Figure 3.13 Residual plot between the residuals and fitted (or predicted) values of LMM model for disease severity.	103
Figure 3.14 Normal quantile-quantile plot of the LMM for disease severity.	104
Figure 3.15 Caterpillar plot of the intercepts of the random effects from each of the 11 weeks of 2017 (with first week converted to Julian date) in the disease severity model.....	104

CHAPTER 1

LITERATURE REVIEW

1.1 Lowbush blueberry production overview

Growing wild blueberries has long been a culturally and economically important practice in northeastern North America. Wild blueberry belongs to the genus *Vaccinium*, which is the most diverse genus in the Ericaceae or Heath family in North America. This genus includes many plants with edible fruits such as low and highbush blueberry, cranberry, huckleberry, bilberry and other species (Freedman, 2014). Members of this family are mostly found in acidic, nutrient-poor and well-drained soils (Freedman, 2014). The two most common wild blueberry species typically found in commercial fields in North America are the low, sweet blueberry *Vaccinium angustifolium* Aiton and *Vaccinium myrtilloides* Michx., commonly called sour top or velvetleaf blueberry (Hall et al., 1979). *Vaccinium angustifolium* is often characterized by shiny, smooth leaves with toothed margins and *Vaccinium myrtilloides* differs in its hairy, non-toothed margins leaves (Hall, 1967). Wild blueberry was first consumed and encouraged to grow by Native Americans using simple methods such as clearing the forests and burning over the fields (Yarborough, 1997).

The habitat range of *V. angustifolium*, the more abundant wild blueberry species, is from the northern Canadian tundra to the New England states, westward to Minnesota and southward to Virginia (Rogers, 1974; Pritts and Hancock, 1984). Nowadays, wild blueberries are commercially grown mostly in Maine, Quebec and the Maritimes provinces of Canada (Strick and Yarborough, 2005). In 2017, wild blueberry production was 28% of the total of North America blueberry production with 7% from Maine and 21% from Canada (Yarborough, 2018). A very small number of wild blueberries are grown in other states of the U.S such as New Hampshire, Massachusetts,

Virginia and the Canadian provinces of Ontario and Saskatchewan (Yarborough, 1997). Currently, wild blueberries are grown on about 44,000 acres in Maine (Yarborough, 2015) with about 17,000 acres bearing fruit in 2018 (USDA, 2018). Approximately, 99% of wild blueberries are sold as frozen products, and only about 1% of the crops are sold fresh for the local retail or farmer markets (Yarborough, 2015).

Lowbush blueberries are unique in their growth habit and life cycle. Most commercial fields, called barrens, are often developed from the naturally occurring blueberries growing in abandoned farmlands or from the understory of woodlands (Hall, 1967). Lowbush blueberry can reproduce sexually from seeds and asexually through its horizontal underground stems called rhizomes (Bell et al., 2009). The seeds may be viable for about 12 years under proper storage (Rogers, 1974). The original plant with its rhizome system is called a clone that can spread to an average size of 75 to 250 square feet (Yarborough, 2015). The blueberry barrens are often comprised of many genetically different clones that result in differences in phenological characteristics and morphological features such as leaf and fruit color, taste, and fruit yield (Vander Kloet, 1978; Smagula et al., 1997).

The blueberry crop typically has a two-year production cycle whereas only half of the growing acres are harvested each year (Yarborough, 1997). In the first vegetative year, the fields produce no fruit and are often sprayed with herbicides or pesticides to control weeds, insects, and pathogens (Yarborough, 2015). In the following year, the overwintering plants will start to produce flowers in early summer and fruit around late July or August. Pesticides or fungicides may be sprayed as needed in the crop year as well. After harvesting, the fields are mowed to the ground or burned to stimulate new growth and reduce diseases by removing infected plants and disrupting the life cycle of the pests (Hall, 1967). Most commercial fields in the present day are mechanically mowed

because not only it is cheaper than traditional burning, but it can reduce harm from burning, such as exposing the plants' rhizomes to the harsh winter environment and from damaging the organic pad (Yarborough, 2015).

Wild blueberry periodically suffers from many diseases and pests, as well as competition from weeds. Mummy berry caused by *Monilinia vaccinii-corymbosi*, blossom & twig blight caused by *Botrytis cinerea*, and several foliar diseases such as leaf rust caused by *Thekopsora minima*, and Valdencia leaf spot caused by *Valdensia heterodoxa*, are among the common problems for wild blueberry every year (Annis et al., 2018). Development of wild blueberry cultivars have been done in the past, but they have not been used in large scale production due to the slow establishment and lack of rhizome production (Jamieson and Nickerson, 2003; Yarborough, 2012). Therefore, the development of a disease resistant cultivar is not a practical idea. External applications of disease control methods such as cultural controls and spraying fungicides are widely used.

In Maine, the wild blueberry growers and researchers from the University of Maine Cooperative Extension are working alongside each other in the integrated pest management (IPM) program to scout for diseases and develop management tools (Yarborough, 2015). Additionally, the program also aims to develop innovative ideas and methods to control and monitor pests as well as reduce the environmental impacts of the control practices.

1.2 *Thekopsora minima*: history, life cycle and disease symptoms on blueberry.

Thekopsora minima (Arthur) Syd. & P. Syd is a native fungal pathogen causing leaf rust in plants of the genus *Vaccinium*, especially blueberry, in Japan and eastern North America (Sato et al., 1993). This fungus was previously thought to belong to the fungal complex of *Pucciniastrum vaccinii* with two different forms: a western form with conical aecia and an eastern form with cylindrical aecia. However, a detailed morphological study from Japan described two fungi: *T.*

minima is the eastern form occurring in Japan and eastern North America, and *Naohidemyces vaccinii* is the western form mostly found in Japan, Europe and western North America (Sato et al., 1993). Blueberry leaf rust outbreaks were not very common and have never been reported before the 2000s (Nickerson and Hildebrand, 2017). However, possibly due to the increase in commercial blueberry production over the years, there has been an increase in reports of the leaf rust in not only native areas but also in many new locations where it has not been found in the past. In the USA, the pathogen was introduced to many western states from the presumed native source in the Northeast, and so far, the newest states with disease incidence reports of *T. minima* include Michigan, Oregon, and California (Schilder and Miles, 2011; Wiseman et al., 2016; Shands et al., 2018). In addition, blueberry production and trade on the global scale might also be the reason for the introduction of the pathogen to countries that are large geographical distances from the native sources such as Mexico, Colombia, Brazil, South Africa, Australia, and China (Rebollar-Alviter et al., 2011; Yepes and Céspedes, 2012; Pazdiora et al., 2019; Mostert et al., 2010; McTaggart et al., 2013; Zheng et al., 2017). The ability of rust spores to travel a far distance via strong wind or hurricanes might also explain the spread of the disease across neighboring countries in South America (Avila-Quezada et al., 2018).

Thekopsora minima is a heteroecious leaf rust fungus in the *Uredinales* order within the Basidiomycota, where all the economically important rust pathogens of plants are found (Maier et al., 2003). Rust fungi are host-specific and obligate biotrophs, which means they need the living host's tissues to complete their life cycle and therefore they are unable to be grown in vitro (Cummins and Hiratsuka, 2003). Their life cycle is often quite involved and can produce up to five types of spore and several other structures on one or two unrelated plant hosts (Maier et al., 2003).

During its life cycle, teliospores of *T. minima* overwinter on leaves of blueberry or other plants of Ericaceae family. Then these spores germinate in the spring to produce basidiospores that can infect its alternate host, hemlock (*Tsuga* spp.) (Sato et al., 1993). Spermata (previously called pycnia) form on the hemlock's needles and subsequently release spermogonia (previously called pycnidiospores) that in turn produce aeciospores that can infect blueberries (Cummins and Hiratsuka, 2003). Infections caused by aeciospores on blueberry plants produce asexual urediniospores that can re-infect other neighboring blueberry plants during the growing season. Teliospores are released again in late fall as overwintering spores and continue the rust life cycle. Leaf rust symptoms often appear around mid-August in blueberry, thus they possibly have minimal effect on the fruit-bearing fields which usually are harvested in August (Annis et al., 2018). However, the pathogen can cause extensive leaf spots and early defoliation of sprout stems that bear flower buds in the vegetative growth fields, which in turn reduces the fruit yield in the subsequent year (Nickerson and Hildebrand, 2017).

Symptoms of rust on blueberry are often not conspicuous until the later stages (Simpson et al., 2017). The early symptoms usually start with water-soaked lesions on the undersides of the leaves around June. In the following months, the lesions move to the upper surface of the leaves and the infected areas become reddish to brown. Yellow pustules or uredinia appear on the underside of the leaves where the lesions are and produce the yellowish orange (rusty) colored urediniospores that are capable of infecting other blueberry plants throughout the growing season (Nickerson and Hildebrand, 2017). The asexual urediniospores are the most noticeable spores with the distinct color of rust pathogens in general (Figure 1.1).



Figure 1. 1 Wild blueberry leaves with rust urediniospores in a field in Maine (Photo: Annis lab)

Defoliation often occurs in severely infected plants and therefore leads to a reduction in yield (Nickerson and Hildebrand, 2017). Due to the impracticality of using resistant cultivars in large scale farming in wild blueberry as mentioned above, blueberry rust is mostly managed by cultural practices and spraying fungicides during the vegetative year when there is no fruit produced (Annis et al., 2018). There is no fungicide resistance reported so far for rust in wild blueberry, but it is necessary to understand the rust disease cycle and dispersal to be able to determine the optimal timing for fungicide applications to reduce the risks of fungicide resistance and the environmental impact of fungicides as well as effectively control rust.

In highbush blueberry production, the evergreen system applied in warmer climate areas is favorable for rust development and thus, disease outbreaks can be more severe. Infection of fruit has been reported in addition to other symptoms and has created a problem of accessing the

markets for growers in the areas with the rust disease epidemic (Simpson et al., 2017). The disease cycle of rust in the northern temperate areas is generally believed to start when the wind carries aeciospores from hemlock plants that infect the young blueberry leaves in early summer (Babiker et al., 2018). Rust infection in highbush blueberries in the southern states of the U.S and warmer production areas, on the other hand, seems to be primarily caused by urediniospores that persist on overwintering blueberry leaves and other native *Vaccinium* species.

A study of rust in highbush blueberry in 2018, confirmed the susceptibility of several *Vaccinium* species except for two accessions from *V. arboreum* and *V. darrowii* (Babiker et al., 2018). Management using fungicides is widely used but fungicide resistance continues to pose a pressing problem for the industry (Simpson et al., 2017). Despite the management efforts, there are still more first reports of disease incidence in the recent years showing that the spreading of the pathogen is still ongoing. Thus, there is a demand for development of highbush cultivars with resistant genes and new alternative methods of chemical control in combating this disease in the highbush blueberry industry (Simpson et al., 2017).

Many early studies on *T. minima* in the past were mainly on its morphology, taxonomy, and host ranges but little is known about its biology (Pfister et al., 2004). So far there is only one study on the temperature effects on urediniospore germination, the incubation period and the efficiency of infecting the leaves (Pfister et al., 2004) and another study on the reactions of a variety of *Vaccinium* spp. to rust infection (Babiker et al., 2018). Thus, there is a need for more studies of blueberry rust's biology and epidemiology in order to effectively control and manage this disease.

1.3 Molecular detection and quantification methodologies

Plant pathogen diagnosis is a crucial step in a disease management system which includes the detection and identification of disease-causing pathogens. Early detection of pathogens can thwart

disease spread and reduce the damage by timely applying the appropriate control methods. Detection of pathogens is traditionally based on visual inspection or microscopic observation of the apparent symptoms and signs from infected plants or cultured plant tissues grown in the laboratory from field samples. However, this approach is often laborious, challenging and requires extensive training in taxonomy (Levesque, 2001). Moreover, many pathogens express symptoms much later after penetration into host plants or remain asymptomatic in some plant varieties and cultivars and are difficult to detect by visual inspection alone (Martin et al., 2016). This challenge has led to the development of many breakthrough molecular detection techniques that have become essential parts of the disease management system in many laboratories nowadays. Molecular detection techniques, although not all perfect, have proved their worth in ensuring accurate results are generated in a much more rapid fashion than traditional techniques.

Many early molecular techniques based on antibodies to detect antigens such as Enzyme-linked immunosorbent assays (ELISA) or on detection of nucleic acids such as Polymerase Chain reactions (PCR) are still among the popular choices today (Levesque, 2001). ELISA, first invented in the 1970s, has become a widely popular immunodiagnostic technique because of its simplicity and potential in high-throughput screening (Martin et al., 2016). The sensitivity and efficiency of the ELISA procedure depends on many factors such as the organism type, freshness and purity of the samples, and pathogen's titer (Schaad et al., 2003; Martin et al., 2016). False positive results and nonspecific detection in ELISA are mostly due to poorly purified samples that still contain proteins of the plant host and co-infecting pathogens or cross-reactivity between protein sequences in other species that resulted in the same target protein being detected (Martin et al., 2016). Other serological techniques besides ELISA include immunostrip assays, western blots, dot-blot

immunobinding assays, and serologically specific electron microscopy (SSEM) (Schaad et al., 2003).

PCR was developed later in 1983 by Kary Mullis and since then has become an essential technique in molecular biology due to its high sensitivity and specificity in detection of target nucleic acids (Mullis, 1987; Schena et al., 2004). The principle of a PCR assay is using the *Taq* DNA polymerase enzyme activity to multiply many copies of nucleic acid. PCR requires two oligonucleotide primers which are specific to a region of the template DNA to create the desired nucleic acid sequences of the target species (Mullis, 1987). PCR is less costly than many serological techniques but highly specific and rapid. Thus, it has become the method of choice for many diagnostic and molecular labs (Martin et al., 2016). PCR is especially useful to detect obligate biotrophic pathogens that cannot be grown in artificial media. Currently, there are many different versions of PCR for different research purposes such as real-time PCR, nested PCR, reverse-transcription PCR, multiplex PCR, etc.

Quantitative or real-time PCR combines the sensitivity of the conventional PCR with fluorescent signals to provide real-time analysis of the amplification reaction and therefore, can quantify specific DNA targets (Schena et al., 2004). Real-time PCR can be either amplicon sequence nonspecific by using intercalating dye such as SYBR Green (Morrison et al., 1998) or ethidium bromide that generates a fluorescent signal when they bind to double-stranded DNA (Higuchi et al., 1992). It can also be amplicon sequence specific by using an oligonucleotide probe and an acceptor dye (quencher) that requires specific hybridization between the probe and the target DNA to generate a fluorescent signal (Schena et al., 2004). The main disadvantage of qPCR is that it requires expensive equipment and technical expertise to perform the procedure (Hodgetts et al., 2015). Another method that has been widely used is Loop-mediated isothermal amplification

(LAMP), and other nucleic based techniques developed are fluorescent in situ hybridization (FISH), DNA fingerprinting, nucleic acid sequence-based amplification (NASBA, also known as 3SR), Rolling Circle Amplification (RCA), Ligase Chain Reaction and AmpliDet RNA (Martinelli et al., 2015; Fakruddin et al., 2013).

The LAMP method was first developed in Japan in 2000 (Notomi et al., 2000) and since then has been a useful tool to detect and amplify nucleic acids. LAMP has been successfully applied in many fields including medical, food science and plant pathology diagnoses and detection research in recent years (Almasi et al. 2012; Elkins et al. 2015; Hodgetts et al. 2015; Villari et al. 2017). It is highly sensitive and able to detect even a very minimal amount of DNA (Notomi et al., 2000). LAMP has an advantage over PCR in that it is done in a shorter time and can amplify DNA with high efficiency under isothermal conditions without being significantly influenced by non-target DNA (Notomi et al., 2000). The LAMP method uses auto-cycling strand displacement DNA synthesis with the help of *Bst* DNA polymerase and a set of two inner primers (forward inner primer -FIP and backward inner primer-BIP) and two outer primers (forward outer primer- F3 and Backward outer primer-B3) that can recognize four to six sequences on the target DNA. The reaction produces million copies of stem loop DNA with inverted repeats and many loop structures of the DNA target (Notomi, 2000). Loop primers can also be added to accelerate the speed of the reaction and increase the reaction sensitivity (Nagamine et al., 2002).

The LAMP method has been used in some recent research in plant pathology such as gray leaf spot disease in turfgrass (Villari et al., 2017) and banana *Xanthomonas* wilt caused by *Xanthomonas campestris* pathovar *musacearum* (Hodgetts et al., 2015) with the goal for field implementation. The assay condition for LAMP is often isothermal, which means the assays can be done in a heat block or water bath. This makes it less costly than PCR and can be potentially

developed to use outside the laboratory setting and in the field. LAMP can be developed into a quantifying method (qLAMP) by addition of fluorescent dyes such as SYBR Green or Eva Green and detection instrumentations such as bioluminescence, fluorescence readers or a turbidimeter (Seyrig et al., 2015). LAMP assay results were often reported to be more sensitive than PCR in many aspects and they tend to be either comparable or less sensitive than qPCR (Notomi et al., 2000; Fukuta et al., 2013; Shen et al., 2016; Ravindran et al., 2012). LAMP results can be assessed visually by observation of changes in turbidity from the formation of magnesium pyrophosphate or by addition of dyes such as SYBR Green, Hydroxynaphthol blue (HNB), Calcein, or Berberine that change the color of the resulting products (Mori et al., 2001; Fischbach et al., 2015).

There are some drawbacks of the LAMP or RT-LAMP techniques, however, such as the inability to be multiplexed or detect multiple targets in one reaction, a high number of false positives, post-amplification contamination, and the assay's reliability might be compromised by inhibitors (Ball et al., 2016). To solve these problems, multiplex LAMP with the incorporation of QUASR (quenching of unincorporated amplification signal reporters) technique was developed to use in a single step, closed tube and multiplex reaction (Ball et al., 2016). Many other improvements of LAMP techniques are still being developed to increase the efficiency of the assays and optimized to best amplify the target DNA or RNA.

There are several LAMP kits being developed or even used currently to detect specific pathogens in a more rapidly fashion. For instance, Eiken Chemical Co., Ltd., the company where the LAMP method was developed, has a few kits available for detection of *Listeria monocytogenes*, *Salmonella* spp., *Campylobacter jejuni* and *Campylobacter coli* that causes food poisoning (Tsukioka, 2005, Eiken genome site). Other isothermal amplification techniques besides LAMP includes Recombinase polymerase amplification, Helicase-dependent amplification, Ramification

amplification method and others (Fakruddin et al., 2013). LAMP appears to be a promising low cost and effective alternative to other detection methods and can potentially be used in portable detection and quantification methods in the field or rural settings.

1.4 Internal transcribed spacer (ITS) regions in fungi

Molecular assays for pathogen detection and quantification such as PCR and LAMP are initiated by developing primers that are specific to a target DNA sequence. In detecting fungal pathogens, many studies chose specific primers from the internal transcribed spacer (ITS 1 and ITS 2) regions that are located between the small subunit (SSU, 18S), the highly conserved 5.8S and the large subunit (LSU, 28S) coding sequence within the nuclear ribosomal DNA genes of fungi (Gardes and Bruns, 1993) (Figure 1.2).



Figure 1.2 Internal transcribed spacer region of the fungal rDNA complex

The function of these spacer regions is still unclear except for that they separate the functional DNA sequences of the various rDNA genes (Iwen et al., 2002). Mutations within these spacer regions often occur at high frequency. Therefore, they are highly variable not only in different major groups of species but even within species of the same genus (Iwen et al., 2002). Therefore, these regions have been intensively studied for direct fungal sequence analysis, rDNA restriction fragment length polymorphism (RFLP) analysis, species-specific primers and oligonucleotide probe development (Iwen et al., 2002). In fungi, the entire ITS region often has a length that ranges from 600 to 800 bp and can be amplified using the “universal primers” developed by White et al.

(1990). The size of each ITS region alone might vary between 156 to 293 bp (Iwen et al., 2002). The “universal primers” for most fungi (White et al., 1990) mentioned earlier, or enhanced ones that target fungi of the Basidiomycota (Gardes and Bruns, 1993) are often generic to a broad range of fungal species. Therefore, to study one fungal species, it is necessary to develop specific primers within the ITS regions that target only that species. Specific primers are essential for detection of obligate fungal pathogens that are often difficult to grow outside the living hosts or of those whose early infection stages show little to no visible symptoms on the hosts. A few examples of these type of studies include molecular detection and differentiation of *Phakopsora pachyrhizi* and *P. meibomia* that cause soybean rust (Frederick et al., 2002), *Venturia nashicola* that causes scab on Japanese pear and Chinese pear (Le Cam et al., 2001), detection of *Phymatotrichopsis omnivora*, the causal pathogen of root rot in cotton (Arif et al., 2014), and *Pseudocercospora macadamiae* that causes husk spot in macadamia nuts (Ong et al., 2017).

1.5 Airborne spore sampling methods and weather factor analysis for development of disease warning systems

The air contains different particles and reproductive means for many organisms such as viruses, bacterial cells, protists, spores of fungi, algae and spores or pollen from plants (Lacey, 1996; Lacey and West, 2006). Fungi normally produce different types of microscopic spores during their life cycle. The spores can travel by air, water or animals to a new destination or hosts. Generally, the air is a common means of transportation for many terrestrial fungi. For example, fungi of the rust order *Uredinales* can produce a maximum of five spore types, and a majority of them are airborne and often are transported by wind to the new hosts of either the same or unrelated plant species (Maier et al., 2003). Understanding the pattern of spore dispersal and the ability to quantify the spore number is essential to study fungal diseases and develop strategies to manage them.

Phillip H. Gregory, a British mycologist who is famous for his pioneer work in aerobiology, the study of biological matters in the atmosphere, is believed to have inspired the development of many current air sampling principles and methods nowadays (Lacey et al., 1997; Lacey and West, 2006). Gregory was working as one of the lead scientists at Rothamsted Research in Harpenden, UK, on epidemiology, spore dispersal and disease gradients of plant pathogens. He also developed the very first drafts for a spore collecting instrument with components like the cascade impactor with sticky slides and cylinders or Petri dishes to catch *Lycopodium* spores. This instrument inspired his colleague Jim Hirst to develop the Hirst volumetric spore trap, a revolutionized tool to study fungi in both medical and phytopathological research in the past 60 years (Lacey and West, 2006).

The Hirst volumetric trap was developed based on the similar principle to Gregory's idea but replacing the sticky cylinders with a more reliable suction trap and an electric motor to automatically move the airstream to collect spores (Lacey and West, 2006; West and Kimber, 2015). The particles are deposited into a Vaseline-coated microscope slide that moves 2mm per hour past an orifice (Hirst, 1952). Early applications of the Hirst spore trap at Rothamsted Research were to collect spores of the allergens causing asthma in an indoor environment such as *Cladosporium*, *Ustilago*, *Hypholoma*, *Bolbitius* and *Ganoderma* (Gregory and Hirst, 1952). The Hirst spore trap has been used widely in many allergen and plant fungal studies and significantly contributed to our understanding of many different airborne spore types that were overlooked before, such as basidiospores and ascospores (Sterling et al., 1999). The Hirst spore trap was commercially produced and further improved in designs to a few different types of spore traps such as the Lanzoni VPPS Hirst-type trap and the Tilak air sampler (Lacey and West, 2006). Burkard seven-day volumetric spore trap (Figure 1.3), was also developed from the Hirst spore

trap by Burkard Manufacturing Co Ltd (Rickmansworth, UK) in 1966 to collect spores weekly automatically.



Figure 1.3. Solar powered Burkard 7-day spore trap on a blueberry barren. (Photos: Annis Lab)

In plant pathological research, spore trap devices are often used to collect airborne fungal spores to study disease epidemiology with a focus on spore dispersal gradients. Identification and quantification of spore number collected using spore traps were most often done by observing the fungal structures and spore morphology through a microscope. As mentioned in the previous section, using microscopy for fungal spore identification and quantification tends to be tedious and difficult. Moreover, a study that compared sequencing with the microscopy method found that over 85% of fungal genera were not detected by microscopy compared to sequencing (Pashley et al., 2012). Therefore, many molecular detection methods, such as PCR- based and LAMP-based methods, were developed to aid in accelerating detection. For example, a Burkard spore trap was used in combination with PCR method to detect smut fungi *Ustilago scitaminea* in sugarcane (Magarey et al., 2008) and qPCR was used to detect and quantify *Sclerotinia sclerotiorum* inoculum in oilseed rape (Rogers et al., 2008).

In addition, changes in weather patterns are also studied with spore traps to assist in the assessment of how weather factors affect the airborne spore production and dispersal (Lacey and West, 2006). Weather factors that have been considered include atmospheric temperature, relative humidity (RH), leaf wetness duration (LWD) and rainfall (precipitation) (Gleason et al., 2008). Other factors like wind direction, wind speed, and solar radiation are also considered in some warning systems (Gleason et al., 2008). These weather factors can directly or indirectly affect the intensity, speed and range that spores travel as well as their viability and infection rate (Cordo et al., 2017; Gleason et al., 2008).

Temperature is one of the most critical environmental factors that affects each stage of infection of the fungal pathogen and is common to measure in many studies regarding the weather effects on disease (Huber and Gillespie, 1992). For example, a study on the effect of temperature in *T. minima* showed that the germination rate of urediniospores and germ tube growth rate was lower and incubation period were 3 to 4 days longer at a temperature range of over 30°C and below 15°C compared to the rates in optimal conditions (Pfister et al., 2004). Moreover, this study also found that temperature also affects the infection rate and production of urediniospores. On the other hand, relative humidity and leaf wetness duration, or the period that water is present on the crop's canopy surface, has an effect on the transport of inoculum, germination of fungal spores and the penetration rate into the plant tissues, especially on those that cause foliar diseases (Huber and Gillespie, 1992; Rowlandson et al., 2015). In another example, a study of spore dispersal in *Zymoseptoria tritici* that causes leaf blotch in wheat found that relative humidity was positively correlated with ascospores release (Cordo et al., 2017). A study of *Puccinia striiformis* causing stripe rust in wheat found that the fungi had a minimum wet period of 3 hours and optimum length was 8 hours (Shaner et al., 1971). Rainfall and water splash can have some effect on spore dispersal

as well. Although the distance the spores travel is often less than 15 cm in each rain splash event, rain overall gives a favorable environment for fungi to spread infection in plants (Madden, 1997).

Both weather data and spore quantification are often incorporated to develop disease warning systems. The disease warning system (DWS) is an important component of a successful integrated pest management (IPM) strategy that not only manages the disease but also reduces pesticide use. Implementation of these systems can help growers achieve many significant benefits. Firstly, the DWS can increase the effectiveness of disease control practices and other management methods when they are applied at the right timing. Secondly, more precise timing of disease control means that there may be a reduction in the spraying frequency of fungicides that might be harmful for the environment. Therefore, the growers not only can reduce the cost of disease control and increase their profit but also improve their company's image to customers by being more environmentally friendly. There are many DWS currently in use for crops, such as a relative humidity-based warning system for sooty blotch and flyspeck fungal disease in apples (Rosli et al., 2017) or a LWD based warning system for strawberry diseases such as Anthracnose and Botrytis fruit rot (Montone et al., 2016) and mummy berry in lowbush blueberry (Annis, 2009). Most disease warning systems are promising methods to study fungal epidemiology and provide many benefits for growers, but they are still not completely perfect, and improvement is still necessary to increase their accuracy and efficacy.

1.6 Thesis objectives

There are two main objectives for this project:

- Developing a specific molecular amplification assay for faster and more accurate detection and quantification of airborne spores of *T. minima*.

- Assessing how weather factors affect *T. minima* spore production and dispersal pattern. Understanding the association of weather factors and spore dispersal pattern will be valuable to potentially develop a disease warning system for blueberry rust disease.

CHAPTER 2: DEVELOPMENT OF MOLECULAR ASSAYS FOR DETECTION AND QUANTIFICATION OF *T. MINIMA*

2.1 Introduction

Identification and quantification of reproductive propagules of fungal pathogens such as spores are important for studying many aspects of disease epidemiology to improve disease control management. Microscopy is frequently used to assess the presence of the inoculum of these pathogens, but this is often time consuming and not very reliable (Pashley et al., 2012). Using molecular assays is generally more practical to accurately identify and assess the number of fungal spores compared to microscopy (Levesque, 2001). *Thekopsora minima*, a leaf rust of blueberry, is an obligate fungal pathogen that can only grow in a living host plant (Cummins and Hiratsuka, 2003). Studies of *T. minima* are scarce, and there are no studies available regarding what environmental factors affect production and dispersal of spores. Since rust is an important and large family of plant pathogens, there were many species-specific molecular assays developed for different rusts, such as real-time Polymerase Chain Reaction (qPCR) for *Puccinia triticina*, a rust of wheat and a quantitative loop mediated isothermal amplification (LAMP) for *Puccinia kuehnii*, a rust in sugarcane (Duvivier et al., 2016; Chandra et al., 2016). Molecular assays developed in these studies have helped improve identification and quantification of rust spores from environmental samples and have great potential for studying the relationship between rust spores and the environmental factors that might affect their production and dispersal (Duvivier et al., 2016). Therefore, a molecular assay for *T. minima* spore detection and quantification would potentially be a great tool to aid in diagnostic but also epidemiological studies of blueberry leaf rust.

As mentioned in chapter 1, polymerase chain reaction (PCR) based assays are common methods for identification and quantification of target nucleic acids due to their sensitivity and reliability. The LAMP method is based on PCR and potentially a more cost effective and sensitive technique than PCR and qPCR, and it can be used as a quantitative method as well (Cheng et al., 2016; Villari et al., 2017). Specificity in detecting only target genes and sensitivity in terms of the lowest copy number of DNA detected are two important factors in evaluating a molecular assay efficiency (Duvivier et al., 2016). Reproducibility is also an important aspect when evaluating an assay and can be assessed by running a reaction in duplicate or triplicate replications to ensure similar results can be obtained from each replication. Conventional PCR and LAMP assays are regularly used for detection of nucleic acids and require post amplification verification by staining the DNA with a dye to observe the separation of amplified DNA by gel electrophoresis (Shipley, 2006). In the case of LAMP assays, the addition of dyes such as HNB, SYBR Green I, Calcein or Berberine that react with the resulting chemicals in the products also helps with visualization of the amplified products (Mori et al., 2001; Fischbach et al., 2015). Quantitative PCR (qPCR) and LAMP (qLAMP) are useful for detection of amplification of nucleic acids in real-time and tend to be more sensitive than the conventional assays (Notomi et al., 2000; Fukuta et al., 2013; Shen et al., 2016; Ravindran et al., 2012). Post amplification verification is optional but not necessary because the results are already visualized by fluorescent signals generated by dyes or probes and can be assessed using the computer programs associated with the real-time devices (Shipley, 2006). Target regions for molecular detection assays like PCR and LAMP are often species specific to avoid amplifying non-target DNA, especially in environmental samples (Brankatschk et al., 2012). The internal transcribed spacer regions in the ribosomal RNA gene complex, for example, are common choices to develop fungal specific primers (Martin and Rygiewicz, 2005).

The primers and other assay components such as the annealing temperature (T_m) and the reagents are commonly tested under different conditions or concentrations to find out the optimal assay conditions.

There are two main methods for quantifying the products of molecular assays, such as qPCR, which are relative (RQ) and absolute quantification (AQ). Relative, or also called the comparative quantification method, compares the relative change in gene expression levels of the unknown samples and a reference or “housekeeping” gene (Livak and Schmittgen, 2001). This reference gene can be of any transcript, as long as the sequence is known (Bustin, 2002). The level of expression is measured by the difference (Δ) between the threshold cycle C_t or C_q (cycle threshold or quantification cycle) (Pfaffl, 2004). This method is generally useful in measuring gene expression and does not require external standards (Livak and Schmittgen, 2001).

Absolute quantification, on the other hand, translates the strength of PCR amplification signal to the copy number of template DNA by using an external calibration or standard curve (Pfaffl and Hageleit, 2001). The standard curve is generated by using a dilution series of known concentration of DNA called standards, of the target species to accurately estimate the precise number of copies of unknown DNA (Whelan et al., 2003). The types of DNA used as standards can be DNA of the target sequence from a PCR assay, plasmid DNA containing the target sequence or commercially available DNA (Dhanasekaran et al., 2010). The standards are used to generate a linear standard curve of the dilution series that represents a plot of cycle threshold value (C_t or C_q) over the log of starting concentrations of the template DNA to subsequently calculate the number of copies in the sample (Brankatschk et al., 2012). A standard curve is also a useful tool to determine the quality of the molecular assay and the primers used. The fit of the linear regression line represented by the

coefficient of determination (R^2) can be used to calculate the assay's efficiency, which is an indication of how well the reaction performed (Adams, 2006).

The AQ method is often used when obtaining the accurate number of target nucleic acids is necessary (Livak and Schmittgen, 2001). The reliability of an AQ qPCR assay depends on the similar amplification efficiencies between the target DNA used in the standard curve and the unknown DNA templates (Souazé et al., 1996). The AQ method is often more tedious to perform because the standard dilutions are needed in every run and precise pipetting technique is required for accurate dilution of the standards. However, the resulting quantification values can be used without the need for normalization of data (Adams, 2006). The AQ qPCR method is often used for quantifying DNA from environmental samples and other epidemiological studies of plant pathogens. For instance, the AQ method was used in qPCR quantification of *Puccinia triticina* in wheat and *Verticillium dahliae* in spinach (Duvivier et al., 2016; Duressa et al., 2012).

The main objective of this chapter is to develop and evaluate PCR-based and LAMP-based amplification assays for spores of *T. minima* to increase the accuracy of detection and quantification of this pathogen. The absolute quantification method was used to assess assay efficiency and estimate the *T. minima* DNA copies in spore extraction samples. The most efficient amplification assay would become a helpful tool in epidemiological research and future management strategies of *T. minima*.

2.2 Material and Methods

2.2.1 *T. minima* urediniospores collection and DNA extraction

Blueberry stems with rust infected leaves that were producing urediniospores were collected from several fields in the downeast region of Maine from 2015 to 2018 for DNA extraction and analysis (Table 2.1).

Table 2.1 Summary of collected spore samples with confirmed *T. minima* presence. The sequences were compared with available *T. minima* sequences from GenBank.

Field site	Collection date	Isolate code name	Query Cover (%)	Identity (%)	E value	GenBank accession number
Blueberry	9/24/2015	BBHF9.24.15	73	99.57	0.0	MH029898.1
Hill Farm,	10/8/2015	BBHF10.8.15	86	99.57	0.0	MH029898.1
Jonesboro	10/15/2015	BBHF10.15.15	87	99.35	0.0	MH029898.1
Spring Pond,	9/22/2016	SP9.22.16_1A	98	99.06	5e ⁻¹⁵⁹	KX813713.1
	9/22/2016	SP9.22.16_2A	82	99.57	0.0	MH029898.1
Deblois	9/22/2016	SP9.22.16_3A	73	99.57	0.0	MH029898.1
	9/18/2017	SP9.18.17	88	99.57	0.0	MH029898.1
Airport,	9/25/2018	AP9.25.18_1	94	99	0.0	MH029898.1
Deblois	9/25/2018	AP9.25.18_2	100	99	0.0	MH029898.1

The leaves of these stems were observed under a dissecting microscope to check for the presence of urediniospores. The urediniospores were vacuumed into a 1000µl micropipette tip (VWR International, Radnor, PA) that was previously wet with 0.05% Tween 20, an emulsifying agent, and was connected by a short clear tube to a mini vacuum pump. A filter was placed in between the tube and the tip and parafilm was wrapped around this connection joint to secure the tip. The filter helped prevent spores being sucked straight into the vacuum line (Figure 2.1). Collected spores were stored in 1.5ml microcentrifuge tubes and the 0.05% Tween 20 solution was removed after pelleting the spores to the bottom of the tube using a microcentrifuge (Eppendorf, Hamburg, Germany). The spore pellet was extracted using a bead-beating method with the Power Plant Pro DNA Isolation kit (MO Bio, Germantown, Maryland). The samples were heated at 65°C on a heat block in ten minutes prior to the bead-beating step which used Vortex Genie 2 (Fisher,

Hampton, NH). The extraction of spores was also performed using liquid nitrogen grinding and the SP Fungal DNA Mini E.N.Z.A. kit (Omega Bio-tek, Norcross, GA) according to the manufacturer's manuals. The final elution volume was reduced from 100 μ l to 30 μ l to increase the DNA concentration. The resulting DNA were run on 0.8% agarose gel, previously stained with 1 X GelStar (Lonza, Basel, Switzerland), and with a Lamda HindIII DNA ladder (Promega, Madison, WI) to estimate the quantity and quality of the DNA. Concentration of DNA was determined by checking the samples on a Nanodrop (NanoDrop 2000, Thermo Scientific).

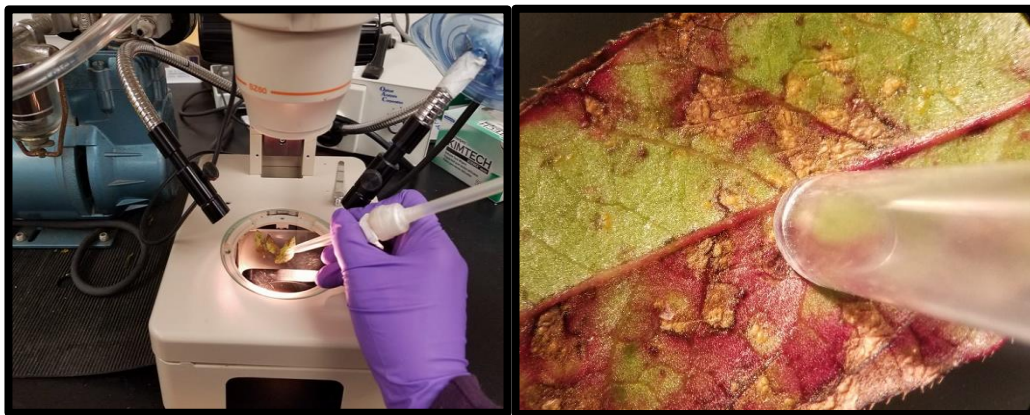


Figure 2.1 Urediniospores collection from infected blueberry leaves. Spore collection using a 1000 μ l micropipette tip attached to a mini vacuum under a dissection microscope (left). A close-up photo of the tip vacuuming spores (right).

2.2.2 Identification of *T. minima* DNA in spore samples

Polymerase chain reactions were performed using the ITS1 and ITS4 universal fungal primers (White et al, 1990.) to amplify the entire length of the fungal DNA ITS regions (including ITS 1, 5.8S and ITS 2) and to assess whether there were other fungal species present in the samples besides *T. minima*. PCR components in a 25 μ l reaction included 1 X OneTaq standard reaction

buffer (NEB, Ipswich, MA), 1.25mM dNTP (Promega, Madison, WI), 1.25 μ M each of ITS1 and ITS4 primers, 0.625 units OneTaq DNA Polymerase (NEB, Ipswich, MA), 5-10ng/ μ l of template DNA and sterilized MilliQ water (MilliporeSigma, Burlington, MA). PCR reaction conditions were 94°C for 5 min, 30 cycles of 95 °C for 1 min, 55 °C for 1 min, 72 °C for 1 min and a final step of 72 °C for 10min. The PCR products were mixed with 2 μ l of 6X Purple Loading Gel Dye (NEB, Ipswich, MA) and run on 1.2 % agarose gel. A 100-base pair (bp) ladder (NEB, Ipswich, MA) was run alongside the samples to assess the amplicon length in base pairs. Amplicon bands appearing on the gel were excised and purified using the QIAEX II gel extraction kit (Qiagen, Germantown, MD) and then sequenced at the UMaine sequencing facility.

2.2.3 DNA from non-target species.

DNA samples of non-target species for primer specificity tests were collected either from collections of previous students' projects, from lab cultures isolated originally from infected plant tissues or from DNA extraction of field samples (Table 2.2). The samples of *Pucciniastrum goeppertianum* (WB2 and WB3), a fungal pathogen that causes Witches' Broom disease in blueberry were collected from a highbush blueberry plant in a residential area in Orono, and two samples of *Coleosporium* sp. (GR1 and GR2), a rust in goldenrod, were collected by extracting DNA from goldenrod collected in a blueberry field. DNA extractions were done using the SP Fungal DNA Mini E.N.Z.A. kit (Omega Bio-tek, Norcross, GA). PCR and DNA sequencing were performed as above using the two universal primers ITS1 and ITS4 (White et al, 1990.).

Table 2.2: List of non-target species used in assay specificity tests.

Species	Code Name	Location
<i>Monilinia vaccinii-corymbosi</i>	MonIso1	Deblois, ME
<i>Monilinia vaccinii-corymbosi</i>	MonIso2	Deblois, ME
<i>Monilinia vaccinii-corymbosi</i>	H3C1	Deblois, ME
<i>Monilinia vaccinii-corymbosi</i>	O24A1	Deblois, ME
<i>Valdensia heterodoxa</i>	VMR5A1	Lubec, ME
<i>Valdensia heterodoxa</i>	VBT1B5	Beddington, ME
<i>Valdensia heterodoxa</i>	VKM3C1	Liberty, ME
<i>Valdensia heterodoxa</i>	VEL141	Ellsworth, ME
<i>Valdensia heterodoxa</i>	VKP4D	Jonesport, ME
<i>Valdensia heterodoxa</i>	VKP6B	Jonesport, ME
<i>Valdensia heterodoxa</i>	VMC7F	Lubec, ME
<i>Pucciniastrum goeppertianum</i>	WB2	Orono, ME
<i>Pucciniastrum goeppertianum</i>	WB3	Orono, ME
<i>Phomopsis sp.</i>	Ph 1	Cherryfield, ME
<i>Phomopsis sp.</i>	Ph3B	Cherryfield, ME
<i>Pestalotia sp.</i>	P1	Cherryfield, ME
<i>Pestalotia sp.</i>	P2	Cherryfield , ME
<i>Gloeosporium sp.</i>	G1C	Cherryfield , ME
<i>Gloeosporium sp.</i>	G1E	Cherryfield , ME
<i>Coleosporium sp.</i>	GR1	Monteville, ME
<i>Coleosporium sp.</i>	GR2	Monteville, ME

2.2.4 Cloning and identification of possible *T. minima* PCR products

When multiple PCR products were amplified and observed on the agarose gel, a DNA cloning method was applied to accurately separate and identify the different bands of DNA to confirm the presence of *T. minima* DNA. The resulting plasmid DNA were used as standards in the qPCR assay to assess the quality of the assay. Cloning was done using the Promega pGEM-T Easy Vector System I kit (Promega US, Madison, WI, USA). Ligation reactions were performed on the PCR product following the manufacturer's protocol. After ligation reactions, the transformation of the plasmid DNA into the bacteria (*Escherichia coli*) procedure was done using High Efficiency Competent Cells (VWR International, Radnor, PA) grown in SOC medium (Super Optimal broth with Catabolite repression) (Chan et al., 2013) and incubated for 1.5 hour at 37°C with shaking. The transformed bacteria were streaked on Luria Broth (LB) plates with 100µg/ml ampicillin (Sigma-Aldrich, St. Louis, MO) that were previously spread with 0.5mM IPTG (Promega US, Madison, WI, USA) and 80µg/ml X-Gal (VWR International, Radnor, PA). The plates were incubated overnight at 37°C. The bacteria colonies grown on the LB plates were color-screened on the following day for white colonies (with inserts) and blue colonies (without inserts).

The bacteria colonies containing plasmid with insert picked from the LB plates were grown in a LB broth in a 37°C incubator overnight then spun down and extracted using the *Small-Scale Preparations of Plasmid DNA* method (Sambrook et al, 1989) and purified with *Preparation of Plasmid DNA: A Modified Mini Alkaline-Lysis/PEG Precipitation Procedure* (Applied Biosystems Inc, 1991). The colonies were extracted and purified in later attempts using the Promega's kit Wizard Plus SV Minipreps DNA purification system (Promega US, Madison, WI, USA). The extracted plasmid DNA was tested using restriction digestion reactions of NotI-HF restriction enzyme (Promega US, Madison, WI, USA) to determine whether the target DNA was

successfully inserted into the vector. Purified plasmid DNA with insert were sent for sequencing. Two bacterial cultures confirmed to contain plasmid with *T. minima* were grown. Plasmid DNA was extracted and purified one more time in 2018 to be used as standards for qPCR assays.

The extracted and purified plasmid DNA were assumed to be pure plasmid DNA containing *T. minima* insert DNA. Each plasmid was assumed to contain one copy of the *T. minima* ITS region. The number of plasmid DNA copies per nanogram of DNA were estimated first by checking the concentration (ng/μl) of the plasmid DNA samples using Nanodrop.

The total copies of plasmid DNA per μL can be calculated using the equation below (Godornes et al., 2007):

$$\text{DNA copies number (molecule) / } \mu\text{L} = \frac{\text{Avogadro's number} \left(\frac{\text{molecules}}{\text{mol}} \right) \times \text{plasmid concentration (g/}\mu\text{L)}}{\text{Length of DNA (bp)} \times 660 \left(\frac{\text{g}}{\text{mol}} \right) / \text{bp}}$$

2.2.5 PCR and LAMP primer development

The DNA sequences obtained from the field samples were checked using the BLAST program (NCBI, 1988), Altschul et al., 1997) against several existing *Thekopsora* sp. sequences in GenBank (NCBI) (Appendix A). The PCR fragments that were identified as *T. minima* (Table 2.1 and 2.4) were aligned using the online version of MAFFT (Kato et al, 2009), a multiple sequences alignment program and then manually analyzed using BioEdit (Hall, 2013), a sequence editor software. Most of the current *T. minima* sequences in GenBank did not include the information on the exact location of each ITS region in the sequences and several do not have both ITS1 and ITS2 sequences, therefore, the location of the ITS regions and the 5.8S gene were estimated based on the available full ITS 1, 5.8S and ITS 2 regions of the sequences from the closely related *Thekopsora areolata* in GenBank (Accession ID: DQ087231, EF363336 and DQ445902). The

sequences of all of the *Thekopsora* spp. available (Appendix A) were aligned to estimate the location of the highly conserved 5.8S region, where most of the sequences were well-aligned. The IT1 and IT2 regions were estimated based on the known range of the full ITS region, which is often from 600-800 bp (Gardes and Bruns, 1993) and from the provided exact location of regions from the *T. areolata* sequences mentioned above. At first, the forward primers for the PCR assay were chosen from ITS 1 region and backward primers were chosen from ITS 2 region. However, the primer sets were re-adjusted to have a shorter length amplicon from 100bp to 250bp to also work with the qPCR assay. The criteria of choosing primers included being specific to *T. minima* especially in the 3' end of the sequence, having sequence lengths from 16 to 28 nucleotides long, and having GC contents from 35% to 65%.

LAMP primer sets were generated by using the Primer Explorer V5 online program (Fujitsu Limited, Tokyo, Japan) using all available *T. minima* ITS sequences from field collected samples and also the available GenBank sequences as listed in Appendix A. Following the instruction manual of PrimerExplorer V5, the primer sets were chosen with ΔG threshold less or equal to -4.0 kcal/mol to ensure primer's stability according to primer design guide from Lucigen (Lucigen Corporation, Middleton, WI). The primers were also checked for self-annealing structures and also whether they can be used to generate two loop primers as well. The two regions F1C and F2 were combined into the long forward inner primer (FIP) and likewise with B1C and B2 to form backward inner primer (BIP). Each primer set files were generated again using Primer Explorer V5 software for backward loop primer LF (or BL) and forward loop primer LB (or FL). The estimate arrangement of the LAMP primers on the DNA sequence including six primers F3, B3, F2, B2, F1C, B1C with the LB and LF are illustrated in Figure 2.2.

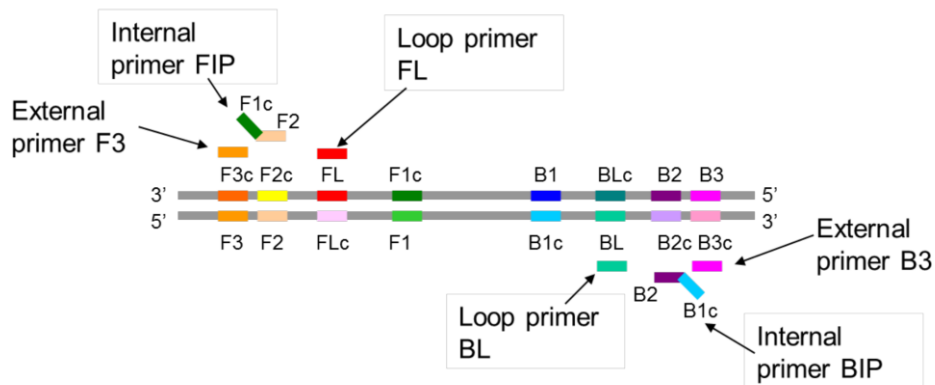


Figure 2.2 Illustration of LAMP primers' location (Source: Eiken Genome Site, Eiken Chemical Co. Ltd)

The potential primer sequences were checked using the BLAST program for possible matches with other blueberry fungal pathogens besides *T. minima* and then they were analyzed by an online program OligoCalc (Kibbe, 2007) for potential problems such as hairpin formation, 3' complementary and self-annealing. This online tool also automatically calculated the predicted GC content percentage and annealing temperature (T_m) for the each of the sequences. The resulting primers were manufactured by IDT (Integrated DNA Technologies, Coralville, USA). The name of the six LAMP primers was changed to TM7F3, TM7B3, TM7FFIP, TM7BIP, TM7LB and TM7LF to avoid confusion with other species' LAMP primers (Table 2.3).

Table 2.3: Primer set for LAMP that targets ITS regions of *T. minima*.

LAMP Primer Name	Sequence (5'-3')	Type	GC content (%)	Length (bp)	Tm (°C)
TM7F3	5'-AAAATTATGGGATGTTGGAAC-3'	Forward outer primer	31.8	22	50.4
TM7B3	5'-CATCCATCACCAACTCCTT-3'	Backward outer primer	47.4	19	52.0
TM7FIP	5'-TCTGCAATTCCCATTACTTATCA CAATAACTTTTAGCAATGGATCTCTTG- 3'	Forward inner primer	34	50	63.3
TM7BIP	5'-GTGAATCATCGAATCTTTGAACG CTGAGAGGGTTTCATGACACT-3'	Backward inner primer	43.2	44	65.5
TM7LF	5'-TGGTATTCCAAAAGGTACACCTGT-3'	Forward loop primer	41.7	24	56.1
TM7LB	5'-ACCTTGCACCTTTTGGTATTCC-3'	Backward loop primer	45.5	22	55.7

2.2.6 PCR and qPCR assay development

The PCR primers were paired up based on their close similarity in Tm and by their locations in the ITS regions. Initially they were tested with each other and with the previously developed primers ITS1F and ITS 4B that amplified ITS regions in Basidiomycetes and rust fungi in general (Gardes et al, 1993). The initial Tm of each primer set was chosen by using the lowest Tm of the primers in a primer set. There were eleven primer combinations (set 1 to 11 in Table 2.6) that were initially tested on two different *T. minima* DNA samples extracted from spores collected on infected blueberry leaves (BBHF10.8.15 and BBHF10.15.15). Primer sets 1 to 11 (Table 2.6) have a forward primer in the ITS1 region and a reverse primer in the ITS2. The last four sets (12 to 15) have both forward and reverse primers in one ITS region to shorten the length of the resulting amplicon to make them more suitable for use in a qPCR assay. The primer sets (set 2, 5, 6, 8, 9, 10) that successfully amplified both *T. minima* samples were later tested for specificity using one or more positive *T. minima* samples and two non-target fungal pathogens of blueberry, *Valdensia heterodoxa* and *Monilinia vaccinii-corymbosi*. DNA of these two species were used as non-target

DNA to test specificity of the assay because they were grown in vitro for DNA extraction and thus, did not have possible field contamination.

The initial running conditions for PCR was 95 °C for 5 minutes, 95 °C for 1 minute, T_m (see initial T_m for each set in Table 2.6) for 1 minute, then 72 °C for 1 minute for 30 cycles and finally 72 °C for 10 minutes before reducing to 4°C. The PCR assays were run on a Bio-Rad C100 Touch thermal cycler (Bio-Rad Technologies, Hercules, CA). The components of each 25 µl PCR reaction included 1.25U of GoTaq DNA Polymerase, and 1X Colorless or Green GoTaq Reaction Buffer (Promega US, Madison, WI, USA), 0.2 µM of each primer, 0.2 mM dNTP, 1 mM MgCl₂ and about 5ng to 10 ng of template DNA. Optimization of MgCl₂ concentration was done for primer set 2 (TMITS1B and TMITS2B) using 0.5 mM, 0.6 mM and 0.9 mM of MgCl₂ to try to improve specificity towards *T. minima*. Primer set 8 (TMITS1A and TMITS2C) was also tested with three MgCl₂ concentration of 0.5, 0.8 and 0.9mM and set 10 (TMITS1C and TMITS2B) with 0.8 mM and 0.9mM of MgCl₂. The results were run on 1.2% agarose gel as described above. Each reaction was run in duplicate. Four primer sets 12 to 15 (Table 2.6) were tested for their usefulness in both PCR and qPCR assays by testing specificity and detection limit. An annealing temperature gradient from 49°C to 61°C was run for set 15 and then three annealing temperatures of 57°C, 58°C and 59°C was tested in PCR to find the optimal T_m. The optimal T_m 59°C was used for a detection limit test later for this set.

The qPCR assays for primer sets 11 to 15 (Table 2.6) were run on the CFX96 Touch Real-Time PCR Detection System (Bio-Rad Technologies, Hercules, CA) in a total reaction volume of 20µl, which contained 1X of Luna Master Mix (NEB, Ipswich, MA), 0.25µM of forward and reverse primers, 5ng to 10 ng of template DNA and sterilized Milli Q water to make up 20 µl. A T_m gradient of from 54°C to 62°C was run first to determine the optimal T_m that produced C_q

values that were the lowest and most consistent between three replications using the plasmids containing *T. minima* DNA as the template (BBHF1A or WL2A samples) and a non-template control (NTC) using sterilized MilliQ water. The qPCR running conditions were 95 °C for 1 minute, 95 °C for 15 seconds and an T_m gradient from 54°C to 65°C for 30 seconds then 72 °C for 1 minute in 30 cycles, a final 72 °C for 10 minutes. Melting temperature curve analysis was also applied by heating the samples to 95 °C, and then at 65 °C for 1 min to assess whether the assay produced only *T. minima* products. The optimal annealing temperature at 61°C was used in the specificity and sensitivity tests afterward. A 10-fold dilution series of plasmid from 2.45x10⁷ to 2.45x10¹ DNA copies/μl was used to check for the detection limit as well as generating the standard curve to calculate the efficiency and check for the reproducibility of the assay. The first standard concentration was later reduced to 2.45x10⁶ DNA copies/μl to conserve the assay reagents. Some of the non-target species listed in Table 2.2 were also run to test the specificity of the assay towards *T. minima*. The assay was run in triplicate including non-template controls using Milli Q water.

2.2.7 LAMP and qLAMP assays development

LAMP assays were initially run for four LAMP primers (TM7F3, TM7B3, TM7FIP and TM7BIP) and loop primers (TM7LB and TM7LF) to check for specificity and detection limits. A T_m test of a low 2.45x10⁴ and a high 2.45x10⁹ number of plasmid copies was performed under three isothermal annealing temperatures of 54°C, 55°C and 56°C. The LAMP assay was first run based on recommendations of the *Bst* DNA polymerase large fragment (NEB, Ipswich, MA) manufacturer's protocol for 25 μl. The initial components of each LAMP reaction included 0.2μM of each TM7F3 and TM7B3 primers, 1.6 μM of each TM7FIP and TM7BIP primers, 0.8 μM of each TM7LB and TM7LF primers, 0.8 μM of Betaine (Fisher Scientific, Hampton, NH), 1X of

ThermoPol reaction buffer (NEB, Ipswich, MA), 6mM of Mg₂SO₄, and 1.4 mM of dNTP (Promega, Madison, WI). The reaction started with heating at 95 °C on a heat block for 5 minutes before *Bst* DNA polymerase was added, then chilled on ice for 5 minutes before 1-hour incubation period at the T_m (54°C, 55°C or 56°C) and then 80 °C for 10 minutes for reaction termination. The reactions were done using a Bio-Rad C100 Touch thermocycler (Bio-Rad Technologies, Hercules, CA). The resulting products were run by electrophoresis on a 1.2% agarose gel to see which T_m couldn't amplify both the high and low copies of plasmid DNA and produce the expected ladder-like pattern of amplified products on the gel. The T_m that amplified both concentrations of plasmid in the LAMP reaction was chosen for testing of different LAMP components.

LAMP assay components were optimized without the loop primers first. The first assay component tested was the inner and outer primers (TM7FIP: TM7BIP to TM7F3: TM7B3) concentration ratio of 2:1 (0.4µM:0.2µM), 4:1(0.8µM:0.2µM), 6:1(1.2µM:0.2µM) and 8:1(1.6µM:0.2µM) in 25µl. Each reaction was done in duplicate. Other components tested were the different *Bst* DNA polymerase concentrations of 2U, 4U, 6U and 8U and dTNP concentrations of 0.5mM, 1mM, 1.2mM, and 1.4mM. The concentration of Mg₂SO₄ were also tested with 2mM, 4mM, 6mM and 8mM. These tests were done using a positive control of *T. minima* DNA plasmid, a non-target sample (*P. goeppertianum* (WB2) or *V. heterodoxa* (VMC7F)) and a NTC. Results of the LAMP assay were visualized by electrophoresis in an agarose gel as described above, or adding 1.25 µl of 3mM Hydroxynaphthol Blue (HNB) dye (Acros Organics) to obtain the final concentration of 150µM in each LAMP reaction as recommended by previous LAMP studies (Goto et al., 2009; Duan et al., 2014; Liu et al., 2015). HNB is a colorimetric indicator that reacts with the change in Mg²⁺ ion concentration during the reaction and turns the color of the positive samples from violet (negative) to sky blue (positive) (Goto et al., 2009).

The quantitative LAMP (qLAMP) assay was done using similar components of the optimized LAMP assay but with an addition of 1X Eva Green DNA fluorescent intercalating dye (Biotium LLC, Fremont, CA) instead of HNB. The qLAMP assay was also run on a CFX96 Touch Real-Time PCR Detection System (Bio-Rad Technologies, Hercules, CA) in a similar manner to qPCR. A T_m gradient was run from 53°C to 60°C to determine the optimal assay T_m. The test was run three times with three replicates each. The conditions of the qLAMP reactions were also 95 °C for 5 minutes on heat block before adding *Bst* DNA polymerase and Eva Green dye, followed by 50 cycles of T_m (temperature gradient from 53°C to 60°C) for 15 seconds and 45 seconds to make up 50 minutes and then 80 °C for 10 minutes. The 50 cycles were added so the C_q values would be generated although the T_m did not change for 50 minutes. A melting temperature curve analysis at 60 °C to 95 °C was also run after the last step. The specificity test of the optimized LAMP assay was done for other non-target species including *Phomopsis* sp., *Pestalotia* sp., *Gloeosporium* sp., along with two samples each of *V. heterodoxa* and *M. vaccinii-corymbosi*.

2.3 Results

2.3.1 Collection of DNA of *T. minima* and other species

The collection of *T. minima* spores using the mini vacuum was tedious and took more than 2 hours to collect from one location with approximately 100 grams of leaves. The spore vacuum was unable to stop collection of other particles and leaf material from being sucked up along with the spores. Extraction of the spore suspension using the DNA kits mentioned in section 2.2.1 with the bead beating method or liquid nitrogen resulted in a very low concentration of DNA (less than 10ng/ µl). The 260/280 ratio obtained from Nanodrop analysis of these samples indicated that they were mostly low in purity and not within the range of 1.8 to 2.1 which indicates “pure” DNA (Desjardins, and Conklin, 2010). DNA from seven non-target fungal species was collected with

six species of fungal pathogens of blueberries and *Coleosporium* sp., which is a rust of goldenrod (Table 2.2). The DNA concentration from the extraction of non-target species grown in lab such as *V. heterodoxa* and *M. vaccinii-corymbosi* were generally much higher than the *T. minima* and showed higher purity of DNA. *Puccinia goeppertianum* and *Coleosporium* sp., on the other hand, although having higher DNA concentrations, had lower purity compared to *V. heterodoxa* and *M. vaccinii-corymbosi* since they were from environmental samples.

2.3.2 PCR and gel electrophoresis for *T. minima* DNA

The universal ITS fungal primers amplified DNA and showed one to multiple bands from *T. minima* samples (Figure 2.3). *T. minima* DNA presence was confirmed through sequencing of the single strong PCR products and BLAST comparison to *T. minima* in GenBank. *Thekopsora minima* was found at all three field locations: BBHF in Jonesboro, Spring Pond and Airport in Deblois, Maine (Table 2.1).

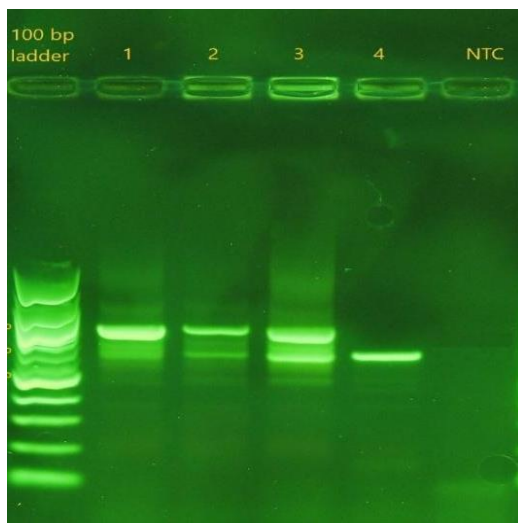


Figure 2.3 Gel electrophoresis of PCR products from three field samples. Spring Pond field, Deblois, ME (SP9.22.16_1A (1), SP9.22.16_2A (2), SP9.22.16_3A (3)) and one from BBHF, Jonesboro, ME BBHF9.24.15 (4) and a non-template control (NTC) using the ITS universal

primers. Bands of around 700 bp and 900 bp were cut out and cleaned up for sequencing. The 100 bp ladder used is from 100 bp to 1517 bp.

2.3.3 Plasmid cloning and estimation of DNA copies

Multiple PCR products were cloned from amplifications of two DNA samples from Wesley field (1A and 1B) and two from the BBHF location (2A and 2B) which had amplification of two to three bands of similar size range (Figure 2.4). Extraction of plasmid DNA using the method from Sambrook et al. (1989) resulted in very high amount of DNA (around 1000 to 7000 ng/ μ l). However, attempts to purify the 16 plasmid samples after extraction for sequencing using the alkaline-lysis method afterwards resulted in a very low concentration of plasmid (less than 5 ng/ μ l) even though the starting plasmid DNA concentration was very high. Plasmids were re-grown and purified in four more attempts, but the resulting concentrations were still very low. Due to time constraints, the number of plasmids used for extraction and purification were reduced to six samples instead of sixteen. Samples chosen had the highest DNA copies from the extraction step.

Plasmid DNA extraction and purification using the Promega kit had much higher concentrations of purified plasmid (from 26 to 183.3 ng/ μ l). There were six purified samples that were sent for sequencing and resulted in a total of three plasmid samples confirmed with *T. minima* presence, which were BBHF1A, WL2A and WL2B (Table 2.4). There was one sample without a result, one was confirmed as *Valdensia heterodoxa* and one was an unknown fungus.

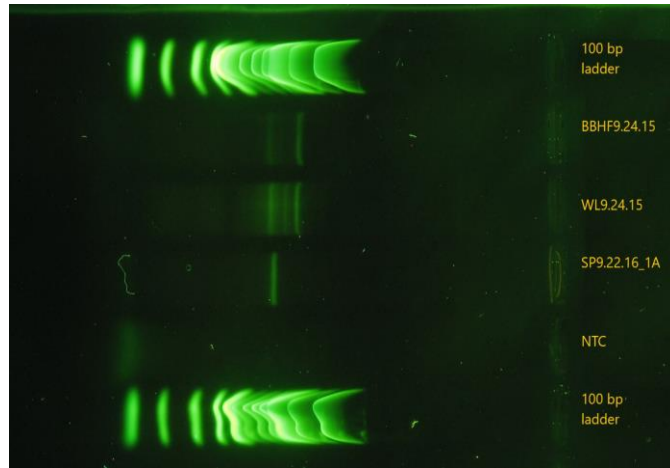


Figure 2.4 Gel electrophoresis of samples that were used for plasmid cloning. Samples BBHF9.24.15 from BBHF, Jonesboro and WL9.24.15, Wesley, ME were in the top two lanes. Sample SP9.22.16_1A with confirmed *T. minima* DNA was used as a positive control and sterile Milli Q water as a non-template control (NTC). The 100 bp ladder used is from 100 bp to 1517 bp.

Table 2.4 Plasmid extraction samples from two locations BBHF and Wesley. There were three plasmid samples BBHF1A, WL2A and WL2B that were confirmed as *T. minima* by sequencing and comparing with GenBank sequences.

Field site and Collection date	Sample Code Name	Sequencing Result	Query Cover (%)	Identity (%)	E value	GenBank Accession number
BBHF 9.24.15	BBHF1A	<i>T. minima</i>	61%	99.57%	0.0	MH029898.1
Wesley 9/24/2015	WL2A	<i>T. minima</i>	60%	99.57%	0.0	MH029898.1
Wesley 9/24/2015	WL2B	<i>T. minima</i>	57%	98.61%	3e ⁻¹⁷⁸	KX813713.1
Wesley 9/24/2015	WL2C	<i>Valdensia heterodoxa</i>	72%	100.00%	0.0	KU306729.1
Wesley 9/24/2015	WL2D	Unknown fungus	87%	94.93%	1xe ⁻¹⁶²	KP889805.1

2.3.4 PCR and qPCR assays development

There was a total of nine *T. minima* DNA sequences, three from ITS 1 region and five from ITS2 region, which were selected as candidates for possible primers (Table 2.5). These primers were combined with each other and with ITS1F and ITS4B for development of a species-specific assay for *T. minima*. Preliminary testing of 11 primer sets (Table 2.6) resulted in six sets (2, 5, 6, 8 9, and 10) that could amplify both *T. minima* samples BBHF10.8.15 and BBHF10.15.15. The estimated length of the DNA amplicons was from about 500 bp to 700bp (Figure 2.5 and 2.6). The primer sets 1, 3, 4, 7 and 11 did not amplify both *T. minima* samples and were eliminated from

further testing. Four more primer sets were chosen with one set from ITS 1 (set 12) and three from ITS2 region (set 13, 14 and 15) (Table 2.6). These primer sets were chosen from either ITS1 or ITS 2 regions to shorten the resulting amplicon length to 100 to 250 bp for them to be applicable for qPCR assays as well.

Table 2.5: PCR primer sequences list. Potential PCR primers from ITS 1 and ITS 2 regions of *T. minima* and two known Basidiomycota ITS primers from (Gardes et al., 1993)

Primer name	Location	Sequence (Forward)	Reverse Complimented Sequence (Reverse)	GC (%)	Length (Bp)	Tm (°C)
TMITS1A	ITS1	5'-CTTATTGGAGTGCACITTTATTGTGACTC-3'	5'-GAGTCACAATAAAGTGCACAATAAG-3'	39	28	57
TMITS1B	ITS1	5'-GTCCTTGTGTGCTCTAACGAGTATAGCA -3'	5'-TGCTATACTCGTTAGAGCACACAAGAC-3'	44	27	58.2
TMITS1C	ITS1	5'-GGAGTGCACITTTATTGTGACT-3'	5'-AGTCACAATAAAGTGCACCTCC-3'	43	21	50.5
TMITS2A	ITS2	5'-GGAGTTGGTGATGGATGTTG-3'	5'-TCA ACA TCC ATC ACC AAC TCCT-3'	50	22	51.8
TMITS2B	ITS2	5'-GTGATGGATGTTGAGTGTGCCG-3'	5'-CGGCAACACTCAACATCCATCACC-3'	50	24	59.1
TMITS2C	ITS2	5'-GAGGAAACCATATAAGAGTGG-3'	5'-CCA CTC TTA TAT GGT TTC CTC-3'	43	21	50.5
TMITS2E	ITS2	5'-TATTCATCAAGGAGTGTGGTGGG-3'	5'-CCCACCACACTCCTTGATGAATA-3'	48	21	55.3
TMITS2F	ITS2	5'-GAAACCCCTCATATAATTC -3'	5'-GAATTATGATGAGAG GGT TTC-3'	35	20	56.3
TMITS2G	ITS2	5'-CAAGGAGTGTGGTGGGTTTAC -3'	5'-GTA AAC CCC ACC ACA CTC CTT G-3'	54.5	22	65
ITS1F (Gardes et al., 1993)	ITS 1	5'-CTTGGTCATTTAGAGGAAAGTAA-3'		36.4	22	49.7
ITS4B (Gardes et al., 1993)	ITS 2	5'-CAGGAGCTTGTACACGGTCCAG-3'		56	25	60.3

Table 2.6 List of 15 primer sets that were tested in PCR and qPCR assays development.

Only sets 12 to 15 were tested under qPCR conditions.

Primer set number	Forward primer	Reverse primer	Initial Tm(°C)	Optimal Tm (°C) and [MgCl ₂] (mM)	Amplicon size (bp)	Specificity Results	Detection Limit Results	Additional tests
1	TMITS1A	TMITS2B	51.3	ND	454	NA	ND	ND
2	TMITS1B	TMITS2B	51.3°C	ND	369	Nonspecific	ND	MgCl ₂ concentration of 0.5, 0.6 and 0.9 mM
3	TMITS1A	TMITS2A	45.6	ND	444	NA	ND	ND
4	TMITS1B	TMITS2A	45.6	ND	375	NA	ND	ND
5	TMITS1A	ITS4B	55 °C	ND	~700	Nonspecific	ND	ND
6	TMITS1B	ITS4B	58 °C	ND	~700	Nonspecific	ND	ND
7	TMITS1C	TMITS2C	52.8°C	ND	445	Nonspecific	ND	ND
8	TMITS1A	TMITS2C	56.6°C	56 °C, 0.8mM	511	Specific to <i>T. minima</i> in PCR	Up to 2.45x10 ³ DNA copies	MgCl ₂ concentration of 0.5,0.8 & 0.9mM
9	TMITS1B	TMITS2C	56.6°C	ND	433	NA	ND	ND
10	TMITS1C	TMITS2B	56 °C	56 °C, 0.8mM	482	Specific to <i>T. minima</i> in PCR	Up to 2.45x10 ⁴ DNA copies	MgCl ₂ concentration of 0.8 and 0.9 mM
11	TMITS1C	ITS4B	52.8°C	ND	~700	NA	ND	ND
12	TMITS1A	TMITS1BR	57 °C	56 °C	119	Specific to <i>T. minima</i> PCR not in qPCR	2.45x10 ⁵ in PCR 2.45x10 ⁰ in qPCR	ND
13	TMITS2A	TMITS2CR	57 °C	57 °C	134	Specific to <i>T. minima</i> in PCR not in qPCR	2.45x10 ⁴ in PCR; 2.45x10 ⁰ in qPCR	ND
14	TMITS2B	TMITS2ER	62 °C	62 °C	128	Specific to <i>T. minima</i> in PCR not in qPCR	2.45x10 ⁴ in PCR; 2.45x10 ⁰ in qPCR	ND
15	TMITS2F	TMITS2GR	59°C	59°C in PCR and 61 °C in qPCR	182	Specific to <i>T. minima</i> in qPCR	Up to 2.2x10 ⁰ copies in both PCR and qPCR	ND

(Note: NA means primer set did not amplify all *T. minima* samples, ND means test was not done for the primer set)

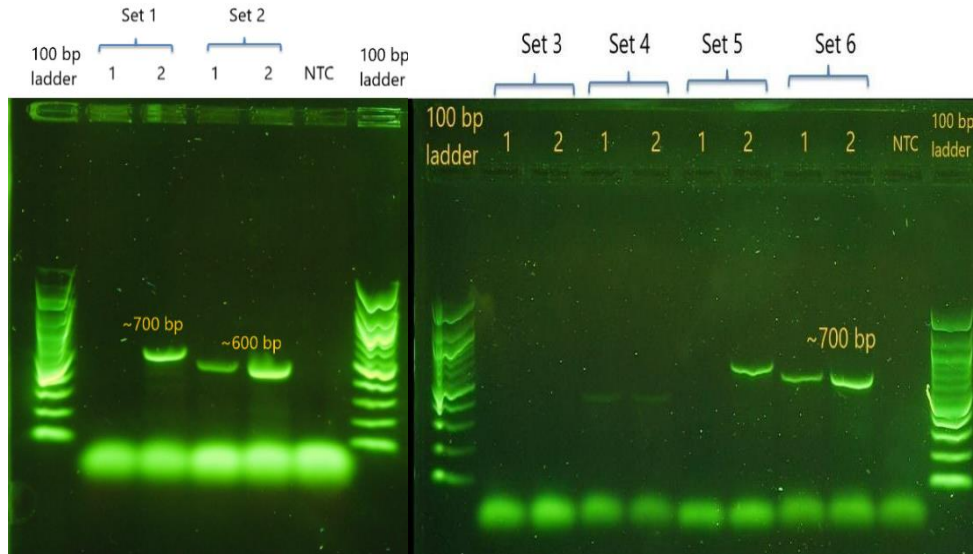


Figure 2.5 Gel electrophoresis of initial tests of six primer sets to amplify *T. minima*. DNA samples were BBHF 10.8.15 (1) and BBHF10.15.15(2). Set 2 (TMITS1B/TMITS2B) on the left gel and set 6 (TMITS1B/ ITS4B) on the right gel amplified both *T. minima* DNA samples. Sets 1, 3, 4 did not amplify both *T. minima* samples and were eliminated from further testing. Amplified bands showed up from 600-700 bp.

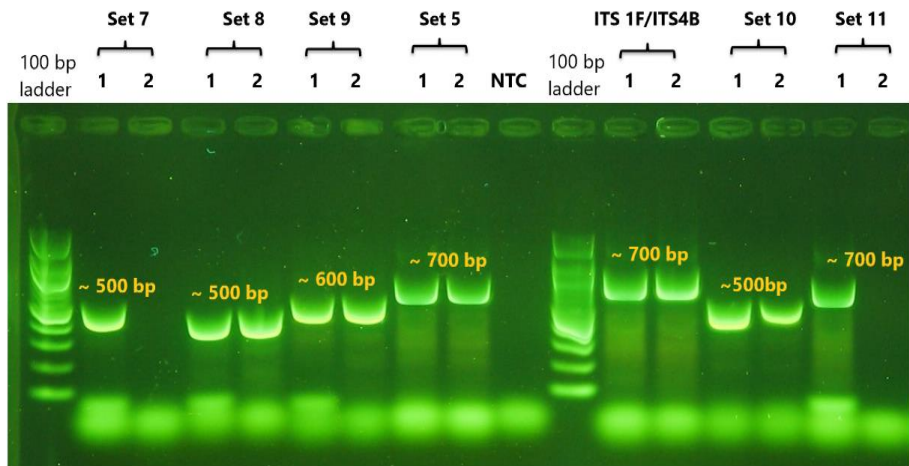


Figure 2.6 Gel electrophoresis of initial tests of primers ability to amplify two *T. minima* DNA samples. The samples were BBHF10.8.15 (1) and BBHF10.15.15(2). The Basidiomycetes primer set ITS1F and ITS4B (Gardes et al., 1993) was included for comparison. There were four primers sets (5, 8, 9, 10) that were able to amplify *T. minima* and two sets (7 and 11) that did not amplify

both samples. Amplified bands were from about 500 -700bp. The 100 bp ladder used is from 100 bp to 1517 bp.

Specificity tests of the primer sets 2, 5, 6, 8, 9 and 10 found sets 5, 6, 9 amplified non-target DNA and set 2, 8 and 10 were specific to *T. minima* (Table 2.6). Attempts to increase the specificity for primer sets 2, 8, and 10 was done by decreasing the concentration of MgCl₂. Set 2 showed specificity to *T. minima* at optimized PCR conditions with T_m at 52°C and MgCl₂ concentration of 0.5mM (Figure. 2.7). However, the assay was not reproducible and showed amplification of non-target species in later runs and no further tests were done for this set. Set 8 showed specificity to *T. minima* and had a detection limit at 2.45x10³ DNA copies at a PCR conditions with T_m at 52°C and MgCl₂ concentration of 0.5 mM (Figure. 2.8 and 2.9). Set 10 was also specific to *T. minima* with a detection limit at 2.45x10⁴ DNA copies under T_m at 56°C and MgCl₂ concentration of 0.8mM (Figure. 2.8 and 2.9).

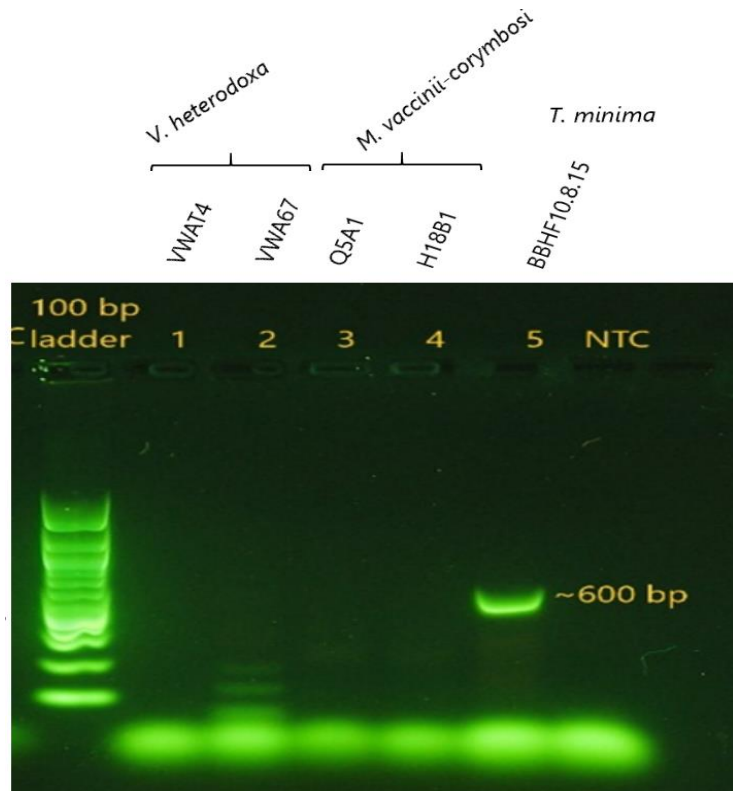


Figure 2.7 Specificity test results of primer set 2 (TMITS1B and TMITS2B). DNA amplification was seen only in the *T. minima* sample from BBHF (BBHF10.8.15) in lane 5 with a band around 600 bp. *Valdensia heterodoxa* samples (2, 3) and *M. vaccinii-corymbosi* samples (4, 5) did not amplify. The 100 bp ladder used is from 100 bp to 1517 bp.

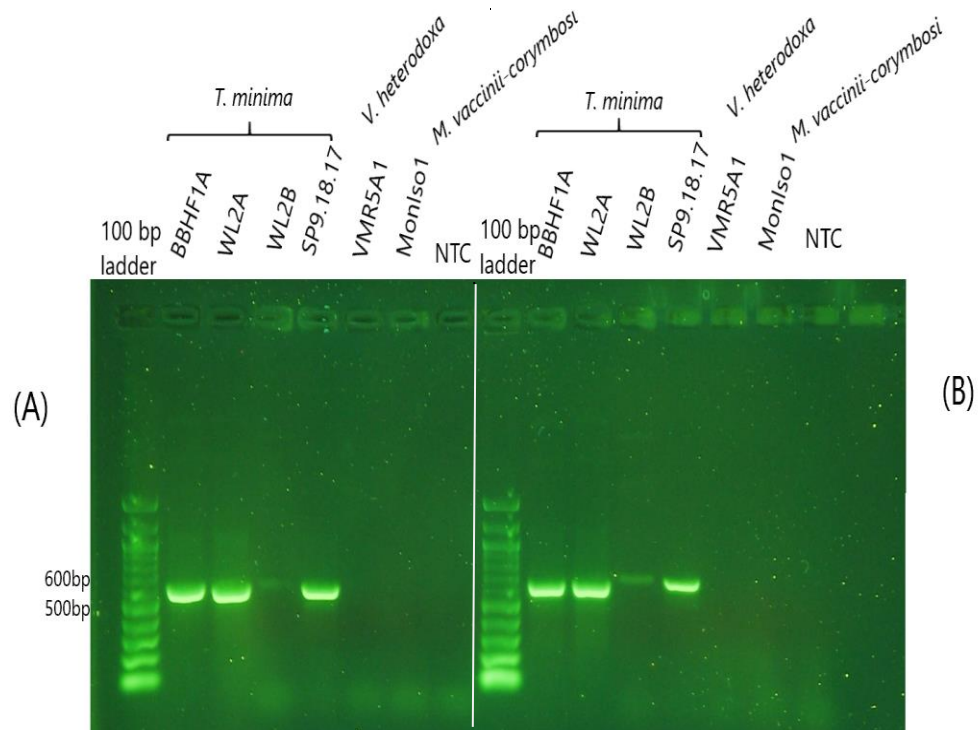


Figure 2.8 Results of PCR specificity test for primer set 8 and 10. Primer set 8 (TMITS1A & TMITS2C) (A) and 10 (TMITS1C & TMITS2B) (B). DNA bands at around 600 to 700 bp were amplified from four *T. minima* samples BBHF1A, WL2A, WL2B and SP9.18.17 (lane 1 to 4) but not with *Valdensia heretoroxa* (VMR5A1) and *M. vaccinii-corymbosi* (MonIso1) (Lane 5 and 6). The 100 bp ladder used is from 100 bp to 1517 bp.

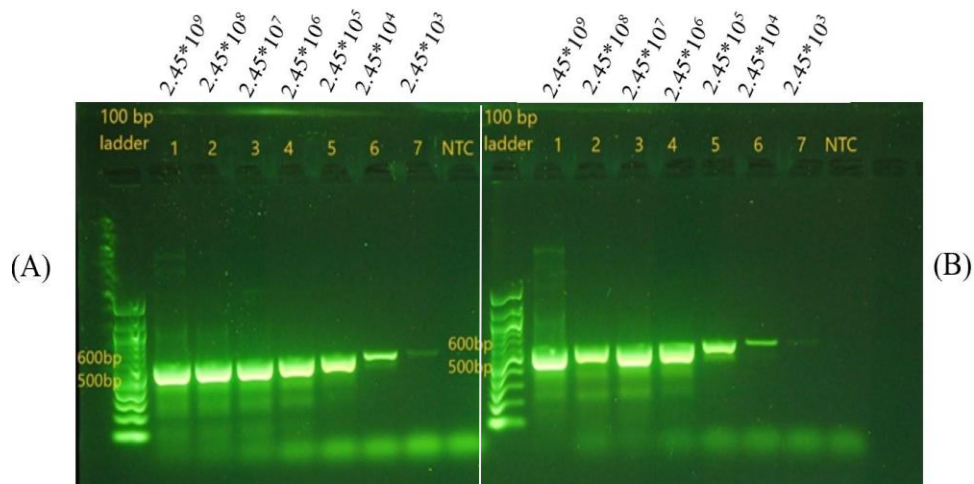


Figure 2.9 PCR detection limit tests for primer set 8 and 10. Set 8 (A) and 10 (B) showed amplification of sample BBHF1A down to 2.45×10^3 for set 8 and 2.45×10^4 copies for set 10.

The primer set 12 (TMITS1A and TMITS1BR) from the ITS 1 region was tested for specificity under the initial T_m of 56°C with *P. goeppertianum*, *Coleosporium* sp., *V. heterodoxa* and *M. vaccinii-corymbosi*. The assay showed no amplification for the non-target species (Figure 2.10). A detection limit test for primer set 12 found the amplification of the plasmid down to 2.45×10^5 copies (Figure 2.11). Primer set 12 was tested in a qPCR setting first by running a T_m gradient from 55°C to 63°C with *T. minima* samples BBHF1A and WL2A, and non-target DNA of *M. vaccinii-corymbosi* (MonIso2) and *V. heterodoxa* (VMR5A1). The primers amplified the plasmid samples and the non-target samples at a cycle threshold (Cq) larger than 32. Due to the nonspecific results of this primer set in the qPCR setting, no further testing was done for this set.

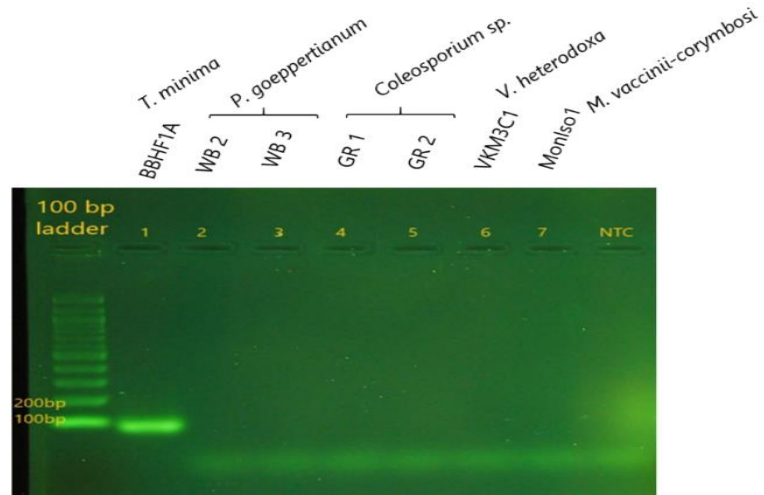


Figure 2.10 Specificity test of primer set 12. Set 12 (TMITS1A & TMITS1BR) showed amplification of the *T. minima* sample (BBHF1A) in lane 1 at around 100 bp. Non target DNA of *Pucciniastrum goeppertianum* (2,3), *Coleosporium sp.*(4,5) *V. heterodoxa* (6) and *M. vaccinii-corymbosi* (7) did not amplify.

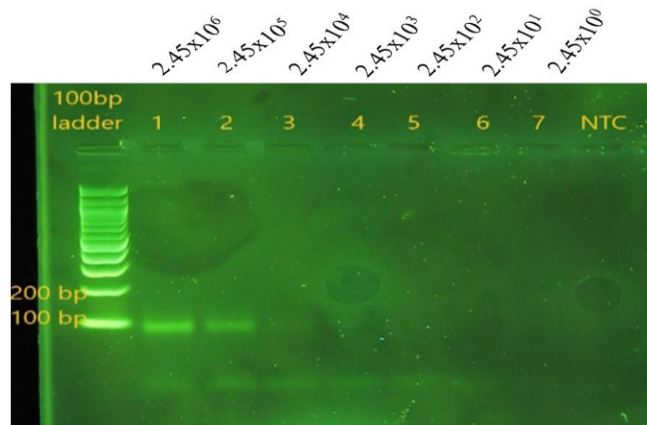


Figure 2.11 Detection limit test of PCR assay using primer set 12. Set 12 (TMITS1A and TMITS1BR) at T_m of 56°C showed amplification of BBHF1A at 2.45x10⁶ and 2.45x10⁵ DNA copies (lane 1 and 2). Bands of amplified DNA were at around 100 bp.

Two other primer sets (13 and 14) from the ITS2 region were tested with PCR for their specificity and detection limit at an annealing temperature of 57°C for set 13 and 62°C for set 14. The two primer sets were specific to *T. minima* DNA under PCR conditions (Figure 2.12 B and D). The detection limit of set 14 was 2.45×10^4 of *T. minima* DNA copies and set 13 could weakly detect down to 2.45×10^3 DNA copies (Figure 2.12 A and C). An annealing temperature gradient from 54°C to 62°C was used initially for the qPCR test of these two primers using one *T. minima* plasmid sample (BBHF1A) and a NTC. The T_m chosen for further testing of both set 13 and 14 was 62°C based on the reproducibility between the three replicates and lower C_q values. In qPCR specificity tests, both primer sets appeared to amplify non-target fungi at C_q about more than 28 cycles and showed multiple bands on gel electrophoresis in non-target samples (Figure 2.13). Therefore, both primers were excluded from further testing.

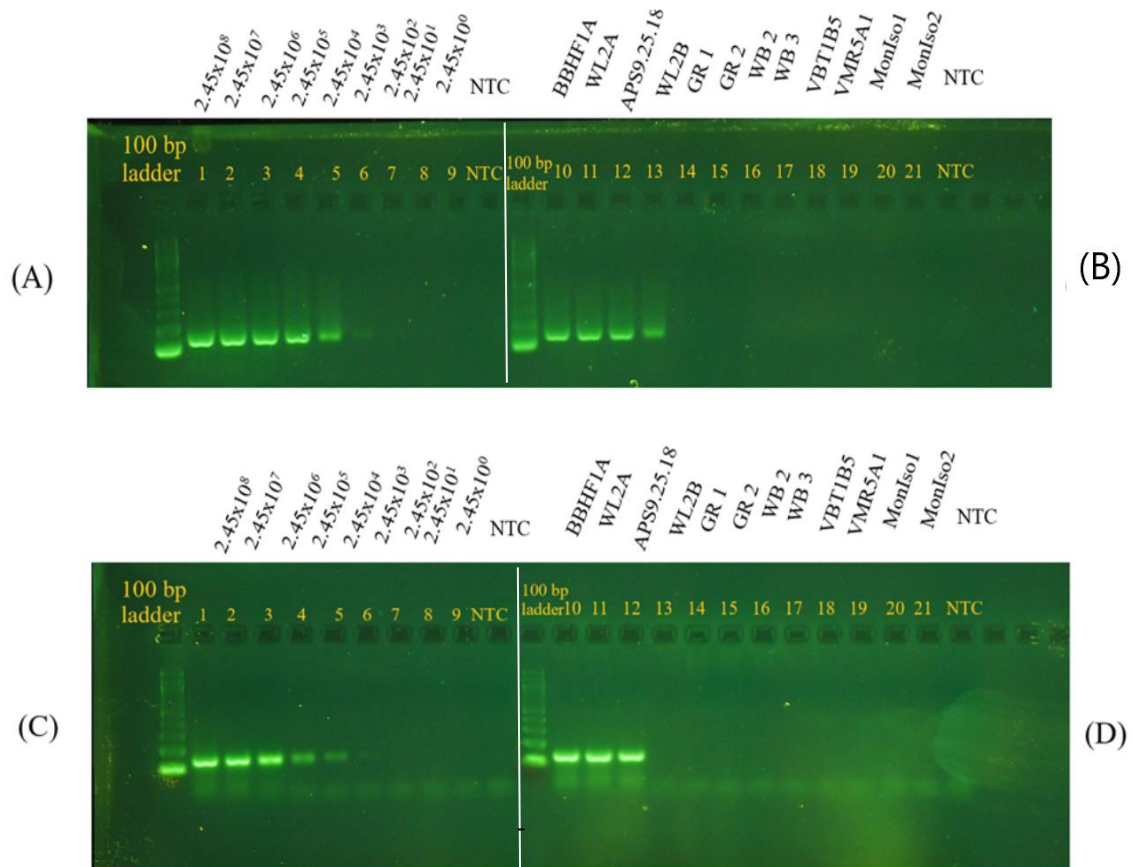


Figure 2.12 PCR detection limit and specificity results for primer set 13 and 14. Set 13 (TMITS2A and TMITS2ER) (Gel A and B) and set 14 (TMITS2B and TMITS2ER) (Gel C and D). Detection limit tests were run with 2.45×10^8 to 2.45×10^0 *T. minima* plasmid DNA copies (Gel A and C). Specificity tests (Gel B and D) were run with *T. minima* DNA (lanes 10, 11, 12, 13) and non-target DNA included *Coleosporium* sp. (lanes 14, 15), *P. goeppertianum* (16, 17), *V. heterodoxa* (18, 19), and *M. vaccinii-corymbosi* (20, 21). All amplified bands were around 100 to 200 bp.

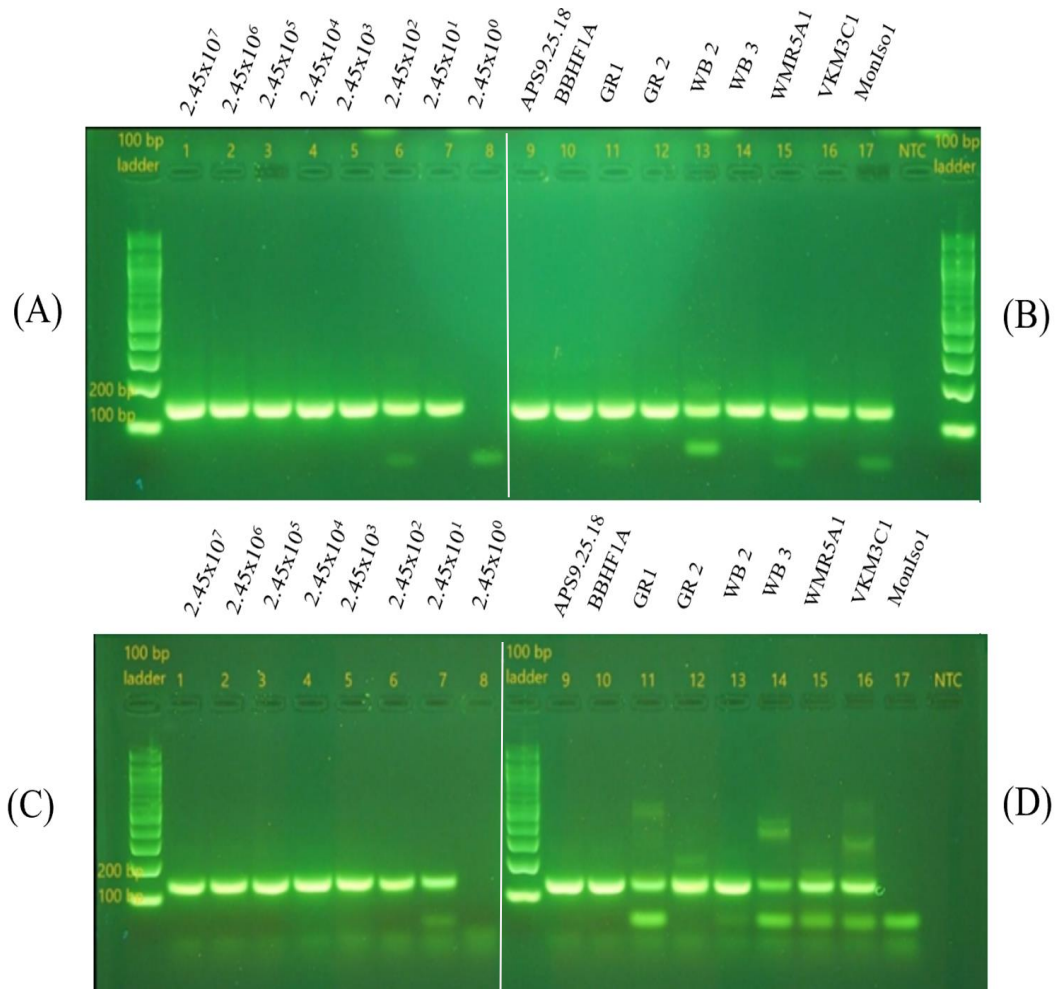


Figure 2.13 The gel electrophoresis of the qPCR detection limit and specificity tests for primer set 13 and 14. Detection limit (Gel A and C) and specificity (Gel B and D) results for primer set 13 (TMITS2A and TMITS2ER) (Gel A and B) and set 14 (TMITS2B and TMITS2ER) (Gel C and D). The primers could detect from 2.45×10^8 to 2.45×10^0 *T. minima* plasmid DNA copies (1 to 8). Specificity tests were run with *T. minima* DNA (9, 10) and non-target DNA included *Coleosporium* sp. (11,12), *P. goeppertianum* (13,14), *V. heterodoxa* (15,16), *M. vaccinii-corymbosi* (17). All amplified bands were around 100 to 200 bp.

The last primer set 15 (TMITS2F and TMITS2GR) was first tested for the optimal T_m using a gradient from 48°C to 61°C in a PCR setting. The resulting *T. minima* amplicon size of this set was about 182bp. The assay was run initially for two samples, a plasmid contains *T. minima* DNA (WL2A) and a NTC. At an annealing temperature from 56.1°C to 61°C, the assay could amplify the plasmid DNA and not the NTC and showed bands in between 100 bp and 200 bp (data not shown). Primer set 15 could detect as low as 2.45×10^0 *T. minima* DNA copies in the PCR assay (Figure. 2.14)

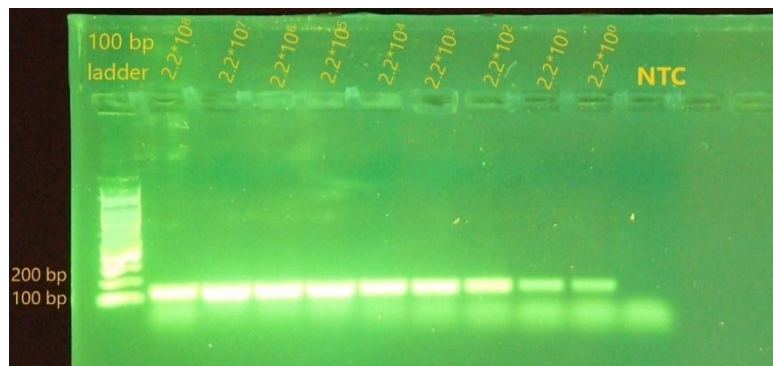


Figure 2.14 PCR detection limit test for primer set 15. Set 15 (TMITS 2F & TMITS2GR) showed amplification down to 2.2×10^0 copies of plasmid DNA sample (WL2A) at the T_m of 59°C.

Primer set 15 was shown to be specific to *T. minima* and did not amplify any other fungi besides *T. minima* and *P. goeppertianum* in the qPCR (Figure 2.15). The cycle threshold of *T. minima* was about 25 and *P. goeppertianum* sample was about 35 (Figure 2.15). To confirm whether the amplified product of *P. goeppertianum* was due to contamination with *T. minima* DNA, the qPCR products were run on a 1.2% gel and the amplicon of *P. goeppertianum* was cut out, purified and sent for sequencing (Figure 2.16). The sequencing result showed that the sample with *P.*

goeppertianum was indeed contaminated with *T. minima* DNA and therefore, this sample was excluded from further analysis.

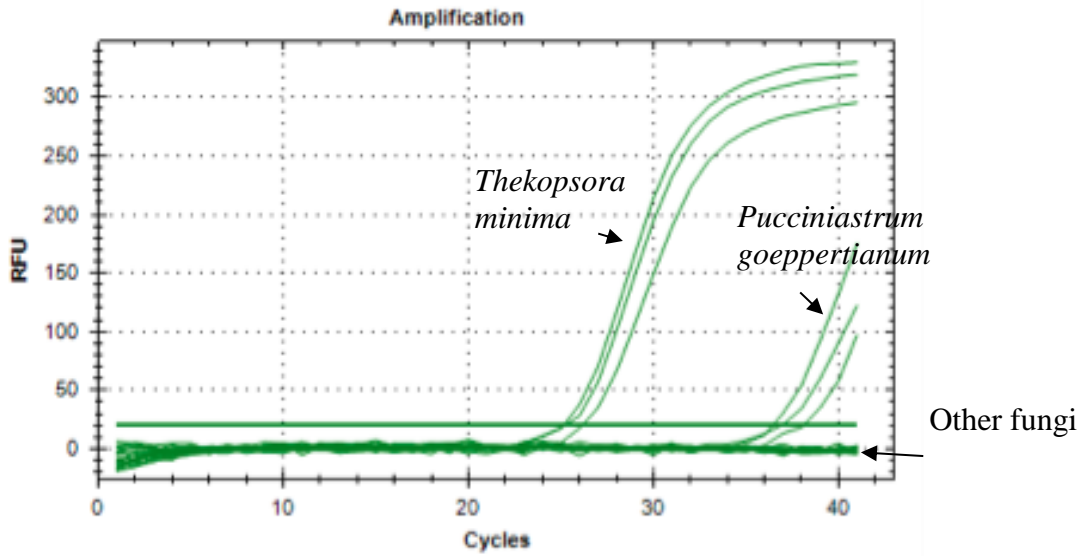


Figure 2.15 Amplification curve in qPCR assay specificity test using primer set 15. The diagram showed amplification of *T. minima* (AP9.25.18) at about 25 cycles and *P. goeppertianum* (WB3) samples at about 35 cycles. No other non-target species was amplified.

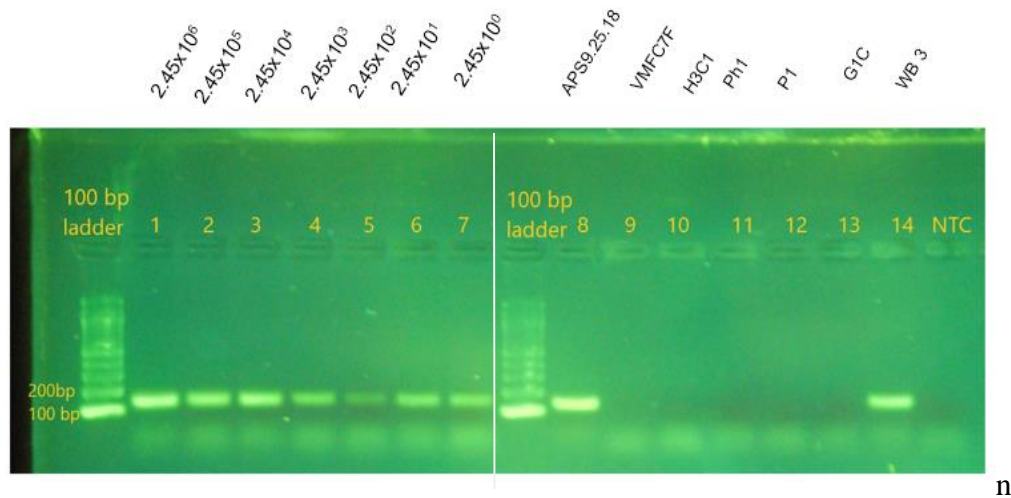


Figure 2.16 Gel electrophoresis of qPCR for detection limit and specificity tests using primer set 15. The detection limit (A) test included 2.45×10^6 to 2.45×10^0 *T. minima* DNA copies

(lanes 1 to 7). Specificity test (B) was run with *T. minima* DNA (8) and non-target DNA included *V. heterodoxa* (9), *M. vaccinii-corymbosi* (10), *Phomopsis* sp. (11), *Pestalotia* sp. (12), *Gleosporium* sp. (13), *P. goeppertianum* (14). All amplified bands were around 100 to 200 bp.

There was inconsistency in amplification of the lowest standard point (2.45×10^0 of *T. minima* DNA copies) across the three replicates in multiple qPCR reactions, which was assumed to be caused by pipetting error in these very low DNA copies number. This level of DNA dilution was excluded from data analysis and was not used for the later tests. Four replicates of the six 10-fold dilution series of plasmid containing *T. minima* DNA from about 2.45×10^6 to 2.45×10^1 DNA copies were used in each qPCR run to generate a standard curve to calculate the estimate quantity and efficiency of the assay. Any replicate that was more than two points higher in Cq value compared to the three other replicates was excluded from analysis with assumption that it was caused by pipetting errors. After excluding the outliers and non-amplified standards, the efficiency of the qPCR assay was 99.5% in the first run and 89.9% in the second run. In the first run, the lowest standard (2.45×10^1 *T. minima* DNA copies) was removed because two replicates did not amplify. The melting curve test showed only one peak at about 77°C for the samples in the first run (Figure 2.17B) and other minor peaks in the second run (Figure 2.18B) The correlation coefficient (R^2) value was 0.843 and the slope was -3.334 in the first run and in the second run, the R^2 was 0.96 and the slope was -3.591. Even though the efficiency was within the acceptable range of 0.90 to 0.110%, the correlation coefficient values were not close to 1 in the first run ($R^2 = 0.843$) due to the variation in amplification of some of the standards (Figure. 2.17A). Pipetting errors during preparation of the reactions was assumed to play the biggest part in the variation of data. Plasmid dilution improvement was attempted by briefly vortexing and then centrifuging the

microcentrifuge tubes contained the dilution before taking a sample to make the next dilution. Plasmid DNA that was thought to be degraded after many freeze thaw cycles was also tested on the Nanodrop to check the number of DNA copies/ μl again. The original purified plasmid copies of samples WL2A and BBHF1A concentration was reduced to 14.3 ng/ μl (3.51×10^9 DNA copies/ μl) and 14.2 ng/ μl (3.48×10^9 DNA copies/ μl), respectively, and the dilution series was recalculated using the new concentrations. After these improvement measures were taken, the standard curves were improved, the range of later standard curves were from 91.3% to 112.6% in efficiency with the best curve obtained had the efficiency of 100% with $R^2 = 0.94$ and the slope was -3.052, which were all within the acceptable range (Figure. 2.19A). Melting curves of all the standards in this run was shown to be of one peak around 77°C (Figure. 2.19B).

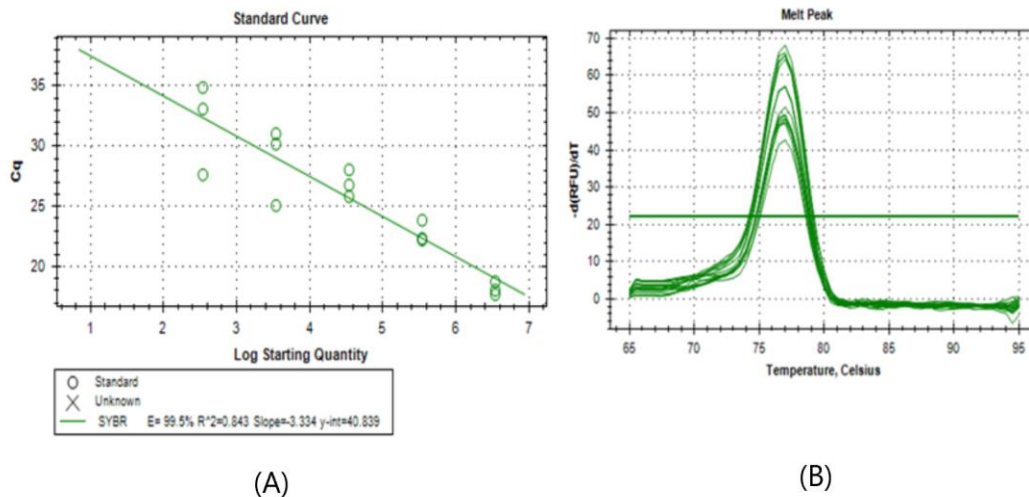


Figure 2.17 Standard curve and melting peak diagram from a qPCR test using primer set 15 in the first run. Standard curves generated from the log of starting DNA copies of *T. minima* (WL2A) and Cq values to assess the quality of the qPCR assay. Standard curve of the first run (A) and the associated melting curve (B).

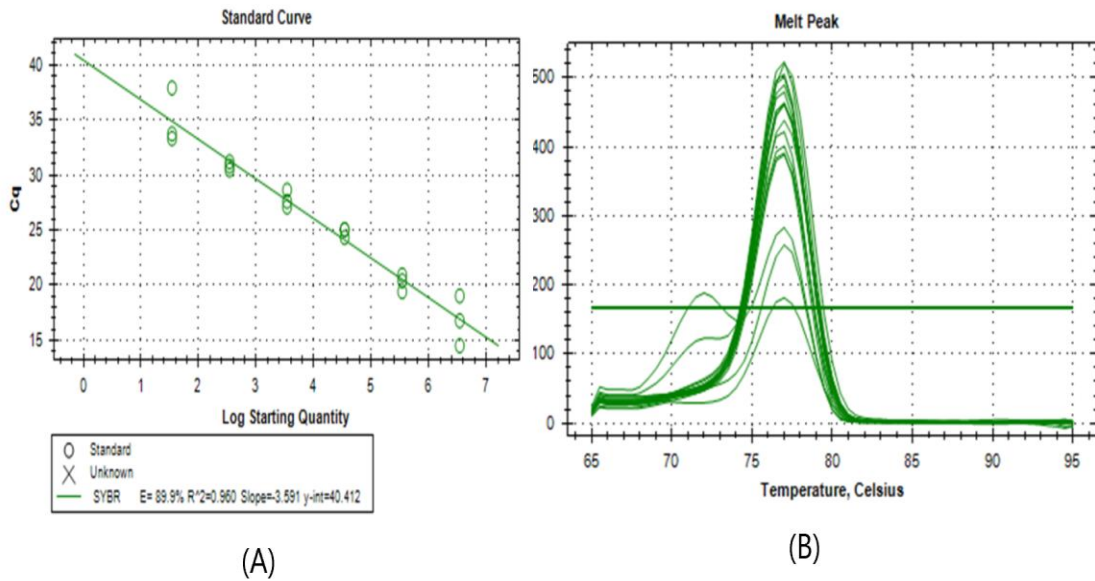


Figure 2.18 Standard curve and melting peak diagram from a qPCR test using primer set 15 in the second run. Standard curve (A) generated from dilution of plasmid copies of *T. minima* (WL2A) and the associated melting curve (B).

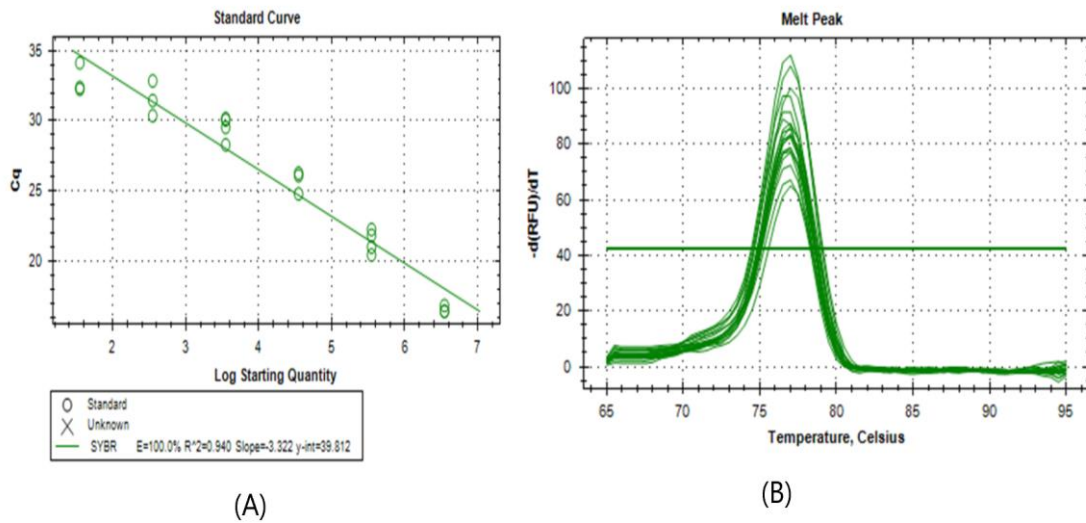


Figure 2.19 Standard curve and melting peak diagram from a qPCR test using primer set 15 in the third run. The standard curve (A) generated from the log of starting DNA copies and

Cq after improvement in dilution of *T. minima* plasmid (WL2A) from 3.48×10^6 to 3.48×10^1 copies. The associated melting curve is shown in B.

2.3.5 LAMP and qLAMP assays development

There were 19 LAMP primer sets generated from the available *T. minima* sequences but there was one set of LAMP primers that had both loop primers available (Table 2.3). The other LAMP primers did not have both loop primers (LB and LF) and were not tested. An initial test of three different T_m points (54°C , 55°C and 56°C) from the lowest T_m of one of the primers and up was conducted for the complete primer set (Table 2.3). The LAMP test used the lowest number of DNA copies the PCR assays could detect (2.45×10^4 copies) and the highest concentration of plasmid copies (2.45×10^9 copies) to see whether LAMP could also detect that range. The primer set amplified the lower concentration of BBHF1A sample at 55°C but not at the other two T_m points (Figure 2.20). The primer set had a $\Delta G = 1.89$ and showed a high specificity to *T. minima* when tested against *V. heterodoxa* and *M. vaccinii-corymbosi* (Figure 2.21). The detection limit ranged from 2.45×10^2 to 2.45×10^1 copies of DNA depended upon the run (Figure 2.22).

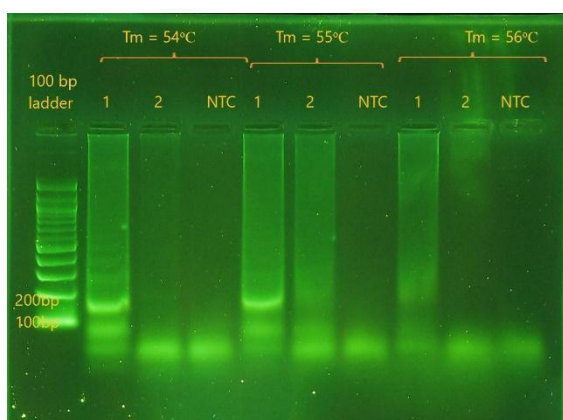


Figure 2.20 Gel electrophoresis of temperature tests for LAMP primer set. Test of three T_m points for LAMP assay using 2.45×10^9 copies (lane 1) and 2.45×10^4 copies (lane 2) of plasmid contains *T. minima* DNA (BBHF1A).

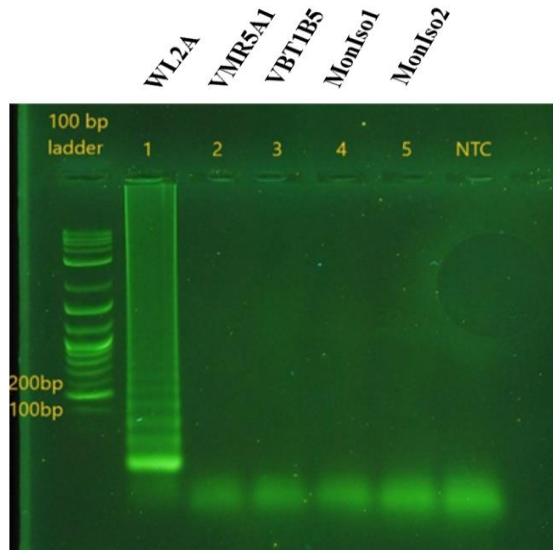


Figure 2.21 Gel electrophoresis of specificity for LAMP primer set. Specificity test for LAMP assay using plasmid containing *T. minima* (WL2A, 1) and non-target samples of *V. heterodoxa* (VMR5A1 in lane 2 and VBT1B5 in lane 3) and *M. vaccinii-corymbosi* (MonIso1 in lane 4 and MonIso2 in lane 5).

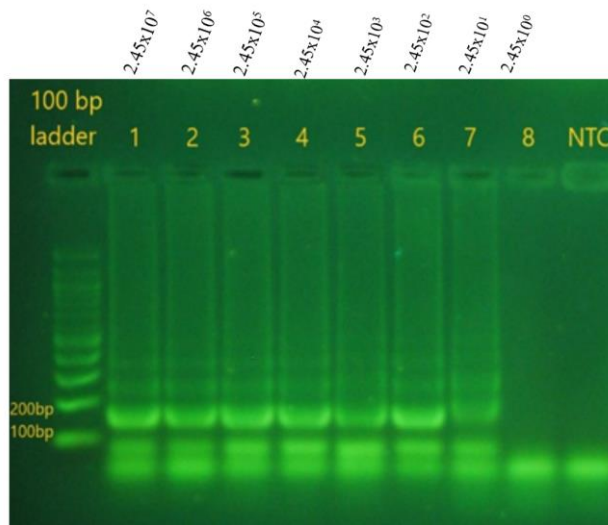


Figure 2.22 Gel electrophoresis of detection limit for LAMP primer set. Detection limit test of LAMP assay using plasmid *T. minima* DNA from 2.45×10^7 to 2.45×10^1 copies.

A test of different primer concentration ratios between F3/B3 and FIP/BIP found that the ratio of 4:1, 6:1 and 8:1 amplified both *T. minima* plasmid samples and did not amplify the non-target DNA samples. The concentrations of 8mM to 10mM of MgSO₄ was the optimal range for the LAMP assay. Tests of *Bst DNA* polymerase concentration, dNTP concentration and betaine usage were inconclusive due to non-reproducible results between runs. Therefore, concentrations of *Bst DNA* polymerase, dNTP and the use of betaine were kept the same as recommended by the manufacturer. Additional testing of the LAMP assay conditions included whether the initial heating at 95°C for 5 minutes of the reagents before adding *Bst DNA* Polymerase was a necessary step and the results concluded it was necessary and no amplification was obtained in reactions with *T. minima* without heating (Figure 2.23A). Detection of LAMP product using HNB dye resulted in positive samples turning to a dark blue color and negative samples remained purple (Figure 2.23 B). Although HNB dye was reported to work when added pre-amplification (Liu et al., 2015), attempts in adding HNB pre-amplification showed all samples with blue color and no other color change was observed post amplification. The reported turbidity of resulting LAMP products was not observed post amplification. The cloudiness of the tubes was observed after the reactions were heated to 95°C and before adding *Bst DNA* polymerase but not after the assay was run. A last specificity test for LAMP with DNA from other fungal pathogens of blueberry resulted in amplification of non-target samples (Figure 2.24) in all three replications.

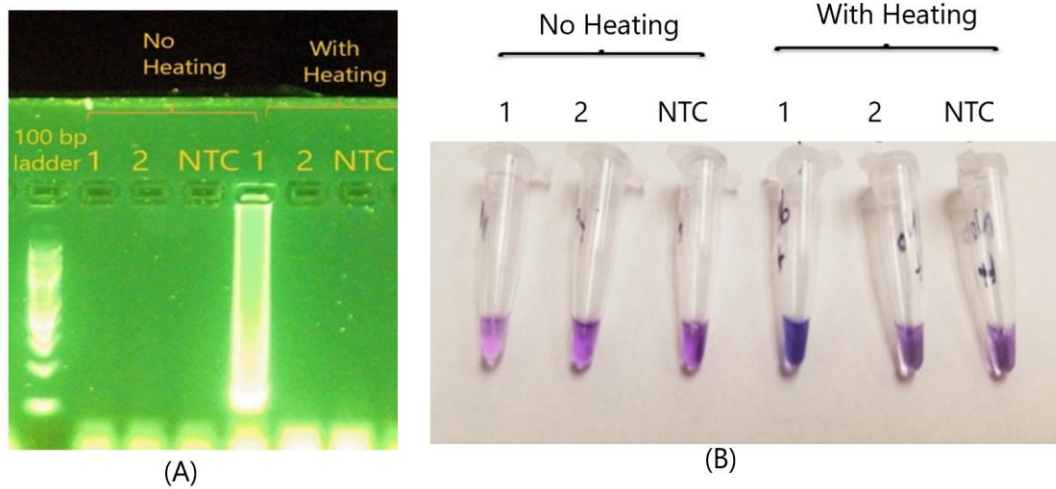


Figure 2.23 Gel electrophoresis of heating test and HNB dye using LAMP assay. Gel electrophoresis (A) and post amplification addition of HNB (B) to LAMP assay of tests of initial heating at 95°C (before adding *Bst* Polymerase) and without heating. *T. minima* DNA from sample APS9.25.19 (lane 1 and tube 1) and *V. heterodoxa* (lane 2 and tube 2) were used. The one tube with color change to blue (tube 4) was the positive sample APS9.25.19 and the other tubes remained purple.

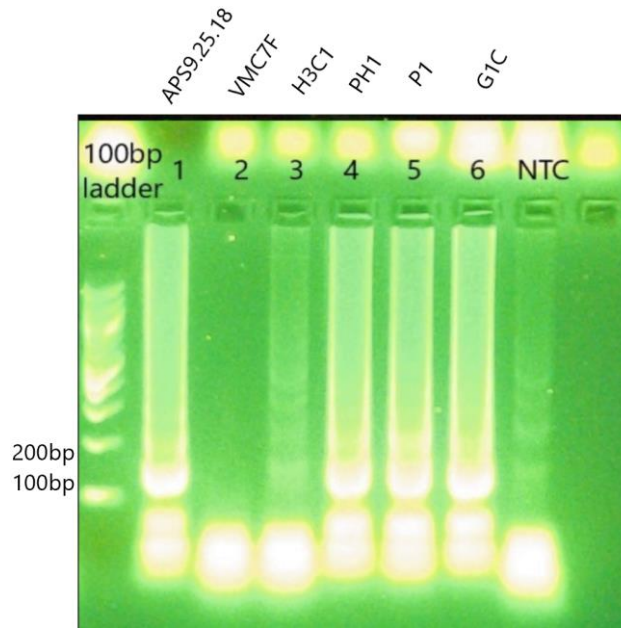


Figure 2.24 Gel electrophoresis of specificity test for LAMP primers. Specificity test of LAMP assay with *T. minima* DNA (1) and non-target DNA included *V. heterodoxa* (2), *M. vaccinii-corymbosi* (3), *Phomopsis* sp. (4), *Pestalotia* sp. (5), *Gleosporium* sp. (6).

The qLAMP assay was first run using similar components with the LAMP assay and a T_m gradient from 55°C to 62°C in triplicate reactions. Amplification of the samples were largely different in C_q values across the replicates. Due to inconclusive results of the T_m gradients in three different runs, the qLAMP assay was deemed to be unsuitable to use for quantification of DNA copies. Both LAMP and qLAMP assays were excluded from any further test.

2.4 Discussion and Conclusion

Development of molecular assays to detect and quantify inoculum of fungal pathogens has been shown to be more beneficial in improving the epidemiological understanding of a pathogen's dispersal and disease cycle compared to traditional microscopy counting of inoculum (Duvivier et al., 2016, Pashley et al., 2012). During the life cycle of *T. minima*, airborne spores such as urediniospores, aeciospores, and basidiospores play significant roles in the initial infection of the

two plant hosts, blueberry and hemlock. Germinated teliospores, the overwintering spores on blueberry, produce basidiospores to infect hemlock in early spring. Aeciospores produced from infected hemlock can infect blueberry initially and the asexual urediniospores that are produced on blueberries can re-infect more blueberries and spread the disease to other blueberries (Nickerson and Hildebrand, 2017). Urediniospores are the most important spore type for spreading of rust infection in blueberry because they are often more abundant due to their asexual reproduction and may cause more economic loss for the blueberry crop by infecting the plants throughout the growing season. Urediniospores are also thought to be the spores that cause blueberry leaf rust epidemics in warmer regions of the world due to their ability to persist on highbush blueberry and other native *Vaccinium* sp. over the mild winters (Babiker et al., 2018). In this study, I concentrated on detecting and quantifying urediniospores which are often conspicuous from summer to late fall during the growing season. Detection and quantification of *T. minima* was previously done by counting the number of visible urediniospores on spore trap tapes using a microscope, which was often quite laborious. Many species-specific molecular assays were developed for detection and quantification of many plant pathogens and other rusts in the past (Crouch and Szabo, 2011, Duvivier et al., 2016, Martin and Rygielwicz, 2005), but according to our knowledge, this study is currently the first in attempts to develop assays that are specific for detecting and quantifying DNA of *T. minima* in North America.

The molecular methods that were used for development of detection and quantification assays of *T. minima* in this project included PCR and LAMP based amplification assays. Attempts to develop LAMP and qLAMP assays were unsuccessful due to the non-reproducibility and non-specificity to *T. minima*. Many LAMP assays developed for plant fungal pathogens were reported to be more sensitive and specific compared to PCR (Hodgetts et al. 2015; Villari et al. 2017).

However, there are a few papers reporting on the lack of sensitivity in LAMP compared to PCR (Deguo et al., 2008) and to qPCR (Fukuta et al., 2013; Shen et al., 2016; Ravindran et al., 2012) due to the presence of possible inhibitors. Sensitivity of the LAMP assay in this study was lower than PCR and qPCR, which could detect as low as 2 copies (with primer set TMITS2F and TMITS2GR). The LAMP assay was able to detect down to about 200 to 20 copies of plasmid containing *T. minima* DNA. Specificity of the LAMP assay was found to be less than the PCR assay when tested with other fungal pathogens of blueberry besides *V. heterodoxa* and *M. vaccinii-corymbosi*. The LAMP assay often got contaminated and had amplification in the non-template control. Moreover, results of the LAMP assay could only be confirmed by observing the ladder-like pattern shown on gel electrophoresis. There are possibilities of confirming LAMP products through sequencing by purifying the gel bands or cloning the amplicons. However, in this study, confirmation of LAMP results was done simply by observing the ladder pattern appearing on agarose gels and by HNB dye indicator. HNB dye was not a very distinct indicator for LAMP products because of the difficulty in differentiating the color change between the positive and negative samples. In the future, other types of indicator dye for endpoint LAMP reactions such as Calcein or Berberine that show color changes under both visible light and fluoresce in ultraviolet (UV) light (Fischbach et al., 2015) could be explored. The unsuccessful results in attempts to develop qLAMP assay might be due to the incompatibility of reagents or unfavorable assay conditions. In future attempt in qLAMP assay development, it might be helpful to use a commercial master mix to avoid variation of reagents or using a turbidimeter to measure the change in turbidity of the resulting products. Nevertheless, the LAMP assay is still a potential cost-effective method for rapid detection of the fungus. In future studies, one might try to test other *T.*

minima LAMP assay conditions with new LAMP primers or try using fluorescent probes to enhance the specificity of the assay (Sun et al., 2015).

The PCR primer sets (set 8, 10, 12, 13, 14 and 15 in Table 2.6) developed in this project were specific to *T. minima* DNA when tested against other fungal pathogens of blueberries. The primers of set 8 and 10 amplified products spanning from both ITS1 and ITS2 regions and was specific to *T. minima*, therefore, they have potential to be used in a PCR assay, but they are too long for use in qPCR assay. The last four primer sets (12 to 15) can also be used in the PCR assays, but only set 15 can be used in qPCR assay. Due to the sensitivity of the qPCR assays, the amplification of non-target species that were not observed in PCR assay using primer sets 12, 13 and 14 appeared at more than 28 cycle thresholds in the qPCR ($C_q > 28$). The qPCR assays often have about 10 to 15 more amplification cycles compared to PCR assays which typically have 25 to 30 cycles. In qPCR assays, we used 40 cycles, which is within the recommended range of cycles (40 to 45) from the qPCR master mix manufacturer (NEB, Ipswich, MA). The assays possibly may have detected artifacts in the later amplification cycles above 30. The amplification of the correct size amplicon in the qPCR assay at around more than 28 cycles from the *Coleosporium* sp. DNA was assumed due to the possible contamination of *T. minima* DNA, since the plant samples were collected from Maine's blueberry fields in the fall when *T. minima* spores are also abundant. The *Coleosporium* sp. DNA sample was excluded afterward, but other non-target DNA also showed amplification at $C_q > 30$ in two of the primer sets, 13 and 14. Therefore, these primer sets were deemed to be nonspecific in the qPCR assay. The last primer set (TMITS2F and TMITS2GR) showed no amplification of non-target species except *P. goeppertianum*. The amplified products from the *P. goeppertianum* sample were confirmed as *T. minima* through sequencing, which might be due to cross contamination between the DNA samples or contamination of *T. minima* spores in the field.

Therefore, the primer set TMITS2F and TMITS2GR was shown to be the most specific to *T. minima*. The internal transcribed spacer regions where the primers were chosen from were confirmed to be useful for finding *T. minima* -specific primers as has been seen for other fungal pathogens mentioned above.

There were many factors that influence the success and reproducibility of a qPCR assay including the extracting techniques for nucleic acids, pipetting techniques, T_m , quality of the template DNA used as standard, and the reagents of the assay (Adams, 2006) The efficiency and correlation coefficient of qPCR assays tend to be affected the most by pipetting errors and degrading DNA templates. Many adjustments of pipetting techniques and sample handling during sample preparation were done to improve the assay's efficiency and reproducibility. Sample preparation was moved from a non-sterilized hood to the sterilized lateral hood, and the pipettes used for qPCR were autoclaved in between use to avoid contamination of plasmid DNA used as standards in this study. The efficiency was improved with these changes, and the range of at least two of three parameters (efficiency, R^2 , and slope) were within an acceptable range during the later runs. The sensitivities of the PCR assays were less than those of the qPCR assays which had a detection limit down to about 2 copies of *T. minima* DNA. At the DNA level of 2 to 10 copies, the results were not usually reproducible as has been found in a previous study (Duvivier et al., 2013). Therefore, 2×10^6 to 2×10^1 *T. minima* DNA copies were later used as the range of DNA templates for generation of standard curves to assess the assay's efficiency and estimate the starting DNA copy number from C_q values of the unknown samples in the next chapter.

In conclusion, the final developed PCR and qPCR assays in this chapter were highly specific to *T. minima*. Therefore, the qPCR was chosen as the real-time detection and quantification method for the rest of the project. The developed molecular assays are based on *T. minima* DNA; thus,

they are potentially helpful diagnostic tools to detect other blueberry *T. minima* spores produced in spring and late summers such as basidiospores and aeciospores.

CHAPTER 3: ASSESSMENT OF WEATHER FACTORS EFFECTS ON DISPERSAL PATTERN AND DISEASE SEVERITY OF *T. MINIMA*

3.1 Introduction

Airborne spores are common propagules for many fungal pathogens, such as *Thekopsora minima* causing blueberry leaf rust, to spread and infect their susceptible plant hosts. Integrating air sampling and molecular methods to identify and quantify spores is a useful way to study a pathogen's epidemiology and environmental factors that influence the disease cycle and spore production and dispersal. Many different air sampling devices have been developed including Hirst and Burkard (Burkard Manufacturing Co Ltd., Rickmansworth, UK) spore traps to collect fungal spores. Identification of fungal spores and other structures using microscopy is more time consuming and frequently requires expertise in a pathogen's morphology. Moreover, many pathogens cannot be cultured in artificial media which makes it difficult to identify and study them (Pashley et al., 2012). Therefore, the development of molecular methods for identification using amplification of nucleic acids such as qPCR assays is more efficient to assess the quantity of pathogen inoculum collected by the air sampling devices. The challenge of these methods is to figure out the relationship between the amount of inoculum detected using an air sampler and the actual inoculum exposed to plants that is causing disease and how to lessen the difference between them (West et al., 2008). This relationship might be affected by the location of where the spore trap devices are placed and the time gap between when the spore are in the atmosphere and when they are exposed to plants and causing disease. In addition, the limits of a qPCR assay include the inability to differentiate between living and dead inoculum, and the high cost of conducting the reactions which means they are not commonly available for in-field detection (West et al., 2008). There is an increasing number of less expensive options available for qPCR systems and even

portable devices for its field implementation such as the Mini8 Plus Real-Time PCR System (Mobitec, Göttingen, Germany) or MyGo Mini Real-Time PCR (Azura Genomics, Raynham, MA). However, it might take a few more years until these methods become as reliable and used as widely as the traditional lab-based methods. Air sampling methods with integration of molecular assays for identification and quantification are useful tools for the development of disease-warning or forecasting systems to help growers make economic decisions to control diseases (Agrios, 2004). Weather data are used in these systems to see if there are correlations between weather factors, the amount of inoculum produced and disease severity during the growing season (Duvivier et al., 2013).

The qualities of a successful disease warning system (DWS) include attributes such as reliability, simplicity, usefulness, availability, and cost-effectiveness (Campbell and Madden 1990). Proper validation of a DWS lies in the assessment of whether the predictions made using a system fall under two of these categories: false positives or falsely predict the presence of inoculum and false negative or predict no inoculum, but it is still present (Madden, 2006). These types of prediction could affect the growers economically if the DWS was not well-validated. There are three types of forecasting strategies available in agriculture (Agrios, 2004; Campbell and Madden 1990). The first type is based on measuring the initial inoculum of a fungal pathogen; an example of this is the forecasting system for Stewart's disease in corn caused by *Erwinia stewartii* (Steven, 1934). The second type is based on weather conditions to forecast the secondary inoculum of a fungal pathogen such as the late blight forecasting system for *Phytophthora infestans* based on temperature and relative humidity that was developed and managed by the USAblight project (USAblight.org). The last type is based on an assessment of the amount of both initial and secondary inoculum used especially for polycyclic diseases such as apple scab caused by *Venturia*

inaequalis (Washington et al., 2002). There are also forecasting systems developed to forecast multiple pathogens at a time, such as the EPPIRE project that was developed in 1983 in the Netherlands that forecasts stripe rust, leaf rust, mildew and cereal aphids for winter wheat (Reinink, 1986).

Weather factors included in epidemiological studies of plant pathogens for development of DWS usually are temperature and moisture in the forms of relative humidity, dew point, leaf wetness duration or rain (precipitation) (Gleason et al., 2008). Temperature fluctuations during the growing season might affect not only the amount of inoculum produced and disease severity but also the plant's level of resistance (Agrios, 2004). Moisture is also an important factor that affects the growth and infection rate of many plant pathogens include bacteria, nematodes and, in particular, oomycetes and fungi (Agrios, 2004). Relative humidity is an essential indicator of moisture level and was found to have a positive correlation, especially with the number of spores produced in spring or autumn in the fungal genera of *Didymella*, *Leptosphaeria*, and *Pleospora* (Oliveira et al., 2009). Dew point is another indicator of moisture with relation to temperature and it was found to be the major source of moisture for the upper canopy of soybean and potentially have an effect on growth of *Phakopsora pachyrhizi*, a soybean rust (Schmitz and Grant, 2009). Leaf wetness duration (LWD), or the time when water is present on the plant surface, was also found to contribute to the infection success of many fungal pathogens that cause foliar disease such as rust. The factors that influence LWD can be rain, fog, irrigation, dewfall or soil distillation (Monteith and Unsworth, 2008). For example, a minimum of LWD of 6 hours and temperature of 15, 20, and 25°C are requirements for infection of *Phakopsora euvitis*, a rust of grapevine and maximum infection was observed at LWD of 12 to 24 hours at 20 °C (Angelotti et al., 2014). LWD and temperature were often implemented into DWS in many crops such as the “Strawberry

Advisory System” for Botrytis fruit rot caused by *Botrytis cinerea* and Anthracnose caused by *Colletotrichum acutatum* in Florida, US (Cordova et al., 2017). The success of an LWD based model is often based on the accuracy of weather data and is often specific to one site (Sentelhas et al., 2005).

In the current wild blueberry disease integrated pest management (IPM) system, a disease forecasting strategy was developed in Nova Scotia and implemented in Maine for *Monilinia vaccinii-corymbosi* that causes mummy berry (Annis, 2009). Weather factors such as temperature and leaf wetness duration during rain or fog events are considered to predict the infection period of *Monilinia* ascospores (Annis, 2009). Several weather stations were placed in different wild blueberry barrens in Maine to collect weather data for forecasting the infection periods of mummy berry and other diseases. Besides *M. vaccinii-corymbosi*, there are many other fungal pathogens of blueberry with unpredictable dispersal patterns that could be monitored such as the leaf rust *T. minima* and *Erysiphe* sp. that causes powdery mildew, to control them more efficiently.

In this chapter, the main objective was using both manual spore counting and a real-time qPCR-based assay developed for *T. minima* in chapter 2 along with the weather data collected using weather stations to assess how weather factors affect the production of spores and disease severity of the blueberry rust. Environmental factors were collected using weather station devices with sensors to record temperature, humidity, leaf wetness, rainfall and the button loggers collected relative humidity and dew point during the growing season. Temperature was found to have a significant effect on the production and germination of uredinia in *T. minima*, and the optimal range for uredinia production was from 17.5°C to 22° F and urediniospores’ optimal range for germination was from 19°C to 23°C in highbush blueberries (Pfister et al., 2004). We expect a positive correlation between the temperature, humidity and leaf wetness period with the number

of urediniospores produced during the growing season based on the previous studies mentioned above. Understanding the correlation between weather factors, disease severity and dispersal patterns of spores can potentially aid in the development of prediction models for a disease warning system for a more precise application of control methods to manage *T. minima*.

3.2 Materials and methods

3.2.1 Spore collection using spore trap samplers:

Airborne spores of *T. minima* were collected using the Burkard 7 days volumetric spore traps (Burkard Manufacturing Co Ltd., Rickmansworth, UK and Burkard scientific, Uxbridge, UK) located in blueberry barrens in the downeast regions of Maine (Table 3.1). Data were used from the spore trap at Blueberry Hill Farm (BBHF) operating for four years from 2014 to 2017. There was one spore trap operating at a field in East Machias (EM), ME in 2015, and there was one spore trap operating in a Spring Pond (SP) field near Deblois, ME in 2017. Spore trap tapes were unavailable for 2016, and they were not included in the analysis. A clear Melinex tape (48mm x12mm) was wrapped around the rotating drum of the Burkard spore trap and then coated with petroleum jelly (Vaseline, company, city) thinned with hexane to collect spores over seven days. After seven days, the drum with tape was taken back to the lab, and the tape was cut into eight sections included six full days and two partial start and end days. Half of the tape of each section was mounted on a microscope slide to count spore under a compound microscope, and the other half was stored in a 1.5ml microcentrifuge tubes at -80°C for later spore extraction. For the analysis, the day of the beginning of each week when the spore tape was replaced was converted into corresponding Julian day in each year.

Table 3.1: Spore trap locations used and weather data collected.

Year	Location	Collection period	Weather data collection interval	Weather factors collected by weather stations
2014	BBHF, Jonesboro	8/5/14 -9/23/14	Every 30 min	Temperature (°F) Leaf Wetness
2015	BBHF, Jonesboro	6/21/15 -10/10/15	Every 30 min	Temperature (°F) Rain
2015	East Machias	6/21/15 – 10/10/15	Every 1 hour	Temperature (°F) Leaf Wetness
2017	BBHF, Jonesboro	8/7/17 – 10/15/17	Every 15 min	Temperature (°F) Rain
2017	Spring Pond, Deblois	8/7/17 – 10/15/17	Every 1 hour	Temperature (°F) Leaf Wetness

3.2.2. *Thekopsora minima* spore counting using microscopy

Blueberry rust urediniospores counting was done by Rachael Martin, research assistant, using a compound microscope (Figure 3.1). Each daily tape section was cut in half and mounted on a microscope slide with fixative (Norland Optical Adhesives No. 61) and marked as 24 equal divisions representing the time of the day. The other half was placed in 1.2 ml or 2 ml microcentrifuge tubes and stored for later spore DNA extraction. The rust urediniospores were counted for each hour of each day using a 0.025 cm x 250 cm grid across the whole hour. The total daily spore number counted was multiplied by the ratio of the total tape area to the counted area to get an estimate of all the spores on the tape. The calculated spore number per day was summed up per week, with the first day being the day when the weekly tape was replaced, and multiplied by two to account for spores on the whole tape.



Figure 3.1 Urediniospores (orange color) observed under 40X lens of the microscope. (Photo: Annis Lab)

3.2.3 DNA extraction of spore trap tapes

DNA extraction of spores on the spore trap tapes from three locations, BBHF, East Machias and Spring Pond in 2014, 2015 and 2017, was first done by disrupting the spores on the daily tape samples. An aliquot of 220 μ L of 0.1% IPEGAL CA-630 (Octylphenoxypolyethoxyethanol, Sigma-Aldrich, St. Louis, MO) a nonionic, non-denaturing detergent, and 0.2g of 0.5mm of Zirconia/Silica beads (BioSpec Products, Inc., Bartlesville, Oklahoma) was added to the 1.5 ml or 2 ml microcentrifuge tubes that contained the daily spore trap tapes. The tubes were shaken in a Mini Beadbeater-16 (BioSpec Products, Inc., Bartlesville, Oklahoma) for two periods of 40 seconds at 3450 oscillations/min with 5 minutes cooling in ice in-between these periods. Then, 220 μ L lysis buffer containing 50 mM Tris, 3% SDS, 50mM EDTA, 0.1% Beta-mercaptoethanol (Duvivier et al., 2013) was added and the tubes were centrifuged for 1 minute at 12,000 rpm to bring all the liquid to the bottom of the tubes. The tubes were incubated on a heat block for one hour at 65°C and stored at -20 °C before continuing the extraction.

The disrupted spore solution from each daily spore trap tape extraction was pooled together into a week sample, and DNA was extracted with a phenol-chloroform method. Each extraction

represented one week of spore tape that included 6 full days plus two partial days (eight samples in total) with the week starting on the day the tape was replaced in the field. The microcentrifuge tubes with individual day samples were centrifuged for 1 minute at 12,000 rpm, and the suspension from the 8 tubes was added together in one 12 ml polystyrene tube for DNA extraction. An equal volume of phenol: chloroform: isoamyl alcohol (25:24:1) was added to the tube and gently mixed until an emulsion was formed. The tubes were centrifuged for 1 minute at 12,000 rpm to separate into two phases: organic (top layer) and aqueous phase (bottom layer). The aqueous phase was transferred to a new polystyrene tube, and this step was repeated once. The aqueous phase was extracted with an equal volume of chloroform twice. The final aqueous solution was placed at -20°C until DNA was precipitated.

DNA in the aqueous solution was thawed before being precipitated using glycogen following the manufacturer's protocol (Thermo Fisher Scientific, Waltham, MA). One-tenth volume of 3M sodium acetate was added to the aqueous solution in the polystyrene tube. Glycogen was added to produce a final concentration of 0.05 µg/µL along with one equal volume of isopropanol. The solution was mixed by gently inverting and incubated at -80°C for 30 minutes. The solution was warmed back to room temperature for 5 to 10 minutes and centrifuged for 15 minutes at 10,000 rpm. The liquid was removed from the tubes, and the resulting pellet was rinsed with 500µL of 70% ethanol kept on ice and air dried in an upside-down position for about 5 to 10 minutes. Finally, the DNA was dissolved in 100µL of sterilized Milli Q water by slightly vortexing, and the DNA solution was transferred to a 1.5 ml microcentrifuge tube. The DNA was kept at -20°C until use.

3.2.4 Determining the detection threshold for qPCR assay

A spore suspension of *T. minima* spores (AP9.25.18), collected by the mini vacuum method from blueberry leaves from Airport field in 2018, was counted using a hemocytometer and adjusted

to a concentration of 200,000 spores/ml by adding a suitable amount of 0.05% Tween 20 solution. An aliquot of 200µl of this solution was added to two 1.2 ml microcentrifuge tubes as the starting solution for a 10-fold dilution series of spores from 4×10^4 to 4×10^0 spores in 200 µl. An aliquot of 100 µl of each dilution was added to a piece of 48 mm x12 mm Melinex tape that was previously spread with Vaseline and hexane. The spore numbers on the tapes ranged from approximately 2×10^4 to 2×10^0 spores. The tapes were dried for about 30 minutes in a fume hood and then placed in 2ml microcentrifuge tubes. The tapes were extracted using the phenol-chloroform method mentioned above and the DNA dissolved in 30µl sterilized Milli Q water. The resulting DNA was checked on a Nanodrop and run in a qPCR assay to obtain the estimate cycle threshold (Cq) values for each spore dilution. The qPCR assay was run two times with three replications for each dilution. The mean Cq values obtained from averaging the three reps from each of the two runs of the dilutions were plotted against the estimated spore number used to generate a linear equation to calculate the spore number based on the cycle threshold (Cq) values for the spore trap tapes. The extraction and quantification process of the spore dilution series was done twice. However, due to dilution errors of the first dilution series, only the data from second run was used to generate the linear equation.

3.2.5 Spore tape quantification using qPCR.

The DNA extracted from the spore tape weekly samples was diluted to 10 ng/µl with sterilized MilliQ water. The number of *T. minima* DNA copies in the spore tape samples were quantified using the qPCR assay developed from chapter 2 to obtain the cycle threshold of the starting DNA used. The reagents in the assay included 1X Luna Universal qPCR Master mix (NEB, Ipswich, MA), 0.25 µM of each primer (TMITS2F and TMITS2GR), 10 ng/µl of DNA and sterilized MilliQ water adding up to a total volume of 20 µl. The running conditions for qPCR included 95°C for 1

minute, and then 40 cycles of 95°C in 15 seconds and an annealing temperature of 61°C for 30 seconds and a final step of melting curve analysis from 65 °C to 95°C. In each qPCR assay, five of 10-fold diluted standards from about 2×10^6 to 2×10^1 DNA copies/ μl of plasmid DNA sample (WL2A or BBHF1A) were run to accurately quantify the cycle quantification threshold (Cq) and starting DNA copies as well as calculate the assay efficiency. The Cq value obtained from each spore tape sample using qPCR assay was converted into the starting number of *T. minima* urediniospores using the linear equation obtained from the detection threshold procedure mentioned above. The estimated total spore number per weekly sample was calculated based on the initial DNA concentration of each sample and then multiplied by two (because the tape was cut in half for microscopy count) using the equation below.

$$T = \left(\frac{(C \text{ ng}/\mu\text{l}) \times S}{10 \text{ ng}} \right) \times 100 \mu\text{l} \times 2$$

In this equation, T is the total spore number on a weekly tape, C is the original DNA concentration (ng/ μl) from the weekly sample and S is the spore number calculated from Cq value indicating the total number of spores in the qPCR reaction. The DNA concentration for each weekly sample was diluted to 10 ng/ μl for the qPCR assay, therefore, the spore number estimated by Cq value was divided by 10 to obtain the spore number in 1ng of DNA. The spore number in 1 ng of DNA was multiplied by the original DNA concentration to get the amount in each 1 μl of original DNA extraction and then multiplied by 100 μl which was the total volume of the DNA solution for each weekly sample of half the spore trap tape. Finally, this number was multiplied by two to have the estimated number of spores for the whole weekly spore trap tape.

3.2.6 Weather data collection and data analyses

Hourly weather data including air temperature and leaf wetness were collected using automated weather stations (Tuctronics, Walla Walla, WA, and Davis Instruments, Hayward, CA). Relative humidity (RH) and dew point were collected using Hygrochron button loggers (iButtonlink Technology, Whitewater WI) placed in blueberry fields with the spore traps from 2014 to 2017. The hourly data of temperature, dew point, and RH were averaged by week for 2014, 2015 and 2017 using the week start date as the date the spore trap tapes were replaced. The number of hours when the temperature (TH) was within the optimal range of 17.5 to 22°C for uredinia production in *T. minima* (Psifer et al., 2004) was also summed up weekly. The leaf wetness duration (LWD) data was calculated by adding the number of hours the rain or leaf wetness sensors detected water daily in 15 minutes, 30 minutes or one-hour intervals depending on the year and field (Table 3.1). The total number of weeks used for analysis was fifty-six weeks with nine in 2014 for BBHF, sixteen weeks each for EM and BBHF in 2015, and nine weeks each for BBHF and SP in 2017.

Principal components analysis (PCA), a data reduction technique, was used to analyze the weekly data of the five weather variables from all three years and three fields to assess the percentage of variance of the data set which was caused by each of the weather variables. All statistical analyses were performed using R version 3.6.0 (R Core Team, 2013). The PCA procedure was chosen to reduce the number of potentially correlated weather variables to a smaller number of uncorrelated weather variables to avoid the collinearity when using them for analysis in linear models. The weather variables chosen to present a principal component were based on the highest absolute value of the factor loadings or the correlation coefficients between the principal component (PC) scores and the factors (Yamamoto et al., 2014). Similar levels of factor

loading values of the variables within a PC also indicate their level of correlation. A biplot of the variables in two dimensions was also generated with addition of principal axes that showed the direction of each weather factor and their correlation. Normality of the spore count data from both qPCR and microscopy of all fields and years was examined using the Shapiro Wilk Test. Log transformation was used for spore numbers quantified by qPCR and square root transformation was used for spore number quantified by microscopy to improve their normality. The Spearman's rank order correlation method was applied to determine the correlation between these two variables.

A linear mixed effect model (LMM) was constructed for the log of spore number quantified by the qPCR and two weather factors including hours of optimal temperature for uredinia production (TH) and LWD, which are highly uncorrelated from PCA results, to see how these weather variables affected the spore number. From the PCA result, average temperature, dew point, and RH were not included in the model to avoid collinearity. The model was run in the R program using the "lme4" and "lmerTest" packages (Bates et al., 2015, Kuznetsova et al., 2017). The response variable was the log of spore number, and the independent variables (or fixed effects) were the weather factors TH and LWD. The random (indirect) effects in the model included the different fields, years, and weeks that spores were collected. Due to the variance in the exact starting date of weekly tape collection data, the first day of each spore trap tape week was converted to Julian date (Appendix B). The random effect from years was 0 and field was 4.81×10^{-10} , which was very low from the preliminary test. Thus, random effects of the model were reduced to only weeks. The resulting model was as followed:

$$Y_i = \beta_0 + X_1\beta_1 + X_2\beta_2 + Z_i u_i + \varepsilon$$

In this model, Y is the log of spore number quantified by qPCR in i^{th} week, X_1 and X_2 were the TH and LWD, respectively. Z was the random effect complements of the fixed effect of i^{th} week and lastly ε was the residual error of the model. The estimated regression coefficients or effect parameters included β_0 as intercept (baseline level of fixed effects), β_1 for TH, β_2 for LWD, r and u are the variance of random effect in the i^{th} week. Three linear nested models with one variable dropped in a sequence were generated to compare to the adjusted model by applying the likelihood ratio test using Chi square distribution to see whether the models were significantly different from each other. Akaike information criterion (AIC) (Akaike, 1974) and the p-value from the likelihood ratio test was examined to see if there was a significant difference between the models. The best model was selected based on the lowest AIC and $p < 0.05$. Confidence levels (CI), the marginal coefficient of determination (marginal R^2), which is the percentage of variance explained by fixed effects, and the conditional coefficient of determination (conditional R^2), which is the percentage of variance explained by both fixed and random effects (Xavier et al., 2018) were calculated for the best-selected model. The residual plot of the model was plotted to evaluate the normality of the distribution (no heteroscedasticity). A similar LMM model was also attempted for log spore number with the two weather effects of temperature and LWD with weeks as the random effects.

Disease severity was rated weekly in 2015 and 2017 for two fields BBHF and SP by Rachael Martin, blueberry disease research assistant; however, the rating methods were different in these two years. Therefore, only the disease severity rating in 2017 was used for analysis. Disease rating was done once a week using a 0.25 m x 0.25 m quadrat frame in four random areas around the field where the weather stations were located. The percentage cover of blueberry leaves with disease within the frame was estimated visually and recorded. The normality of the disease rating

data was checked using the Shapiro Wilk test. The disease severity was square root transformed to improve the normality. Spearman's rank correlation approach was applied for disease severity and the two spore quantification methods. A LMM with random effects of weeks and fields was applied to evaluate the potential effect of the weather factors and log of spore number quantified by qPCR on the disease severity. The response variable in the model was the disease severity rating, and the explanatory or fixed effects were log of spore number, TH, and LWD with field and weeks as the random effects. Preliminary testing of the model excluded random effects from field (variance =0) since it did not have effects on disease severity rating. The model was adjusted to included only week as a random effect; the model's equation is as followed:

$$Y_i = \beta_0 + X_1\beta_1 + X_2\beta_2 + X_3\beta_3 + Z_i u_i + \varepsilon$$

In this model, Y is the disease severity rating in i^{th} week, X_1 , X_2 and X_3 were the TH, LWD and log of spore number quantified by qPCR, respectively. Z was the random effect complements of the fixed effect of i^{th} week and lastly ε was the residual error of the model. The estimated regression coefficients included β_0 as intercept, β_1 for TH, β_2 for LWD, β_3 for log of spore number and u_i is the variance of random effect in the i^{th} week. The fields included were BBHF and SP in 2017 and the weeks were from 8/7/2017 to 10/15/2017. The week of 8/14/2017 - 8/20/2017 in SP did not have weather and spore number data available and was not included in the analysis. Three nested linear mixed models with one variable dropped in a sequence were generated and goodness-of-fit tests were as mentioned above. A residual plot was generated for the model to visually examine the pattern of residuals for constant variance and a caterpillar plot of random effect intercepts was created to observe model random effects.

Additionally, a similar LMM model was generated for disease severity with temperature, LWD and the log of spore number quantified by qPCR with the effect of weeks for two fields BBHF and SP in 2017. The model equation is as followed:

$$Y_i = \beta_0 + X_1\beta_1 + X_2\beta_2 + X_3\beta_3 + Z_i u_i + \varepsilon$$

In this model, Y is the disease severity rating in i^{th} week, X_1 , X_2 and X_3 were the temperature, LWD and log of spore number quantified by qPCR, respectively. Z was the random effect complements the fixed effect of i^{th} week and lastly ε was the residual error of the model. The estimated regression coefficients included β_0 as intercept, β_1 for temperature, β_2 for LWD, β_3 for log of spore number and u_i is the variance of random effect in the i^{th} week. Three nested models were created with one variable dropped in sequence to compare with the full model using similar method as mentioned above. A residual plot and caterpillar plot were created to visually evaluate the pattern of the model residuals and random effects.

3.3 Results

3.3.1 Determining the detection threshold for the qPCR assay

The detection threshold of the qPCR was estimated by using DNA extracted from a dilution series of known *T. minima* urediniospores on the Melinex tape (Table 3.2). The equation used for calculating spore quantity (X) in each qPCR reaction from the Cq value (Y) was:

$$X = e^{((Y-31.861)/-1.193)}$$

The coefficient of determination (R^2) of this linear equation was 0.9576, which indicated that the data from both qPCR runs of the second spore dilution series fit the regression line.

Table 3.2 Results of amplification of spore dilution series extracts. Spore extraction was from 20,000 to 2 spores on a daily segment of Melinex tape using qPCR assay.

Number of spores on tape	Number of spores contributing DNA in qPCR reaction (1)	Mean Cq	Standard deviation
20,000	666.67	23.38	1.43
2000	66.67	27.76	0.68
200	6.67	29.78	1.17
20	0.67	32.13	0.52
2	0.067	34.69	0.65

(1) Total spores on the tape were extracted to a final volume of 30µl and 1µl of this DNA extract was used in each qPCR reaction.

3.3.2 Detection and quantification of rust DNA from spores on spore trap tapes.

DNA extractions of spore trap tape using the phenol-chloroform technique recovered an average of 44.3 ng/µl of DNA from all locations and years. The extraction of rust spores using this technique was able to obtain a higher DNA concentration in general compared to using a DNA extraction kit described in section 2.2.1 (average concentration of 5.98 ng/µl). The qPCR assay had an average cycle threshold within the range of 26.92 to 37.87 for all the spore tape samples. The total number of spore tapes quantified by qPCR assays were 56 samples. In the first run of the tape samples, the efficiency of qPCR had a range of 73.3% to 134% with an R^2 of 0.78 to 0.979, and the slope was from -2.709 to -4.189. In the second run, the efficiency was improved to a range from 92.3% to 112.6% with an R^2 of 0.897 to 0.958, and the slope was from -3.052 to -3.591. The qPCR assay could not amplify DNA from samples of two weeks from 7/6/2015 to 7/11/15 and 10/9/2017 to 10/15/2017 at BBHF location in all three replicates in both runs. Spore counting by

microscopy data was also unavailable for these two weeks. Due to the unreliability data of spore number from these two weeks, they were excluded from further analysis.

3.3.3 Comparison of spore number from the molecular method to microscopy and disease severity rating

The Shapiro Wilk test resulted in both spore data quantified by microscopy and qPCR method, as well as the disease severity in 2017 were not normally distributed ($p < 0.05$). The spore numbers obtained by microscopy and qPCR were compared by using Spearman’s rank order correlation for all fields in three years, 2014, 2015 and 2017. Log transformation was done for spore number quantified by qPCR to improve the normality of the data. The correlation test resulted in significant positive correlation between the two spore count methods (correlation coefficient = 0.323 and $P = 0.0152$). Summary of the average spore number for each method in each field and year is in table 3.3.

Table 3.3 Average spore number per week quantified by microscopy and qPCR methods in three blueberry fields over three years

Year	Field	Average spore number (qPCR)	Average spore number (microscopy)
2014	BBHF, Jonesboro	7907	107
2015	BBHF, Jonesboro	4055	131
2015	East Machias	9104	40
2017	BBHF, Jonesboro	4738	1079
2017	Spring Pond, Deblois	15275	567

The spore number quantified from both microscopy and the molecular methods appeared to increase starting from the early August (weeks starting on Julian dates of 214 and 221) until mid-October (weeks starting on Julian dates of 282 and 289) in all three years and fields (Figures 3.2, 3.3 and 3.4). In 2014 and 2017, there were missing data in early weeks in June and July for all the fields, therefore, the early spore number was not determined. In 2014 at BBHF location, the detection of spore number by microscopy method started on the week starting with Julian date 217 (early August) and had a high peak on the week starting with Julian date 238 (last week of August) before decreasing in spore number in the later weeks (Figure 3.2A). Spore numbers quantified by qPCR method detected more spores than microscopy from the week starting with Julian date 217, and the spore number went up week by week and had the highest peak on the week starting with Julian date 266 (late September) (Figure 3.2 A). In 2015, there was a high number of spores detected by qPCR method in the week starting with Julian date 172 (late June) in both locations, BBHF and EM (Figures 3.2B and 3.3); microscopy only picked up the spore number in week 186 (early July) in EM. Peak of spore number detected by qPCR during this timeline was weeks starting with Julian dates 228 and 249 in BBHF, and 242 and 249 in EM, which was around mid-August to mid-September. On the other hand, the peak of spore number by microscopy was later in the season in BBHF on the weeks starting with Julian dates 256 and 277 (mid-September to early October) and in mid-season in EM with peaks on weeks starting with date 221 and 249 (early August to early September) (Figure 3.2 B and 3.3).

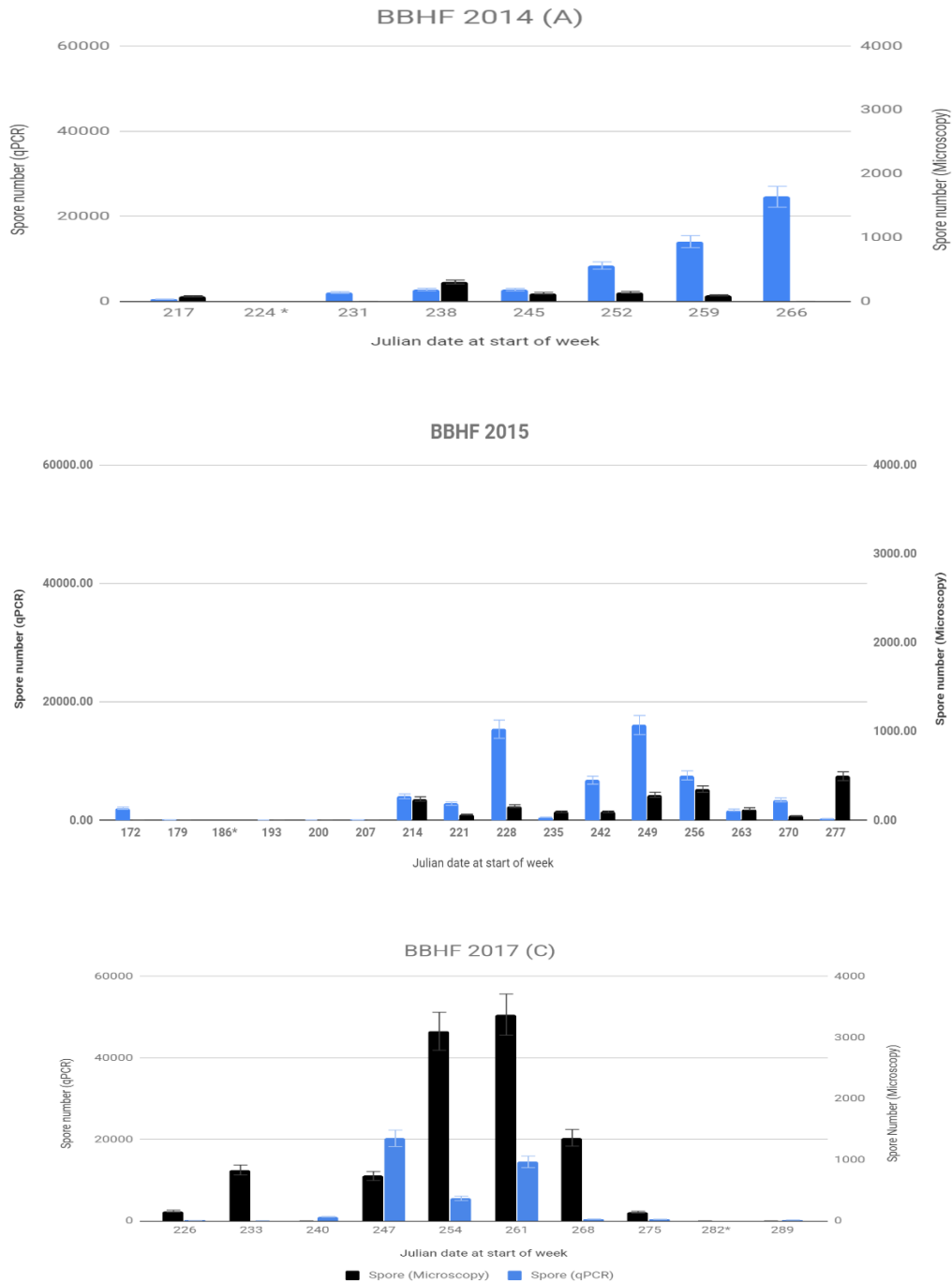


Figure 3.2 Graph of spore numbers quantified using microscopy and the qPCR method. Urediniospore numbers were quantified by qPCR (blue column) and microscopy (black column) in BBHF in three years 2014 (A), 2015 (B) and 2017 (C). Spores were detected the earliest around

late June (Julian date 172) and latest by mid-October (Julian date 289). (*) Week 224 (2014), 186 (2015) and 282 (2017) had no data for both spore number quantified by qPCR and microscopy. Error bars represent standard error of the mean.

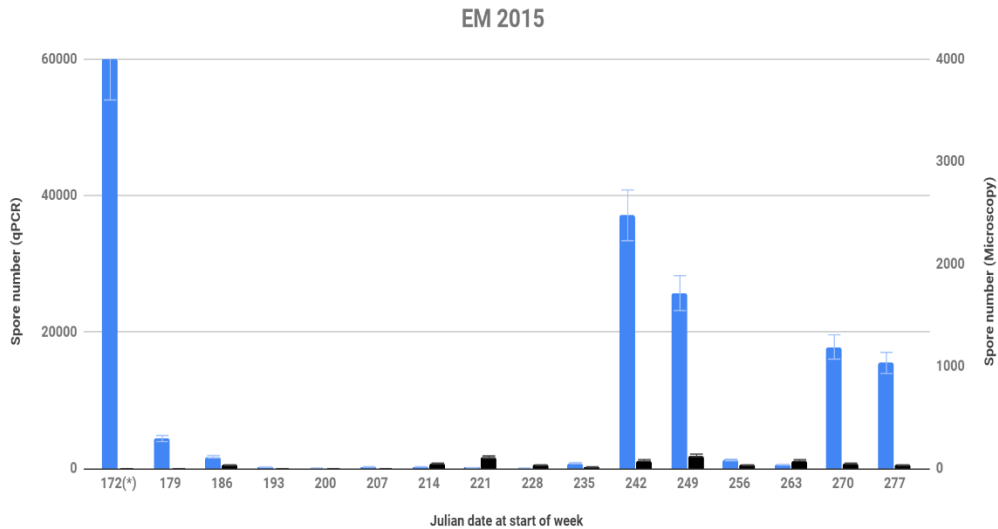


Figure 3.3 Graph of spore number in EM 2015. Spore numbers were quantified by using both qPCR assay (blue column) and microscopy (black column) in East Machias location from the late June (172) to the mid October 2015 (270). Week 172 (*) had a high spore number of 665811 spores detected by qPCR, and Y axis was scaled to 60,000 spores to show other weeks. Error bars represent standard error of the mean.

In BBHF 2017, spore number detected by qPCR had highest peak in weeks starting with Julian dates 247 and 261 (early and mid-September) while microscopy detected the highest peak in weeks starting on 254 and 261 (mid-September) (Figure 3.2 C). This pattern is quite similar in SP 2017, as the highest peaks of spore detected by qPCR and microscopy were in the week starting with Julian date 261 and 254 (mid-September), respectively (Figure 3.4).

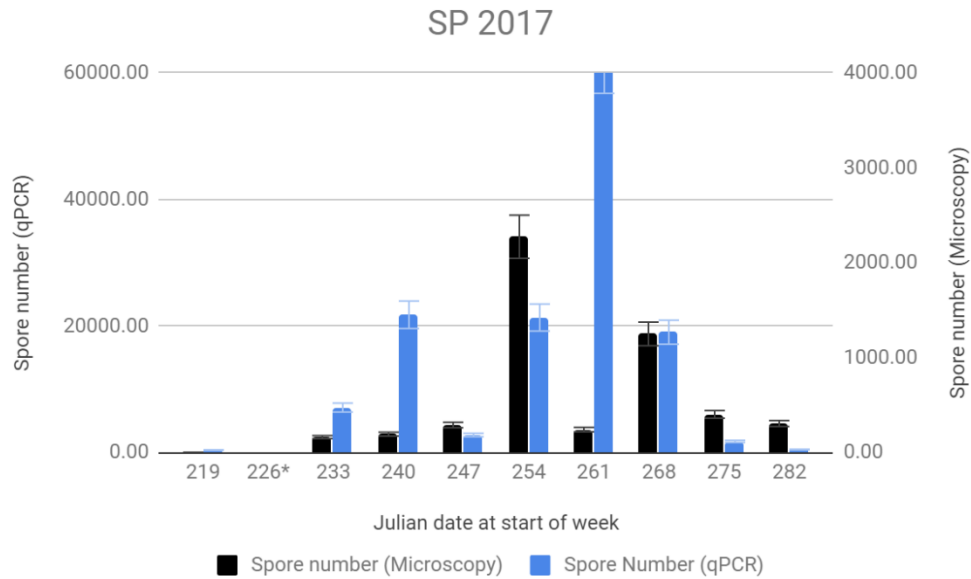


Figure 3.4 Graph of spore numbers in SP 2017. Spore number were quantified by qPCR (blue column) and microscopy (black column) in Spring Pond, Deblois, 2017. (*) Week 226 had no data for both spore number quantified by qPCR and microscopy. Error bars represent standard error of the mean.

The patterns of average temperature for all years and all fields were quite consistent over the growing season with a slightly higher temperature in August and September (Figure 3.5, 3.6 and 3.7). However, the weekly hours of optimal temperature for uredinia production (TH) fluctuated up and down every one or two weeks in all years and fields during the season (Figure 3.5, 3.6 and 3.7). This pattern was also observed with LWD fluctuating every one or two weeks in all years and fields (Figure 3.5, 3.6 and 3.7). In BBHF 2014, the peak of TH was in the week starting with Julian date 238 (late August) and peak of LWD was in the week starting with date 217 (early August) (Figure 3.5 A). Spore numbers in 2014 were not observed to be affected by the weather variables, but the high number of LWD might have initiated the spore numbers to increase in early

August in BBHF. In BBHF in 2015, peak of TH was in the week starting with date 228 (mid-August) and peak of LWD was observed in the week starting with date 172 (late June) (Figure 3.5B). The LWD of BBHF 2015 was lower compared to that of the EM field in the same year. The peak of spore number coincided with the highest peak of TH, but highest peak of LWD was observed in late June (week 179) (Figure 3.5B). In EM 2015, the peak of TH was also observed in the week starting with date 228 (mid-August), and the peak of LWD was in weeks starting with dates 207 and 228, which was during the time spore number was quite low. There was sudden drop in both LWD and TH in week 242, which had the highest peak spore number (Figure 3.5C). This drop in spore number occurred two weeks after week 228, which had the highest number of LWD and TH.

In 2017, the peak of TH was observed in the week starting with date 261 (late September) and LWD in the week starting with date 247 (early September) in BBHF (Figure 3.6). Peaks of TH were observed in weeks starting with date 226, 247 and 261, and LWD in weeks starting with date 261 and 275 (late September and early October) in SP (Figure 3.7). Peaks of spore number quantified by qPCR were observed in weeks with high number of LWD in both fields in 2017. Disease severity increased from mid-August (starting week of Julian date of 247) and reached the highest peak around the early October (week of Julian date of 282) in both BBHF and SP (Figure 3.6 and 3.7).

In summary, spores quantified by both microscopy and the qPCR method were detected from late August to mid-October. The earliest detection of spores was in late June and early July by the qPCR method. The temperature showed not much fluctuation over the summer months and only decreased in late September. The TH and LWD seemed to fluctuate more frequently than temperature for all years and they seemed to be higher from late August to October when the

urediniospores were abundant. However, no clear and consistent pattern was found for spore number and the weather variables in all fields and years that were examined. Disease severity, on the other hand, seemed to increase one or two weeks after the combination of high spore number and increased TH and LWD. Disease severity continued to increase to the end of the season.

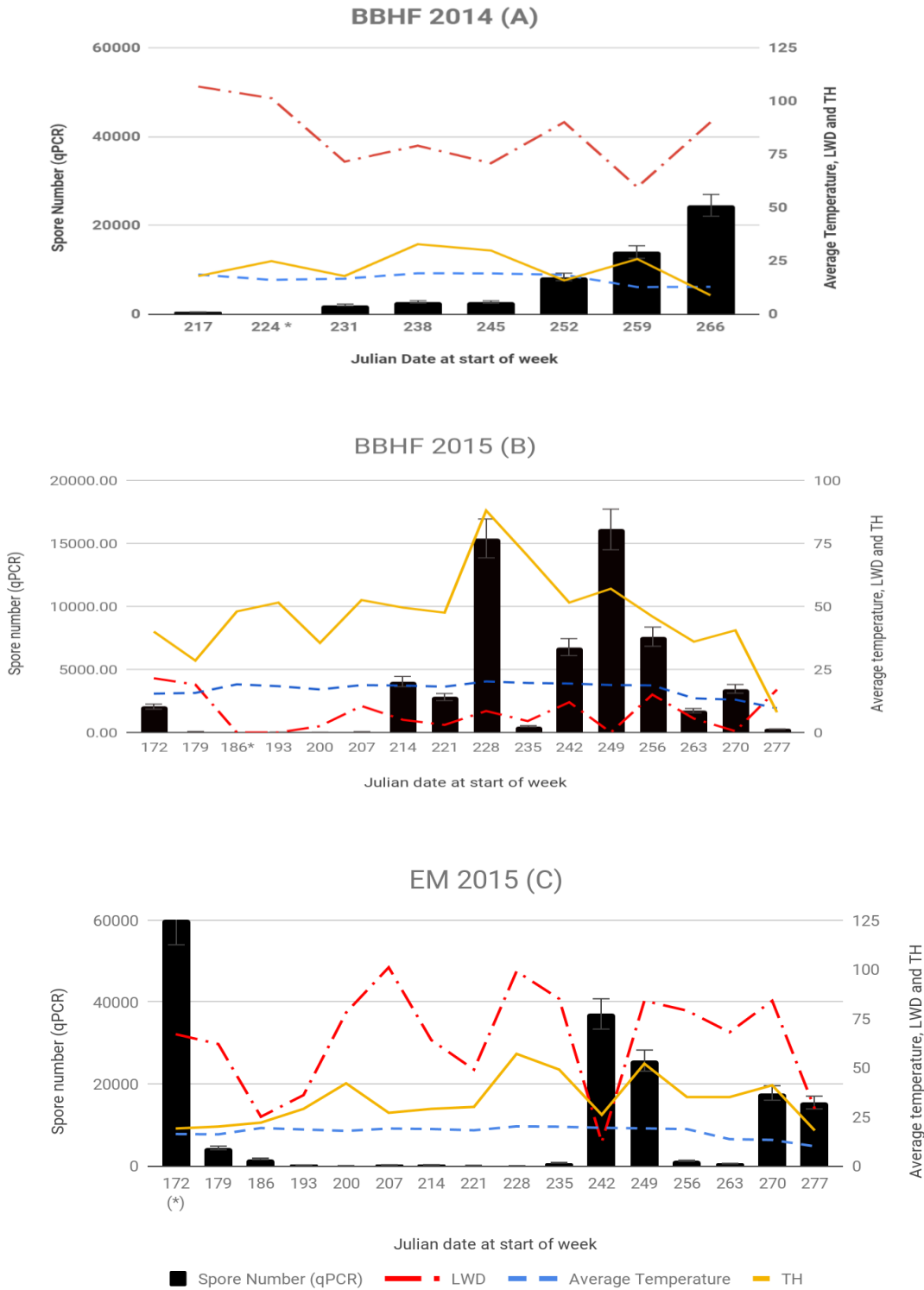


Figure 3.5 Spore numbers and weather factors in BBHF and EM in 2014 and 2015. Spore numbers quantified by qPCR (black columns) were compared to temperature (blue dash line),

LWD (orange dash and dot line). and TH (yellow solid line) in BBHF in 2014 (A), in BBHF (B) and East Machias (C) in 2015. Note that the spore number is on the primary axis and the temperature (C), TH (hours) and LWD (hours) values are on the secondary axis. Error bars represent standard error of the mean. Week 172 (*) in EM 2015 had a high spore number of 665811 spores detected by qPCR and Y axis was scaled to 60,000 spores to show other weeks.

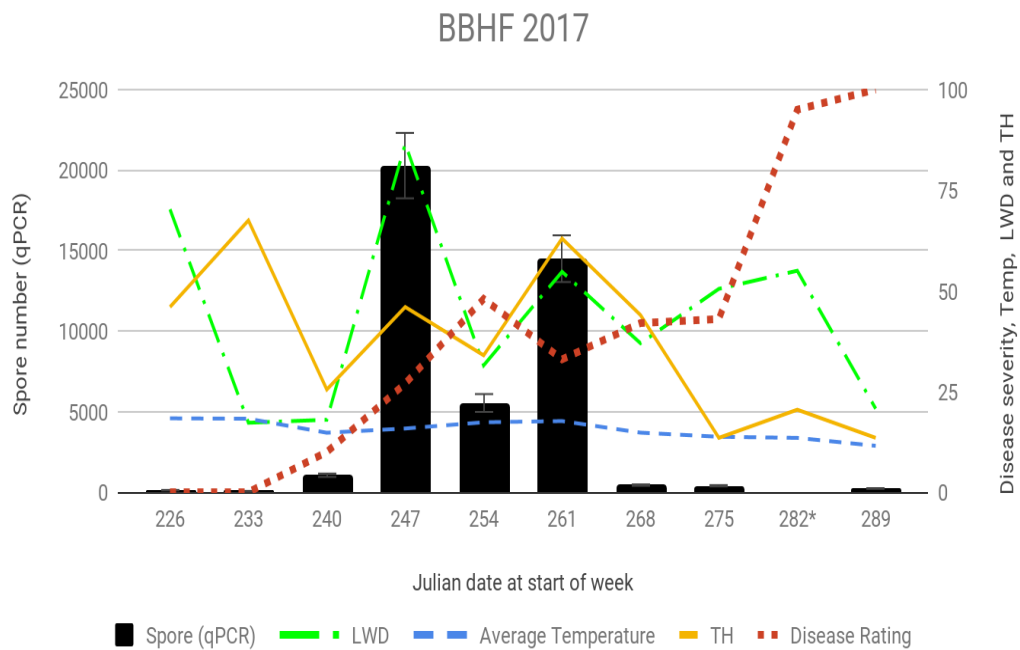


Figure 3.6 Spore numbers, disease severity and weather factors in BBHF in 2017. Spore numbers quantified using qPCR (black column) were compared with disease severity (orange dot line), temperature (blue dash line), TH (yellow solid line), and LWD (green dash and dot line) in BBHF, Jonesboro, ME field. Disease severity is the mean percentage of leaves with rust. is the weather factors included in the graph. Note that the spore numbers are on primary axis and the temperature, TH, LWD and disease ratings are on secondary axis. Error bars represent standard error of the mean.

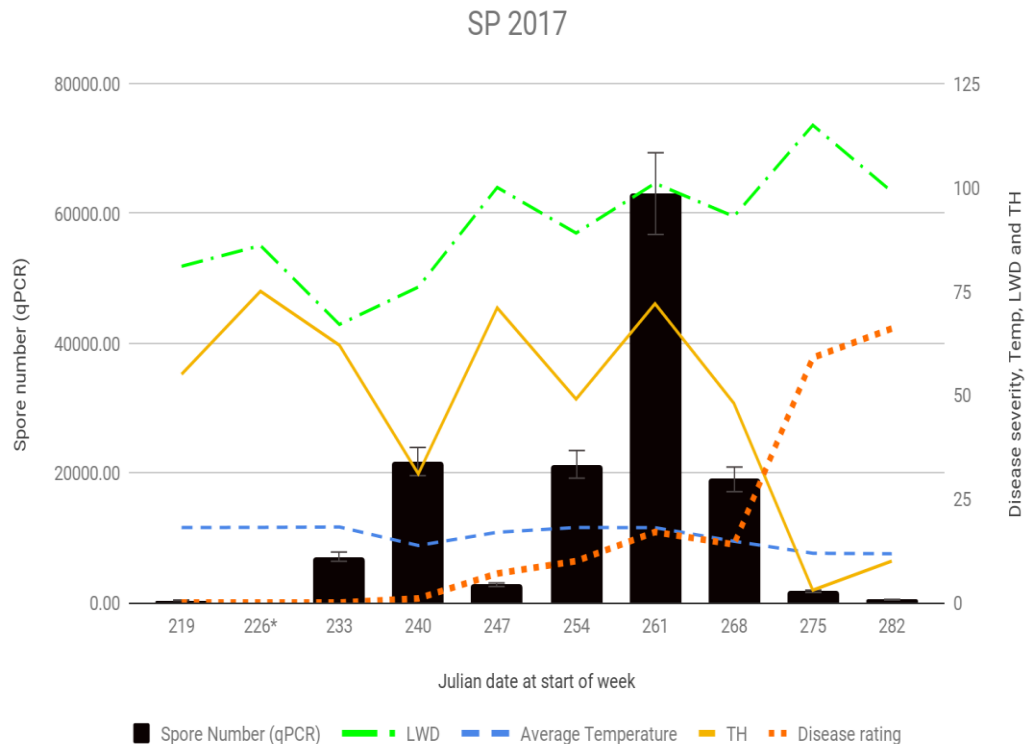


Figure 3.7 Spore numbers, disease severity and weather variables in SP in 2017. Spore numbers quantified using both qPCR (black column) were compared with disease rating (orange dot line), temperature (blue dash line) TH (yellow solid line) and LWD (green dash and dot line) in Spring Pond, Deblois, ME field. Disease severity is the mean percentage of leaves with rust. Note that the spore numbers are on primary axis and the temperature, TH, LWD and disease rating values are on secondary axis. Error bars represent standard error of the mean.

3.3.4 Analysis of weather data and spore numbers using molecular method.

Weather variables, including LWD, average temperature, TH, RH, and dew point, were analyzed by principal component analysis (PCA) for BBHF in 2014, BBHF and EM in 2015, and BBHF and SP in 2017 (Table 3.1) to assess their contribution to the variance of the total weather data and their correlation with each other. Results of the PCA showed that the proportion of

variance was highest in principal component (PC) 1 (47.23%) and PC2 (27.05%), which in combination explained 74.28 % of the variance in the data (Table 3.4). The PC 3 explained 15.18 % and the PC 4 explained 10.19% and PC5 explained only 0.0359% of the variance in the data (Table 3.4). Factor loadings of each variable showed the highest absolute number in PC 1 were from both temperature and dew point, LWD had highest loading in PC 2, TH in PC 3, RH in PC 4 and dew point in PC 5 (Table 3.5).

Table 3.4 Proportion of variance each of five principal components contributed to the variance of the weather data.

	PC1	PC2	PC3	PC4	PC5
Proportion of Variance	47.23 %	27.05 %	15.18 %	10.19%	0.0359%
Standard deviation	1.5367	1.1629	0.8711	0.7138	0.1340
Cumulative Proportion	0.5686	0.8778	0.9971	0.9964	1.00000

Table 3.5 Factor loadings or the correlation coefficients between the weather variables and factors. The variables with the highest absolute value (*) of loading in a PC was chosen as the representative of that PC.

Variable	PC 1	PC 2	PC 3	PC4	PC 5
LWD	-0.18	-0.69*	0.32	0.61	-0.03
Temperature	-0.56*	0.30	-0.31	0.31	-0.63*
RH	-0.43	-0.44	0.16	-0.72*	-0.26
Dew Point	-0.63*	0.04	0.26	0.03	0.73*
TH	-0.26	0.48	0.83*	0.03	0.04

From the factor loadings, temperature and dew point both represented PC1, which indicated a high correlation between them. The PCA biplot with coordinates as the correlation between the variables and principal components confirmed temperature, dew point and TH as all being highly correlated variables (Figure 3.8). Dew point had a higher loading in PC 4 compared to PC1, therefore, this variable represented PC 4 more than PC 1. The LWD and RH also had vectors that were close on the biplot, which indicated their high correlation with each other. Temperature, TH and dew point were negatively correlated with the two highly correlated variables LWD and RH (Figure 3.8). From the results of PCA, the two weather variables dew point and RH were excluded due to their correlation with the other two variables, and the less correlated variables temperature, TH and LWD remained for further analysis.

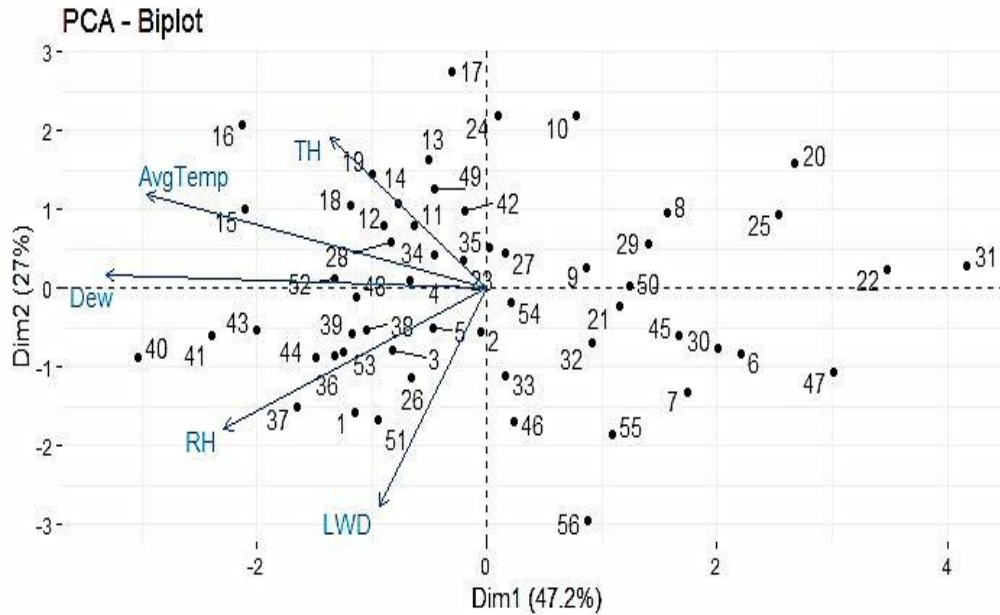


Figure 3.8 A PCA biplot of the five weather variables (Temperature, TH, RH, LWD and dew point). The plot included the weather variable vectors and the mean PC scores of each of the weather variables as vectors on two dimensions.

The linear mixed effects model used to examine the effects of TH and LWD on the log of spore number quantified by the qPCR assays in three years and fields showed no significant effects from both weather variables and the random effect from different years and fields (Table 3.6). The three nested models with an effect taken out in sequence showed no significant difference with the full model which indicated no significant effect came from the fixed effects (Table 3.7). TH and LWD both affected the spore number positively ($\beta_1 = 0.01$ and $\beta_2 = 0.01$). However, these effects were non-significant ($p > 0.05$). The resulting full model explained only 26.61% (conditional R^2) of the variance in the data set, in which the fixed effects from the weather variables explained only 3.54% of the variance (marginal R^2). Visual inspection of residual plot of the model showed a nonrandom (cone-like shaped) pattern, which indicated that the model was not a good fit for

predicting the spore number (Figure 3.8). Attempt to run a similar LMM model for log of spore number replacing TH with temperature also resulted in no significant effects between the log of spore number and two weather variables temperature and LWD (data not shown).

Table 3.6 Summary of the linear mixed effects model of log spore quantified by qPCR and two weather factors of TH and LWD. The model (N=56) included random effects from weeks.

	Variable	Estimated coefficient	Standard error	df	t value	P value	CI lower	CI Higher
Fixed effects	Intercept	5.73	0.94	52.25	6.13	1.19xe ⁻⁷	3.91	7.544
	TH	0.01	0.02	52.62	0.50	0.623	-0.03	0.04
	LWD	0.01	0.01	44.03	1.47	0.150	-0.004	0.03
	Variable	Variance	Standard deviation					
Random effects	Week	1.31	1.14					
	Residual	4.16	2.04					

Note: (*) Significant effects were at $p < 0.05$

Table 3.7 Results of likelihood ratio test on the full model of log spore number with weather variables and three nested models.

Response variable	Fixed effect(s)	Random effect	df	AIC	P value
Log of spore number (qPCR)	TH + LWD	Week	5	259.70	0.61
Log of spore number (qPCR)	LWD	Week	4	257.96	0.15
Log of spore number (qPCR)	None	Week	3	258.01	NA

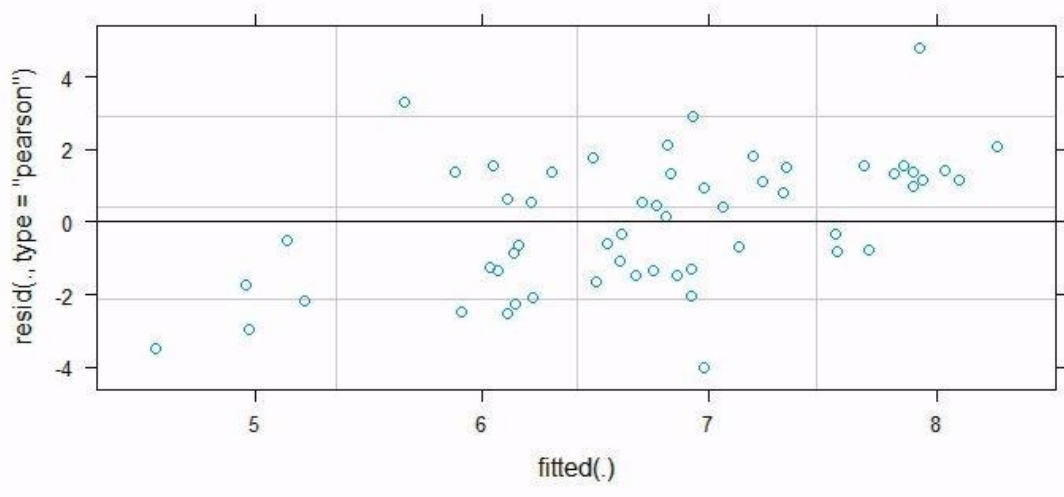


Figure 3.9 Residual plot of the linear model between log of spore number detected by qPCR TH and LWD.

A linear mixed model approach was applied to assess the relationship between the square root of disease severity (DS) with the TH and LWD and log of spore number (by qPCR) in BBHF and SP in 2017 (Table 3.8). The random effects of field and week were added into the model to assess

their effects on the variance of DS. The three nested models with an effect taken out in sequence showed significant difference ($p < 0.05$) between the full model and the three nested models, and the full model had the lowest AIC value (Table 3.9).

Table 3.8 The summary of the LMM model of disease severity rating, log of spore number and two weather factors TH and LWD. The model (N=18) included week and field as random effects (CI= Confidence interval)

	Variable	Estimated coefficient	Std. error	df	t value	P value	CI lower	CI higher
Fixed effects	Intercept	5.34	2.23	1.34	2.40	0.197	1.05	9.571
	TH	-0.10	0.03	13.56	-3.24	0.006*	-0.164	-0.024
	LWD	-0.01	0.02	0.50	-0.56	0.735	-0.051	0.036
	Log of spore number	0.54	0.36	13.28	1.49	0.159	-0.130	1.212
	Variable	Variance	Std. deviation					
Random effects	Week	2.47	1.57					
	Field	0.09	0.29					
	Residual	3.81	1.95					

Note: (*) Significant effects were at $p < 0.05$

Table 3.9 Results of likelihood ratio test on the full LMM model of disease severity with weather variables and two nested models. Full model (*) had the lowest AIC value and p value <0.05.

Response Variable	Independent Variable(s)	Random variable	df	AIC	P value
Disease severity	(*) TH + LWD + log of spore number	Week	7	92.49	0.013 *
Disease severity	LWD + log of spore number	Week	6	96.63	0.177
Disease severity	log of spore number	Week	5	96.46	0.866
Disease severity	None	Week	4	94.48	NA

(Note: * Significant difference were at $p < 0.05$)

The resulting model for predicting disease severity could explain 62.88% (conditional R^2) of the variance, in which the fixed effects accounted for 38.04 % (marginal R^2) of the variance in the square root of DS. Within the model, the effect of TH was significant ($p < 0.05$) and negatively affected the DS ($\beta_1 = -0.10$). The effect of LWD was not significant ($p > 0.05$) and negatively affected the DS ($\beta_2 = -0.05$). Log of spore number had positive effect ($\beta_3 = 0.54$) on disease severity but the effect was not significant ($p > 0.05$). Visual inspection of the residual plot and quantile-quantile plot showed no obvious deviations from normal distribution (Figure 3.9 and 3.10). Random effects of weeks were confirmed, and negative effects were from weeks with lower than average value of DS and positive effects were from weeks with higher than average DS (Figure 3.11).

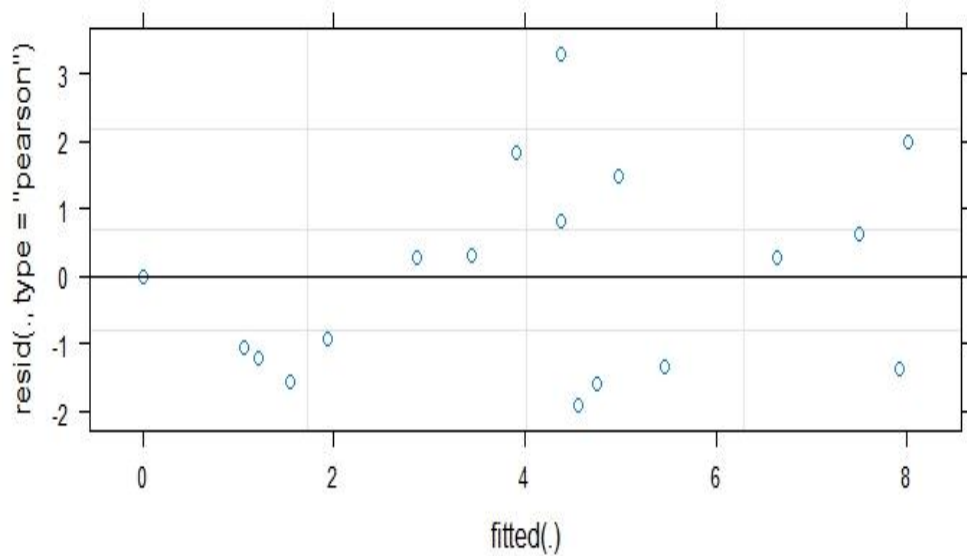


Figure 3.10 Residual plot between the residuals and fitted (or predicted) values. The plot was for the LMM model of square root of DS with log of spore number, TH and LWD as fixed effects and weeks and fields as random effects.

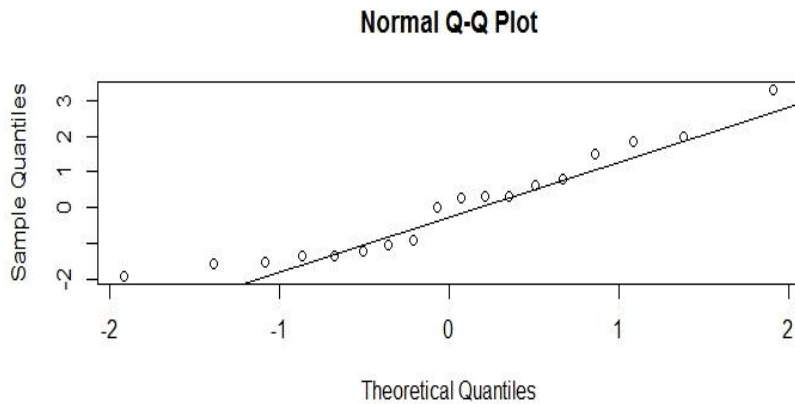


Figure 3.11 Normal quantile-quantile plot of the LMM for disease severity. The plot with log of spore number, temperature and LWD was used for assessment the assumption of normal distribution of the model.

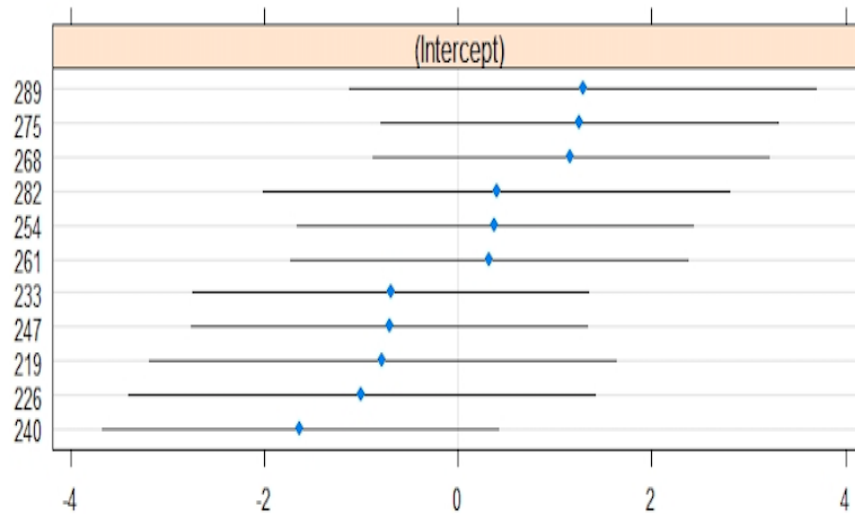


Figure 3.12 Caterpillar plot of the intercepts of the random effects from each of the 11 weeks of 2017 (with first week converted to Julian date) in the disease severity model.

The last LMM model (Table 3.11) for square root of disease severity with fixed effects from temperature, LWD, log of spore number quantified by qPCR and random effects from weeks were generated for two fields, BBHF and SP, in 2017. The resulting model could explain 94.38% (conditional R^2) of the variance in the disease severity with fixed effects from temperature, LWD and log of spore number could explain 64.46% (marginal R^2) of the variance. The temperature ($\beta_1 = -10.93$) and LWD ($\beta_2 = -0.31$) were found to have significantly negative ($p < 0.05$) effects on the disease severity. Log of spore number had no significant effect on disease severity ($p > 0.05$). The likelihood ratio test resulted in a significant difference between the full model and the nested model (Table 3.11). Visual inspection of the residual plot (Figure. 3.13) and normal quantile-quantile plot (Figure. 3.14) showed no obvious evidence of nonrandom distribution. The caterpillar plot of the random effect intercepts showed evidence for the effects of each week on the variance of the disease severity (Figure 3.15).

Table 3.10 Summary of the LMM model of disease severity rating, log of spore number and two weather factors temperature and LWD. The model (N=18) included week and field (CI= Confidence interval).

	Variable	Estimated	Std. error	df	t value	P value	CI	CI
		coefficient					lower	higher
Fixed	Intercept	214.79	35.81	12.57	5.99	5.14e ⁽⁻⁰⁵⁾ *	147.45	294.22
effects	Temperature	-10.93	2.12	12.72	-5.15	0.000201*	-15.69	-6.91
	LWD	-0.31	0.12	9.8	-2.57	0.02844*	-0.53	-0.07
	Log of spore number	0.76	2.12	11.16	0.36	0.725	-3.19	4.62
	Variable	Variance	Std.					
			deviation					
Random	Week	355.98	18.868					
effects	Field	0.0	0.0					
	Residual	66.86	8.177					

Note: (*) Significant effects were at $p < 0.05$

Table 3.11 Summary of the likelihood ratio test on the full LMM model of disease severity with weather variables and two nested models. Full model (*) had the lowest AIC value and p value <0.05.

Response Variable	Independent Variable(s)	Random variable	df	AIC	P value
Disease severity	(*) Temperature + LWD + log of spore number	Week	6	158.76	1.269e ⁽⁻⁵⁾ *
Disease severity	LWD + log of spore number	Week	5	175.82	0.2470
Disease severity	log of spore number	Week	4	175.16	0.2607
Disease severity	None	Week	3	174.42	NA

Note: * Significant difference were at $p < 0.05$

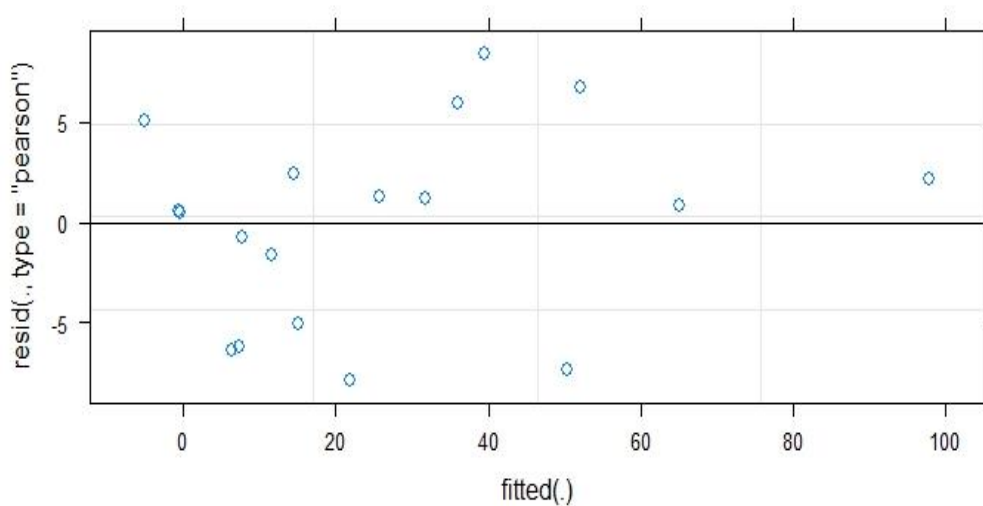


Figure 3.13 Residual plot between the residuals and fitted (or predicted) values of LMM model for disease severity. The LMM model of sqrt disease severity with log of spore number, temperature and LWD as fixed effects and weeks as random effects.

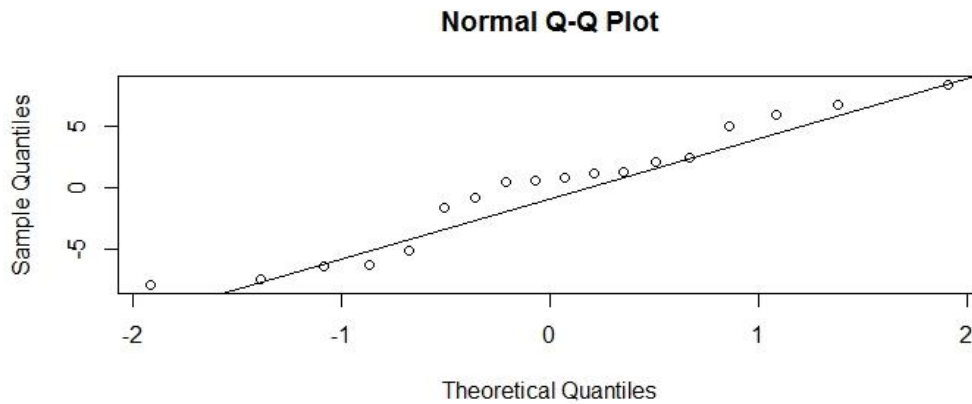


Figure 3.14 Normal quantile-quantile plot of the LMM for disease severity. The LMM model with log of spore number, temperature and LWD for assessment the assumption of normal distribution of the model.

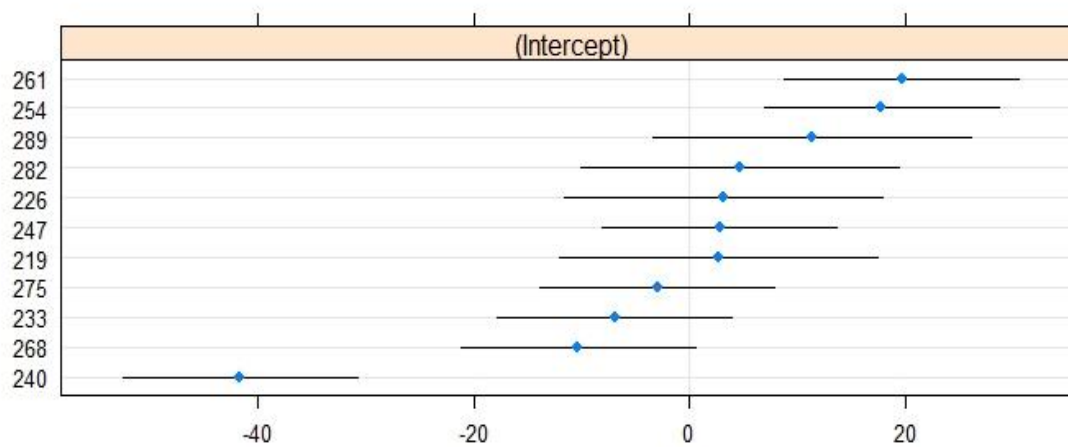


Figure 3.15 Caterpillar plot of the intercepts of the random effects from each of the 11 weeks of 2017 (with first week converted to Julian date) in the disease severity model.

3.4 Discussion and Conclusion

Many fungal pathogens release mainly airborne spores to infect their plant hosts which include many of our common economically important crops. Studies that integrated qPCR methods with air sampling of fungal spores have reported these methods are useful tools to understand the

epidemiology of the pathogens and to monitor the inoculum production as well as the pattern of dispersal (Wieczorek et al., 2014, Almquist et al., 2015, Duvivier et al., 2016). Prediction of spore release timing could be made by the ability to quantify spores and assess what environmental factors affect spore release and build predictive models based on this information.

Thekopsora minima, a fungal pathogen that causes leaf spot in blueberry belongs to the group of polycyclic rust pathogens that release different types of airborne spores, including aeciospores and urediniospores, during the growing season to infect wild blueberries. In this study, the qPCR assay developed using species-specific primers was combined with Burkard air samplers to detect and quantify airborne spores of *T. minima*. The PCR primer set TMITS2F and TMITS2GR from the ITS 2 region of *T. minima* developed in this study was found to be highly specific to rust and can detect as low as two spores on a daily segment of Vaseline/ hexane coated Melinex tape. However, the cycle quantification threshold (Cq) obtained for spores at this level was often irreproducible. A comparable lowest level of spore detection from 2 to up to 10 spores on the Melinex tape, was found in a previous study using a similar technique on *Puccinia triticina*, rust of wheat (Duvivier et al., 2016). The Cq values of the detection range for *T. minima* from 20 to 20,000 spores on the tape was found to be from 34 to 23, respectively. The spore tape extraction method adopted from a previous study (Duvivier et al., 2016) was found to be able to obtain a higher amount of spore DNA compared to using commercial DNA extraction kits. The extraction procedure, which consisted of three steps: spore disruption, DNA extraction and DNA precipitation (Duvivier et al., 2016), took more time than using the kits. Pooling daily samples into one weekly sample saved more time in the extraction procedure and the extraction of about one month of spore (4 weeks) or more can be done in one day by one person. However, weekly spore data obtained instead of daily data caused the data set to be much smaller in sample size compared

to using daily spore data. To increase the capability of inferring a more meaningful analysis from the spore number data, it might be helpful to obtain more weekly data from earlier months (from April to July) and from more blueberry fields to increase the sample size.

There was a statistically significant positive correlation between the two spore count methods found in this study. However, due to the sensitivity of the qPCR assay, there were a large difference in spore numbers quantified using the qPCR and microscopy methods. The microscopy counting method was found to quantify lower spore numbers than the qPCR. Counting spores in small areas of each hour on the tape might have missed some clumps of spores that might have been located outside of the examined area on the tape. DNA extraction and quantification of spores from weekly spore tape samples can be done within 1 or 2 days and considerably faster and more accurately than counting spores manually using microscopy. Spore numbers detected by both the qPCR and microscopy methods were observed to be present in the air starting from late August until early and mid-October for all three years and fields. The abundance of spores during this period is consistent with the previous findings of Nickerson and Hildebrand (2017).

Interestingly, in 2015, tapes from the early weeks of the season had a high number of spores detected by the qPCR method around late June to early July. During this time, urediniospores and rust symptoms are most often not visible on the wild blueberry plants. The detection of high spore numbers in late June indicates that the spore we detected might be the aeciospores of *T. minima* released from hemlock, the rust's alternate plant host, to infect the wild blueberries. However, the exact timing of when aeciospores begin to be produced and are available in the air is still unknown because of the missing data of the earlier weeks in this study. In future studies, it might be helpful to include all the early weeks from April to July to better determine the timing of aeciospores infecting wild blueberries. Nevertheless, the qPCR assay has more potential compared to the

microscopy method for the early diagnosis of *T. minima* and could be used as a tool to aid in future diagnostic studies and development of disease prevention strategies.

Linear mixed models (LMM) were chosen for analyzing the effects of weather data on the spore numbers quantified by qPCR and disease severity with weeks as the random effects. The addition of the random effect of each week was confirmed to be necessary and did contribute to the variance of the models. The variance from each week of the growing season might be due to various factors such as the physiological condition of the wild blueberry plant. Blueberry plants typically do not show rust symptoms in the beginning of the season around June to July but start to senesce in late September to mid-October. There was no statistically significant correlation between the disease severity and spore numbers using qPCR methods for the year 2017 in two different fields BBHF and SP. However, this result is not unexpected due to the incubation and germination time required after the spore lands on the plant hosts' tissues (Agrios, 2004), which may indicate that an increase of spore number alone might not cause an increase in disease severity immediately. The pattern of spore numbers and disease severity observed in 2017 in both BBHF and SP fields showed an increase in disease severity occurred about one or two weeks after an increase of spore numbers. This range of time was within the mean incubation period of 13 to 14 days at the two minimum and maximum temperature range 15°C and 30°C in *T. minima* (Pfister et al., 2004).

The LMM approach was chosen to examine the relationship between spore number and weather variables and to investigate the random effects that might come from the variation of data in different fields, weeks and years. Random effects of fields and years were minimal and therefore, not included in the later models. The proposed preliminary LMM in this study found no statistically significant effects from the number of optimal temperature hours for uredinia

production (TH) and LWD on the log-transformed spore number quantified by qPCR. This result might indicate that within the optimal temperature range, uredinia production might be favorable but not immediately affect the urediniospores production and their presence in the air. There might be a time gap between when the uredinia were produced and when the spores were available in the atmosphere and therefore, resulted in the inability to deduce a meaningful connection between the optimal temperature hours and spore numbers.

On the other hand, the models for disease severity in 2017 in two fields, BBHF and SP, found that the number of optimal temperature hours for *T. minima* and temperature, in general, had significant negative effects on the disease severity, which indicated that a higher number of optimal temperature hours and a higher temperature, in general, might decrease the disease severity. This finding is quite surprising because the optimal temperature range and warmer temperature were expected to encourage the production rate of *T. minima* uredinia, which in turn should have increased the disease severity rating as well. The possible explanations for this phenomenon might be due to the other environmental cofactors such as humidity and leaf wetness duration, that might not complement the temperature and were not included in the previous temperature effect study of *T. minima* by Pfister et al. (2004). Moreover, the optimal temperature range of uredinia production in the temperature study was done for *Rhododendron* sp., a different host plant, and not *V. angustifolium*, and *T. minima* might have a different optimal temperature to infect blueberries. Additionally, an increase in production of uredinia might not influence the spore number immediately, but it might take a few days under favorable weather conditions before urediniospores are produced and dispersed in the air. Weekly effects confirmed using the model showed that it is necessary to take the variance of each week during the growing season into account when analyzing the effects of the environmental factors. The blueberries' physical

conditions and other unexplored seasonal factors during the plant growing months might have affected the disease severity for each week. The peak of disease severity in mid-October was late in the season and spores might have accumulated and infected the plants, which usually senesce at this point, and therefore DS was found to be much higher around this time.

Since *T. minima* spores are mostly airborne, the increase of leaf wetness due to rainfall or dew might have decreased the presence of spores in the atmosphere and washed the spores off the leaf. However, since many fungi need moisture for their development, when spores are present on the leaf surface, the increase in moisture could help increase the disease severity. Through the LMM models, the LWD was found to have no significant impact on the spore numbers in the atmosphere when it was included in the model with either TH or temperature. No significant effect from LWD was also found in the model for disease severity when TH was included in the model. However, in the model that included average temperature, LWD and the spore number, both temperature and LWD were found to negatively impact the disease severity. This later model was better at explaining the variance in disease severity, which indicated that the two weather variables temperature and LWD in a model were a better fit than including TH and LWD in the model. Overall, the findings from these models are in contrast with studies of other rust pathogens which mostly found positive effects of the increased LWD on disease development and spore number (Angelotti et al., 2014, Schmitz et al., 2009). Since we used either rainfall or leaf wetness data collected by different sensors, this might also affect the results. The accuracy of LWD data largely determines the success of the predictive model based on it (Sentelhas et al., 2005); therefore, more accurate data are needed to confirm the results of the predictive models for *T. minima*. Additionally, the preliminary result of the disease severity LMM model was done using a small

number of data points (N=18) in August to mid-October of 2017 from two fields, which might not be representative of the whole growing season and in other years.

In conclusion, the combination of spore tape extraction and quantification using qPCR was more efficient compared to the microscopy counting method and could detect early spores that might be aeciospores in the early months of June and July. Comparisons of spore numbers, disease severity and the weather factors showed that disease severity seemed to increase one or two weeks after an increase in the combination of high spore number, LWD and optimal temperature in 2017, and disease severity reached its highest peak in later part of the season. Temperature and LWD were found to negatively impact the disease severity but not the spore numbers in 2017. More continuous weekly data of disease severity and spore numbers from future growing seasons would be used to develop a better model that could precisely predict the spore number and disease severity of rust based on the weather factors. Nonetheless, this study demonstrated a potential scheme for spore detection and quantification method that can be implemented with weather data into a predictive model to better understand the spore release pattern and infection frequency by developing a model for disease warning system for *T. minima*. Accurate prediction of disease incidence and spore accumulation would aid in disease management and mitigate the cost of production as well as reduce the unwanted effects of fungicide application in the environment.

CITED REFERENCES

Adams, S. P, 2006. Data analysis and reporting. Real-time PCR. Dorak, M. Tevfik. New York; Abingdon [England]; Taylor & Francis.

Agrios, G.N. 2004. Plant Pathology, 5th Ed. Academic Press, San Diego.

Akaike, H. 1974. A new look at the statistical model identification. IEEE Transactions on Automatic Control 19 (6): 716-23.

Almasi, M. A., Aboubakr M., Jaber N., Soraya K., and Mojtaba N. 2012. Assessment of performance ability of three diagnostic methods for detection of potato leafroll virus (PLRV) using different visualizing systems. Applied Biochemistry and Biotechnology 168 (4): 770-84.

Almquist, C., A. C Wallenhammar. 2015. Monitoring of plant and airborne inoculum of *Sclerotinia sclerotiorum* in spring oilseed rape using real-time PCR. Plant Pathology 64 (1): 109-18.

Altschul, S.F., T.L. Madden, A.A. Schäffer, J. Zhang, Z. Zhang, W. Miller, & D.J. Lipman, 1997. Gapped BLAST and PSI-BLAST: a new generation of protein database search programs. Nucleic Acids Research. 25:3389-3402.

Annis, S, Yarborough, D and Martin, R. 2018. Disease Control Guide for Wild Blueberries [Factsheet 219]. The University of Maine Cooperative Extension. Retrieved from: <https://extension.umaine.edu/blueberries/factsheets/disease/219-disease-control-guide-for-wild-blueberries>

Annis, S. 2009. Forecasting Mummy berry fungus infection. The University of Maine Cooperative Extension. Retrieved from: <https://extension.umaine.edu/blueberries/factsheets/disease/mummyberry/>

Angelotti, F., C. R. Scapin, D. J. Tessmann, J. B. Vida, and M. G. Canteri. 2014. The effect of temperature, leaf wetness and light on development of grapevine rust. Australasian Plant Pathology 43 (1): 9-13.

Applied Biosystems Inc. 1991. High-quality template DNA for Taq cycle sequencing using DyeDeoxy™ terminators: An improved preparation procedure. Applied Biosystem Inc. User Bulletin 18

Arif, M., S. Dobhal, P. A. Garrido, G. K. Orquera, A. S. Espíndola, C. A. Young, F. M. Ochoa-Corona, S. M. Marek, and C. D. Garzón. 2014. Highly sensitive end-point PCR and SYBR green qPCR detection of *Phymatotrichopsis omnivora*, causal fungus of cotton root rot. Plant Disease 98 (9): 1205-12.

Avila-Quezada, G. Dolores, A. Melgoza-Castillo, J. F. Esquivel, H. V. Silva-Rojas, S. G. Leyva-Mir, C. J. Garcia-Avila, A. Quezada-Salinas, L. Noriega-Orozco, P. Rivas-Valencia, and D. Ojeda-Barrios. 2018. Emerging plant diseases under a changing climate scenario: Threats to our global food supply. Emirates Journal of Food and Agriculture 30 (6): 443-50.

Babiker, E. M., S. J. Stringer, B. J. Smith, and H. F. Sakhanokho. 2018. Reaction of different *Vaccinium* species to the blueberry leaf rust pathogen *Thekopsora minima*. *HortScience* 53 (10): 1447-52.

Ball, C. S., Y. K. Light, C.Y. Koh, S. S. Wheeler, L. L. Coffey, and R. J. Meagher. 2016. Quenching of unincorporated amplification signal reporters in reverse-transcription loop-mediated isothermal amplification enabling bright, single-step, closed-tube, and multiplexed detection of RNA viruses. *Analytical Chemistry* 88 (7): 3562-8.

Bell, D. J., Rowland, L. J., Zhang, D., & Drummond, F. A. 2009. Spatial genetic structure of lowbush blueberry, *Vaccinium angustifolium*, in four fields in Maine. *Botany*, 87(10), 932+.

Brankatschk, Robert, Natacha Bodenhausen, Josef Zeyer, and Helmut Bürgmann. 2012. Simple absolute quantification method correcting for quantitative PCR efficiency variations for microbial community samples. *Applied and Environmental Microbiology* 78 (12): 4481-9.

Bustin, SA. 2002. Quantification of mRNA using real-time reverse transcription PCR (RT-PCR): Trends and problems. *Journal of Molecular Endocrinology* 29 (1): 23-39.

Chan, W-T., C. S. Verma, D. P. Lane, and S. K. Gan. 2013. A comparison and optimization of methods and factors affecting the transformation of *Escherichia coli*. *Bioscience Reports* 33 (6): e00086.

Chandra, A., A. T. Keizerweerd, and M. P. Grisham. 2016. Detection of *Puccinia kuehnii* causing sugarcane orange rust with a loop-mediated isothermal amplification-based assay. *Molecular Biotechnology* 58 (3): 188-96.

Cheng, N., Y. Xu, X. Yan, Y. Shang, P. Zhu, W. Tian, Z. Liang, and W. Xu. 2016. An advanced visual qualitative and EVA Green-Based quantitative isothermal amplification method to detect *Listeria monocytogenes*. *Journal of Food Safety* 36 (2): 237-46.

Cordo, C. A., C. I. Mónaco, R. Altamirano, A. E. Perelló, S. Larrán, N. I. Kripelz, and M. R. Simón. 2017. Weather conditions associated with the release and dispersal of *Zymoseptoria tritici* spores in the Argentine Pampas region. *International Journal of Agronomy*. 1-13.

Cordova, Leandro G., Achour Amiri, and Natalia A. Peres. 2017. Effectiveness of fungicide treatments following the strawberry advisory system for control of Botrytis fruit rot in Florida. *Crop Protection* 100: 163-7.

Crouch, J. A., and L. J. Szabo. 2011. Real-time PCR detection and discrimination of the southern and common corn rust pathogens *Puccinia polysora* and *Puccinia sorghi*. *Plant Disease* 95 (6): 624-32.

Cummins, G. B., and Y. Hiratsuka. 2003. *Illustrated genera of rust fungi*. 3rd ed. St. Paul, Minn: American Phytopathological Society.

Deguo, W., G., Huo, F. Wang, Y. Li, R., Daxi. 2008. Drawback of loop-mediated isothermal amplification. *African Journal of Food Science*. 2: 83-86.

Desjardins, P., D. Conklin. 2010. NanoDrop microvolume quantitation of nucleic acids. *Journal of Visualized Experiments* (45).

Dhanasekaran, S., T. M. Doherty, J. Kenneth, and TB Trials Study Group. 2010. Comparison of different standards for real-time PCR-based absolute quantification. *Journal of Immunological Methods* 354 (1-2): 34-9.

Bates D., M. Maechler, B. Bolker, S. Walker. 2015. Fitting linear mixed-effects models using lme4. *Journal of statistical software*, 67(1), 1-48. <doi:10.18637/jss.v067.i01>.

Duressa, D., G. Rauscher, S. T. Koike, B. Mou, R. J. Hayes, K. Maruthachalam, K. V. Subbarao, and S. J. Klosterman. 2012. A real-time PCR assay for detection and quantification of *Verticillium dahliae* in spinach seed. *Phytopathology* 102 (4): 443-51.

Duan, Y., C. Ge, X. Zhang, J. Wang, and M. Zhou. 2014. A rapid detection method for the plant pathogen *Sclerotinia sclerotiorum* based on loop-mediated isothermal amplification (LAMP). *Australasian Plant Pathology* 43 (1): 61-6.

Duvivier, M. G. Dedeurwaerder, M. De Proft, J. Moreau, and A. Legrève. 2013. Real-time PCR quantification and spatio-temporal distribution of airborne inoculum of *Mycosphaerella graminicola* in Belgium. *European Journal of Plant Pathology* 137 (2): 325-41.

Duvivier, M., G. Dedeurwaerder, C. Bataille, M. De Proft, and A. Legrève. 2016. Real-time PCR quantification and spatio-temporal distribution of airborne inoculum of *Puccinia triticina* in Belgium. *European Journal of Plant Pathology* 145 (2): 405-20.

Elkins, R. B., T. N. Temple, C. A. Shaffer, C. A. Ingels, S. B. Lindow, B. G. Zoller, and K. B. Johnson. 2015. Evaluation of dormant-stage inoculum sanitation as a component of a fire blight management program for fresh-market bartlett pear. *Plant Disease* 99 (8): 1147-52.

Fakruddin, M, K. S. Bin Mannan, A. Chowdhury, R. M. Mazumdar, M N. Hossain, S. Islam, and M. A. Chowdhury. 2013. Nucleic acid amplification: Alternative methods of polymerase chain reaction. *Journal of Pharmacy & Bioallied Sciences* 5 (4): 245-52.

Frederick, R. D., C. L. Snyder, G. L. Peterson, and M. R. Bonde. 2002. Polymerase chain reaction assays for the detection and discrimination of the soybean rust pathogens *Phakopsora pachyrhizi* and *P. meibomia*. *Phytopathology* 92 (2): 217-27.

Fischbach, J., N. C. Xander, M. Frohme, and J. F. Glökler. 2015. Shining a light on LAMP assays: A comparison of LAMP visualization methods including the novel use of berberine. *Biotechniques* 58 (4): 189-94.

Freedman, B. 2014. Heath family (Ericaceae). In K. L. Lerner & B. W. Lerner (Eds.), *The Gale Encyclopedia of Science* (5th ed.). Farmington Hills, MI: Gale. Retrieved from http://link.galegroup.com.proxy4.ursus.maine.edu/apps/doc/CV2644031088/SUIC?u=maine_orono&sid=SUIC&xid=67ba8120

Fukuta, S., R. Takahashi, S. Kuroyanagi, N. Miyake, H. Nagai, H. Suzuki, F. Hashizume, et al. 2013. Detection of *Pythium aphanidermatum* in tomato using loop-mediated isothermal amplification (LAMP) with species-specific primers. *European Journal of Plant Pathology* 136 (4): 689-701.

Gardes, M., and Bruns, T. D. 1993. ITS primers with enhanced specificity for basidiomycetes -application to the identification of mycorrhizae and rusts. *Molecular Ecology*, 2(2), 113.

Gleason, M. L., K. B. Duttweiler, J. C. Batzer, S. E. Taylor, P. C. Sentelhas, M., J. E. B. Almeida, and T. J. Gillespie. 2008. Obtaining weather data for input to crop disease-warning systems: Leaf wetness duration as a case study. *Scientia Agricola* 65 (spe): 76-87.

Godornes, C., B. T. Leader, B. J. Molini, Arenturion-Lara, and Sheila A. Lukehart. 2007. Quantitation of rabbit cytokine mRNA by real-time RT-PCR. *Cytokine* 38 (1): 1-7.

Goto, Motoki, Eiichi Honda, Atsuo Ogura, Akio Nomoto, and Ken-Ichi Hanaki. 2009. Colorimetric detection of loop-mediated isothermal amplification reaction by using hydroxy naphthol blue. *Biotechniques* 46 (3): 167-72.

Gregory, P. H., and J. M. Hirst. 1952. Possible role of basidiospores as air-borne allergens. *Nature* 170 (4323): 414.

Hall, L. V. 1967. Lowbush blueberry production in Canada. Retrieved from: http://publications.gc.ca/collections/collection_2015/aac-aafc/A63-1278-1967-eng.pdf.

Hall, I.V., L.E. Aalders, N.L. Nickerson, and S.P. Vander Kloet. 1979. The biological flora of Canada. 1. *Vaccinium angustifolium* Ait., Sweet lowbush blueberry. *Can. Field-Naturalist* 93:415-430.

Hall, Tom. 2013. BioEdit Sequence Alignment Editor. Computer software Vers. 7.2.5. <http://www.mbio.ncsu.edu/bioedit/bioedit.html>.

Harrison, C., J. Tomlinson, S. Ostoja-Starzewska, and N. Boonham. 2017. Evaluation and validation of a loop-mediated isothermal amplification test kit for detection of *Hymenoscyphus fraxineus*. *European Journal of Plant Pathology* 149 (2): 253-9.

Higuchi R., Dollinger G., Walsh P. S., Griffith R. 1992. Simultaneous amplification and detection of specific DNA sequences. *Bio/technology* 10 (4): 413-7.

Hirst J.M. 1952. An automatic volumetric spore trap. *Annals of Applied Biology*. 39, 257–265.

Hodgetts, J., J. Hall, G. Karamura, M. Grant, D. J. Studholme, N. Boonham, E. Karamura, and J. J. Smith. 2015. Rapid, specific, simple, in-field detection of *Xanthomonas campestris* pathovar *musacearum* by loop-mediated isothermal amplification. *Journal of Applied Microbiology* 119 (6): 1651-8.

Huber, L., and T. J. Gillespie. 1992. Modeling leaf wetness in relation to plant disease epidemiology. *Annual Review of Phytopathology* 30 (1): 553-77.

Iwen, P. C., S. H. Hinrichs, and M. E. Rupp. 2002. Utilization of the internal transcribed spacer regions as molecular targets to detect and identify human fungal pathogens. *Medical Mycology* 40 (1): 87.

Jamieson, A. R., and N. L. Nickerson. 2003. field performance of the lowbush blueberry propagated by seed, stem cuttings and micropropagation. *Acta Horticulturae* (626): 423-8.

Katoh, K., Asimenos, G., & Toh, H. 2009. Multiple alignment of DNA sequences with MAFFT. *Methods in Molecular Biology* (Clifton, N.J.), 537: 39.

- Kibbe WA. 'OligoCalc: an online oligonucleotide property calculator'. 2007. *Nucleic Acids Research*. 35 (webservice issue): May 25.2018
- Kuznetsova A., Brockhoff, P. B., Christensen R. H. B. 2017. lmerTest Package: Tests in Linear Mixed Effects Models. *Journal of Statistical Software*, 82(13), 1–26. doi: 10.18637/jss.v082.i13.
- Lacey, J. 1996. Spore dispersal — its role in ecology and disease: The British contribution to fungal aerobiology. *Mycological Research* 100 (6): 641-60.
- Lacey, J., M. E. Lacey, and B. D. Fitt. 1997. Philip Herries Gregory 1907-1986: Pioneer aerobiologist, versatile mycologist. *Annual Review of Phytopathology* 35 (1): 1-14.
- Lacey, M. E., and J. S. West. 2006. *The air spora: a manual for catching and identifying airborne biological particles*. Dordrecht: Springer.
- Le Cam, B., M. Devaux, and L. Parisi. 2001. Specific polymerase chain reaction identification of *Venturia nashicola* using internally transcribed spacer region in the ribosomal DNA. *Phytopathology* 91 (9): 900.
- Lévesque, C. A. 2001. Molecular methods for detection of plant pathogens-what is the future? *Canadian Journal of Plant Pathology* 23 (4): 333-6.
- Liu, Z., Xueying Xia, Cuiyun Yang, and Junyi Huang. 2015. Colorimetric detection of maize chlorotic mottle virus by reverse transcription loop-mediated isothermal amplification (RT-LAMP) with hydroxynaphthol blue dye. 6 (1): 73-8.
- Livak, K. J., and T. D. Schmittgen. 2001. Analysis of relative gene expression data using real-time quantitative PCR and the 2(-delta delta C(T)) method. *Methods*. 25 (4): 402.
- “Design of LAMP primers”. lucigen.com.
<https://www.lucigen.com/docs/manuals/Design-of-LAMP-primers-11-2015.pdf> (accessed 3.17.2019).
- Madden, L.V. 1997. Effects of rain on splash dispersal of fungal pathogens. *Canadian Journal of Plant Pathology* 19: 225-230.
- Madden, L. V. 2006. Botanical epidemiology: Some key advances and its continuing role in disease management. *European Journal of Plant Pathology* 115 (1): 3-23.
- Magarey, R.C., K.S. Braithwaite, G. Bade, B.J. Croft, and K.J. Lonie. 2008. Spore trap detection of sugarcane smut: 12 months experience and outcomes. *Proceedings of Australian society of sugar cane technologists*. 72-86.
- Maier, W., D. Begerow, M. Weiß, and F. Oberwinkler. 2003. Phylogeny of the Rust Fungi: An Approach Using Nuclear Large Subunit Ribosomal DNA Sequences. *Canadian Journal of Botany*. 81, 1: 12-23.
- Martinelli, F., R. Scalenghe, S. Davino, S. Panno, G. Scuderi, P. Ruisi, P. Villa. 2015. Advanced methods of plant disease detection. A review. *Agronomy for Sustainable Development*. 35 (1): 1-25.

- Martin, K. J., and P. T. Rygiewicz. 2005. Fungal-specific PCR primers developed for analysis of the ITS region of environmental DNA extracts. *BMC Microbiology* 5 (1): 28.
- Martin, R. R., F. Constable, and I. E. Tzanetakis. 2016. Quarantine regulations and the impact of modern detection methods. *Annual Review of Phytopathology* 54 (1): 189-205.
- McTaggart, A. R., A. D. W. Geering, and R. G. Shivas. 2013. *Thekopsora minima* causes blueberry rust in south-eastern Queensland and northern New South Wales. *Australasian Plant Disease Notes* 8 (1): 81-3.
- Montone, V. O., C. W. Fraisse, N. A. Peres, P. C. Sentelhas, M. Gleason, M. Ellis, and G. Schnabel. 2016. Evaluation of leaf wetness duration models for operational use in strawberry disease-warning systems in four US states. *International Journal of Biometeorology* 60 (11): 1761-74.
- Monteith, J. L., and M. H. Unsworth. 2008. *Principles of environmental physics*. 3rd ed. Amsterdam; Boston; Elsevier.
- Mori, Y., K. Nagamine, N. Tomita, and T. Notomi. 2001. Detection of loop-mediated isothermal amplification reaction by turbidity derived from magnesium pyrophosphate formation. *Biochemical and Biophysical Research Communications* 289 (1): 150-4.
- Morrison, T. B., J. J. Weis, and C. T. Wittwer. 1998. Quantification of low-copy transcripts by continuous SYBR green I monitoring during amplification. *Biotechniques* 24 (6): 954.
- Mostert, L., W. Bester, T. Jensen, S. Coertze, A. van Hoorn, J. Le Roux, E. Retief, A. Wood, and M. C. Aime. 2010. First report of leaf rust of blueberry caused by *Thekopsora minima* on *Vaccinium corymbosum* in the Western Cape, South Africa. *Plant Disease* 94 (4): 478-94 (4), 478.
- Mullis K. 1987. Process for amplifying nucleic acid sequences. U.S. Patent No. 4683202
- Nagamine, K., T. Hase, and T. Notomi. 2002. Accelerated reaction by loop-mediated isothermal amplification using loop primers. *Molecular and Cellular Probes* 16 (3): 223-9.
- National Center for Biotechnology Information (NCBI)[Internet]. Bethesda (MD): National Library of Medicine (US), National Center for Biotechnology Information; (1988). Available from: <https://www.ncbi.nlm.nih.gov/>
- Nickerson, N. L, Hildebrand. 2017. Leaf rust in Compendium of blueberry, cranberry and lingonberry diseases and pests. Eds. Polashock, J. J., F. L. Caruso, A. L. Averill, A. C. Schilder, APS Press, St. Paul, MN, USA.
- Notomi, T., H. Okayama, H. Masubuchi, T. Yonekawa, K. Watanabe, N. Amino, and T. Hase. 2000. Loop-mediated isothermal amplification of DNA. *Nucleic Acids Research* 28 (12): 63-63.
- Oliveira, M., H. Ribeiro, J. L. Delgado, and I. Abreu. 2009. The effects of meteorological factors on airborne fungal spore concentration in two areas differing in urbanization level. *International Journal of Biometeorology* 53 (1): 61-73.

Ong, C. E., J. Henderson, and O. A. Akinsanmi. 2017. Characterization and development of qPCR for early detection and quantification of *Pseudocercospora macadamiae* at different stages of infection process. *European Journal of Plant Pathology* 147 (1): 85-102.

Pashley, Catherine H., Abbie Fairs, Robert C. Free, and Andrew J. Wardlaw. 2012. DNA analysis of outdoor air reveals a high degree of fungal diversity, temporal variability, and genera not seen by spore morphology. *Fungal Biology* 116 (2): 214-24.

Pfaffl, M. W. 2004. Quantification strategies in real-time PCR. In M. W. Pfaffl, A-Z of quantitative PCR. La Jolla, CA, USA: International University Line (IUL).

Pfister, S. E., S. Halik, and D. R. Bergdahl. 2004. Effect of temperature on *Thekopsora minima* urediniospores and uredinia. *Plant Disease* 88 (4): 359.

Pritts, Marvin P.; Hancock, James F. 1984. Independence of life history parameters in populations of *Vaccinium angustifolium* (Ericaceae). *Bulletin of the Torrey Botanical Club*. 3(4): 451-461.

R Core Team. 2013. R: A language and environment for statistical computing. R Foundation for Statistical Computing, Vienna, Austria. URL <http://www.R-project.org/>.

Ravindran, Aravind, Julien Levy, Elizabeth Pierson, and Dennis C. Gross. 2012. Development of a loop-mediated isothermal amplification procedure as a sensitive and rapid method for detection of *Candidatus liberibacter solanacearum* in potatoes and psyllids. *Phytopathology* 102 (9): 899-907.

Rebollar-Alviter, A., A. M. Minnis, L. J. Dixon, L. A. Castlebury, M. R. Ramírez-Mendoza, H. V. Silva-Rojas, and G. Valdovinos-Ponce. 2011. First report of leaf rust of blueberry caused by *Thekopsora minima* in Mexico. *Plant Disease* 95 (6): 772.

Reinink, K. 1986. Experimental verification and development of EPIPRED, a supervised disease and pest management system for wheat. *European Journal of Plant Pathology* 92: 3-14.

Rogers, R. 1974. Blueberries. Gill, John D., William M. Healy, and Northeastern Forest Experiment Station (Radnor, Pa.). 1974. Shrubs and vines for northeastern wildlife. Vol. 9. Upper Darby, Pa: Northeastern Forest Experiment Station.

Rogers, S. L., S. D. Atkins, and J. S. West. 2009. Detection and quantification of airborne inoculum of *Sclerotinia sclerotiorum* using quantitative PCR. *Plant Pathology* 58 (2): 324.

Rosli, H., D. A. Mayfield, J. C. Batzer, P. M. Dixon, W. Zhang, and M. L. Gleason. 2017. Evaluating the performance of a relative humidity-based warning system for sooty blotch and flyspeck in Iowa. *Plant Disease*; PDIS-02-17-0294.

Rowlandson, T., M. Gleason, P. Sentelhas, T. Gillespie, C. Thomas, and B. Hornbuckle. 2015. Reconsidering leaf wetness duration determination for plant disease management. *Plant Disease* 99 (3): 310: 19.

Sambrook, J, E. Fritsch, and T. Maniatis, 1989. Small-Scale Preparations of Plasmid DNA. In *Molecular cloning: A laboratory manual* (2nd ed., pp. 1.25-1.28). Plainview, New York: Cold Spring Harbor Laboratory Press.

- Sato, S, Katsuya, K, and Hiratsuka, Y. 1993. Morphology, taxonomy and nomenclature of Tsuga-Ericaceae rusts. *Transactions of the Mycological Society of Japan*. 34: 47–62.
- Schaad, N. W., R. D. Frederick, J. Shaw, W. L. Schneider, R. Hickson, M. D. Petrillo, and D. G. Luster. 2003. Advances in molecular-based diagnostics in meeting crop biosecurity and phytosanitary issues. *Annual Review of Phytopathology* 41: 305.
- Shaner, G. E., and R. L. Powelson. 1971. Epidemiology of stripe rust of wheat, 1961-1968. Corvallis: Agricultural Experiment Station, Oregon State University.
- Schena, L., F. Nigro, A. Ippolito, and D. Gallitelli. 2004. Real-time quantitative PCR: A new technology to detect and study phytopathogenic and antagonistic fungi. *European Journal of Plant Pathology* 110 (9): 893-908.
- Schena, L., Li, D. N. M. G., Sanzani, S. M., Ippolito, A., Faedda, R., & Cacciola, S. O. 2013. Development of quantitative PCR detection methods for phytopathogenic fungi and oomycetes. *Journal of Plant Pathology*, 95, (1), 7-24.
- Schilder, A. M. C., and T. D. Miles. 2011. First report of blueberry leaf rust caused by *Thekopsora minima* on *Vaccinium corymbosum* in Michigan. *Plant Disease* 95 (6): 768.
- Schmitz, H. F., and R. H. Grant. 2009. Precipitation and dew in a soybean canopy: Spatial variations in leaf wetness and implications for *Phakopsora pachyrhizi* infection. *Agricultural and Forest Meteorology* 149 (10): 1621-7.
- Sentelhas, P. C., T. J. Gillespie, J. C. Batzer, M. L. Gleason, J. E. Monteiro, J. R. M. Pezzopane, and M. J. Pedro Jr. 2005. Spatial variability of leaf wetness duration in different crop canopies. *International Journal of Biometeorology* 49 (6): 363-70.
- Seyrig, G., R. D. Stedtfeld, D. M. Turlousse, F. Ahmad, K. Towery, A. M. Cupples, J. M. Tiedje, and S. A. Hashsham. 2015. Selection of fluorescent DNA dyes for real-time LAMP with portable and simple optics. *Journal of Microbiological Methods*. 119: 223-7.
- Shands, A. C., S. G. Crandall, T. Ho, and T. D. Miles. 2018. First report of leaf rust on southern highbush blueberry caused by *Thekopsora minima* in California. *Plant Disease* 102 (6): 1171.
- Shaner, Gregory Ellis, and R. L. Powelson. 1971. Epidemiology of stripe rust of wheat, 1961-1968. Corvallis: Agricultural Experiment Station, Oregon State University.
- Shen, W., G. Xu, L. Sun, L. Zhang, and Z. Jiang. 2016. Development of a loop-mediated isothermal amplification assay for rapid and sensitive detection of *Sporisorium scitamineum* in sugarcane. *Annals of Applied Biology* 168 (3): 321-7.
- Shipley, L. G, 2006. An introduction to real-time PCR in Real-time PCR. Dorak, M. Tefvik. New York; Abingdon [England]; Taylor & Francis.
- Simpson, M., P. Wilk, D. Collins, D. Robertson, and R. Daniel. 2017. Managing blueberry rust under an evergreen system. *Acta Horticulturae*. 1180: 105-10.

- Smagula JM, W. Litten, Y. Chen, S. Dunham. 1997. Variation of fruit set and fruit characteristics of wild lowbush blueberries (*Vaccinium angustifolium*) in a managed field. *Acta Horticulturae* 446:109-118.
- Souazé, F., A. Ntodou-Thomé, C. Y. Tran, W. Rostène, and P. Forgez. 1996. Quantitative RT-PCR: Limits and accuracy. *Biotechniques* 21 (2): 280-5.
- Sterling, M., C. Rogers, and E. Levetin. 1999. An evaluation of two methods used for microscopic analysis of airborne fungal spore concentrations from the Burkard spore trap. *Aerobiologia* 15 (1): 9-18.
- Stevens, N. E. 1934. Stewart's disease in relation to winter temperatures. *Plant Dis. Rep.* 18:141-149.
- Strick, B.C., and D. Yarborough. 2005. Blueberry production trends in North America, 1992 to 2003, and predictions for growth. *HortTechnology* 15(2): 391–398.
- Sun, G., J. Liu, G. Li, X. Zhang, T. Chen, J. Chen, H. Zhang, D. Wang, F. Sun, and H. Pan. 2015. Quick and accurate detection and quantification of *Magnaporthe oryzae* in rice using real-time quantitative polymerase chain reaction. *Plant Disease* 99 (2): 219-24.
- Tsukioka, A. 2005. Eiken chemical to release LAMP-based *Listeria monocytogenes* reagent test kit. JCNN News Summaries - Japan Corporate News Network.
- U.S. Department of Agriculture/ National Agricultural Statistics Service. 2018. Non-Citrus Fruit and Nut 2017 Summary. Available online. Accessed on 01/26/2019)
- Vander Kloet, S.P. 1976. A comparison of the dispersal and seedling establishment of *Vaccinium angustifolium* (the lowbush blueberry) in Leeds County, Ontario and Pictou County, Nova Scotia. *Canada Field Nature*. 90: 176-180.
- Villari, C., W. F. Mahaffee, T. K. Mitchell, K. F. Pedley, M. L. Pieck, and F. P. Hand. 2017. Early detection of airborne inoculum of *Magnaporthe oryzae* in turfgrass fields using a quantitative LAMP assay. *Plant Disease* 101 (1): 170-7.
- Washington, W. S., N. Kita, and D. Bardon. 2002. The use of weather and ascospore data for forecasting apple and pear scab in Victoria, Australia. *Australasian Plant Pathology* 31 (3): 205-15.
- West, J. S., S. D. Atkins, J. Emberlin, and B. D. L. Fitt. 2008. PCR to predict risk of airborne disease. *Trends in Microbiology* 16 (8): 380-7.
- West, J. S., and R. B. E. Kimber. 2015. Innovations in air sampling to detect plant pathogens. *Annals of Applied Biology* 166 (1): 4-17.
- Whelan, J. A., M. A. Whelan, and N. B. Russell. 2003. A method for the absolute quantification of cDNA using real-time PCR. *Journal of Immunological Methods* 278 (1): 261-9.
- White, T. J., Bruns T, Lee S., Taylor J. 1990. Amplification and direct sequencing of fungal ribosomal RNA genes for phylogenetics. In: Innis MA, Gelfand DH, Sninsky JJ, White TJ (eds) *PCR Protocols: A Guide to Methods and Applications*. Academic Press, NY. 315-322.

Wiseman, M. S., M. I. Gordon, and M. L. Putnam. 2016. First report of leaf rust caused by *Thekopsora minima* on northern highbush blueberry in Oregon. *Plant Disease* 100 (9): 1949.

Wieczorek, T. M., L. N. Jørgensen, A. L. Hansen, L. Munk, and A. F. Justesen. 2014. Early detection of sugar beet pathogen *Ramularia beticola* in leaf and air samples using qPCR. *European Journal of Plant Pathology* 138 (4): 775-85.

Yamamoto, H., T. Fujimori, H. Sato, G. Ishikawa, K. Kami, and Y. Ohashi. 2014. Statistical hypothesis testing of factor loading in principal component analysis and its application to metabolite set enrichment analysis. *BMC Bioinformatics* 15 (1): 51.

Yarborough, D. E. 1997. Production trends in the wild blueberry industry in North America. *Acta Horticulturae* (446): 33-6.

Yarborough, D. E. 2012. Establishment and management of the cultivated lowbush blueberry (*Vaccinium angustifolium*). *International Journal of Fruit Science* 12 (1-3): 14-22.

Yarborough, D. E., J. M. Smagula, F. Drummond, S., Annis, 2009. Organic production of wild blueberries iii. Fruit quality. *Acta Horticulturae*, (810), 847-852.
doi:10.17660/ActaHortic.2009.810.113

Yarborough, D, E. 2015. Wild Blueberry Culture in Maine, Fact sheet No. 220. The University of Maine Cooperative Extension. Retrieved from: <https://extension.umaine.edu/blueberries/factsheets/production/wild-blueberry-culture-in-maine/>

Yarborough, D, E. 2018. Wild blueberry newsletter. The University of Maine Cooperative Extension. Retrieved from: <https://extension.umaine.edu/blueberries/newsletters/july-maine-wild-blueberry-newsletter/>

Yepes, M. S, and Céspedes P. B., 2012. Nuevos registros de royas (*Pucciniales*) en plantas de interés agronómico y ornamental en Colombia. New rusts (*Pucciniales*) records on crops and ornamental plants in Colombia. *Revista Facultad Nacional De Agronomía* 65 (2): 6691-6.

Zheng, X., G. Tang, Y. Tian, X. Huang, X. Chang, H. Chen, H. Yang, S. Zhang, and G. Gong. 2017. First report of leaf rust of blueberry caused by *Thekopsora minima* in China. *Plant Disease* 101 (5): 835.

APPENDIX A

LIST OF SEQUENCES USED TO DEVELOP PCR PRIMERS

Number	Species	Isolate Code Name or GenBank accession ID	Location	Collection Date
1	<i>Thekopsora minima</i>	SP092216_1A	Spring Pond, ME	9/24/15
2	<i>Thekopsora minima</i>	SP092216_2A	Spring Pond, ME	9/24/15
3	<i>Thekopsora minima</i>	BBHF10.8.15	Blueberry Hill Farm, ME	10/8/15
4	<i>Thekopsora minima</i>	BBHF10.15.15	Blueberry Hill Farm, ME	10/15/15
5	<i>Thekopsora minima</i>	SP9.22.16	Spring Pond, ME	9/22/16
6	<i>Thekopsora minima</i>	SP9.19.16	Spring Pond, ME	9/29/16
7	<i>Thekopsora minima</i>	1A-1-1	Wesley, ME	9/24/2015
8	<i>Thekopsora minima</i>	2A-1-1	Wesley, ME	9/24/2015
9	<i>Thekopsora minima</i>	2B-2-1	Wesley, ME	9/24/2015
10	<i>Thekopsora minima</i>	9.2C-T7	Maine	NA
11	<i>Thekopsora minima</i>	11.2C-T7	Maine	NA
12	<i>Thekopsora minima</i>	13.1B-T7	Maine	NA
13	<i>Thekopsora minima</i>	13.1C-T7	Maine	NA
14	<i>Thekopsora minima</i>	13.1D-T7	Maine	NA
15	<i>Thekopsora minima</i>	GU355675	GenBank	NA
16	<i>Thekopsora minima</i>	HQ661383	GenBank	NA
17	<i>Thekopsora minima</i>	KX813713	GenBank	NA
18	<i>Thekopsora rubiae</i>	KC415800	GenBank	NA
19	<i>Thekopsora rubiae</i>	KC415804	GenBank	NA
20	<i>Thekopsora nipponica</i>	KC415795	GenBank	NA

21	<i>Thekopsora nipponica</i>	KC415793	GenBank	NA
22	<i>Thekopsora areolata</i>	KJ546897	GenBank	NA
23	<i>Thekopsora areolata</i>	DQ445905	GenBank	NA
25	<i>Thekopsora areolata</i>	EF363336	GenBank	NA
26	<i>Valdensia heterodoxa</i>	SP092216_3B	Spring Pond, ME	9/24/15
27	<i>Valdensia heterodoxa</i>	2A 2-1	Wesley, ME	9/24/2015
28	<i>Valdensia heterodoxa</i>	Isolate 4	Maine	NA
29	<i>Valdensia heterodoxa</i>	Isolate 5	Maine	NA
30	<i>Valdensia heterodoxa</i>	Isolate 6	Maine	NA
31	<i>Valdensia heterodoxa</i>	KT121733	GenBank	NA
32	<i>Valdensia heterodoxa</i>	KU306730	GenBank	NA
33	<i>Erysiphe vaccinii</i>	BBHF_PM-1	BBHF, ME	NA
34	<i>Erysiphe vaccinii</i>	BBHF_PM2	BBHF, ME	NA
35	<i>Erysiphe vaccinii</i>	BBHF_PM3	BBHF, ME	NA
36	<i>Erysiphe vaccinii</i>	Deblois_PM_4	Deblois, ME	NA
37	<i>Erysiphe vaccinii</i>	Wesley_PM_6	Wesley, ME	NA
38	<i>Erysiphe vaccinii</i>	Wesley_PM_7_	Wesley, ME	NA
39	<i>Botrytis cinerea</i>	KT266232	GenBank	NA
40	<i>Botrytis cinerea</i>	KX443701	GenBank	NA
41	<i>Septoria albopunctata</i>	DQ019362	GenBank	NA
42	<i>Septoria sp.</i>	KF251564	GenBank	NA
43	<i>Gloeosporium sp.</i>	EF672242	GenBank	NA
44	<i>Gloeosporium sp.</i>	KF572449	GenBank	NA
45	<i>Exobasidium vaccinii</i>	KP322983	GenBank	NA
46	<i>Monilinia vaccinii-corymbosi</i>	Z73796	GenBank	NA
47	<i>Cladosporium cladosporioides</i>	11.2B-T7	Maine	NA
48	<i>Pleosporales sp</i>	9.1A-T7	Maine	NA
49	<i>Sporobolomyces phaffii</i>	9.1F-T7	Maine	NA
50	<i>Heterocephalacria arrabidensis</i>	9.2A-T7	Maine	NA

51	<i>Genolevuria bromeliarum</i>	9.2B-T7	Maine	NA
52	<i>Heterocephalacria arrabidensis</i>	9.2F-T7	Maine	NA
53	<i>Cryptococcus keelungensis</i>	11.1C-T7	Maine	NA
54	<i>Alternaria sp.</i>	IsolateR52	Maine	NA
55	<i>Pucciniastrum goeppertianum</i>	WB2	Orono, ME	7/22/2018
56	<i>Pucciniastrum goeppertianum</i>	WB3	Orono, ME	7/22/2018
57	<i>Pucciniastrum goeppertianum</i>	L76509_1_	GenBank	NA

APPENDIX B

LIST OF FIELDS AND WEEKS of SPORE TRAP TAPES USED IN THIS STUDY

Field	Year	Week	Julian Date (Start)	Julian Date (End)
BBHF	2014	8/5/2014 - 8/11/2014	217	223
BBHF	2014	8/19/2014 - 8/25/2014	231	237
BBHF	2014	8/26/2014 - 9/1/2014	238	244
BBHF	2014	9/2/2014 - 9/8/2014	245	251
BBHF	2014	9/9/2014 - 9/15/2014	252	258
BBHF	2014	9/16/2014 - 9/22/2014	259	265
BBHF	2014	9/23/2014 - 9/29/2014	266	272
BBHF	2014	10/5/2014 - 10/11/2014	278	284
BBHF	2015	6/21/2015 - 6/27/2015	172	291
BBHF	2015	6/28/2015 - 7/4/2015	179	178
BBHF	2015	7/5/2015 - 7/13/2015	186	185
BBHF	2015	7/12/2015 - 7/18/2015	193	199
BBHF	2015	7/19/2015 - 7/25/2015	200	206
BBHF	2015	7/26/2015 - 8/1/2015	207	213
BBHF	2015	8/2/2015 - 8/8/2015	214	220
BBHF	2015	8/9/2015 - 8/15/2015	221	227
BBHF	2015	8/16/2015 - 8/22/2015	228	234
BBHF	2015	8/23/2015 - 8/29/2015	235	241
BBHF	2015	8/30/2015 - 9/5/2015	242	248
BBHF	2015	9/6/2015 - 9/12/2015	249	255
BBHF	2015	9/13/2015 - 9/19/2015	256	262
BBHF	2015	9/20/2015 - 9/26/2015	263	269
BBHF	2015	9/27/2015 - 10/3/2015	270	276
BBHF	2015	10/4/2015 - 10/10/2015	277	283
BBHF	2017	8/7/2017 - 8/13/2017	226	232
BBHF	2017	8/21/2017 - 8/27/2017	233	239
BBHF	2017	8/28/2017 - 9/3/2017	240	246
BBHF	2017	9/4/2017 - 9/10/2017	247	253
BBHF	2017	9/11/2017 - 9/17/2017	254	260
BBHF	2017	9/18/2017 - 9/24/2017	261	267
BBHF	2017	9/25/2017 - 10/1/2017	268	274
BBHF	2017	10/2/2017 - 10/8/2017	275	281
BBHF	2017	10/9/2017 - 10/15/2017	289	295
EM	2015	6/21/2015 - 6/27/2015	172	178
EM	2015	6/28/2015 - 7/4/2015	179	185
EM	2015	7/5/2015 - 7/11/2015	186	192

EM	2015	7/12/2015 - 7/18/2015	193	199
EM	2015	7/19/2015 - 7/25/2015	200	206
EM	2015	7/26/2015 - 8/1/2015	207	213
EM	2015	8/2/2015 - 8/8/2015	214	220
EM	2015	8/9/2015 - 8/15/2015	221	227
EM	2015	8/16/2015 - 8/22/2015	228	234
EM	2015	8/23/2015 - 8/29/2015	235	241
EM	2015	8/30/2015 - 9/5/2015	242	248
EM	2015	9/6/2015 - 9/12/2015	249	255
EM	2015	9/13/2015 - 9/19/2015	256	262
EM	2015	9/20/2015 - 9/26/2015	263	269
EM	2015	9/27/2015 - 10/3/2015	270	276
EM	2015	10/4/2015 - 10/10/2015	277	283
SP	2017	8/7/2017 - 8/13/2017	219	225
SP	2017	8/21/2017 - 8/27/2017	233	239
SP	2017	8/28/2017 - 9/3/2017	240	246
SP	2017	9/4/2017 - 9/10/2017	247	252
SP	2017	9/11/2017 - 9/17/2017	254	260
SP	2017	9/18/2017 - 9/24/2017	261	267
SP	2017	9/25/2017 - 10/1/2017	268	274
SP	2017	10/2/2017 - 10/8/2017	275	281
SP	2017	10/9/2017 - 10/15/2017	282	288

BIOGRAPHY OF THE AUTHOR

Nghi S. Nguyen was born in Ho Chi Minh City in southern Vietnam in spring 1989. She came to Dallas, Texas with her family in 2007 after graduating high school and started her undergraduate study at Collin County Community College and North Texas university with a major in Biology. After graduation, she worked as a pharmacy technician at Walgreens in Oklahoma and later went to work for Oklahoma Blood Institute in Oklahoma City as a quality control lab technician for two years. She developed her interest in botanical studies and taking a few plants related classes at the University of Central Oklahoma. In 2016, she applied for an internship in North Florida Education and Research center, an extension of University of Florida and spent six months there working on many different projects and assisted in the Plant Pathology clinic. The internship has inspired her to study more about plant pathology and crop science. She is a candidate for Master of Science degree in Botany and Plant Pathology from the University of Maine in August 2019.